Institut für Pharmakologie und Klinische Pharmazie
Fachbereich Pharmazie

Interaction dynamics between heterotrimeric G-proteins and type V adenylyl cyclase determine sensitivity of effector regulation

Dissertation
zur Erlangung des
Doktorgrades der Naturwissenschaften
(Dr. rer. nat.)

dem
Fachbereich Pharmazie
der Philipps-Universität Marburg

vorgelegt von

Markus Milde

aus **Dortmund**

Marburg 2013

Vom Fachbereich Pharmazie

der Philipps-Universität Marburg als Dissertation am _____ angenommen.

Erstgutachter: Prof. Dr. Moritz Bünemann

Zweitgutachter: Prof. Dr. Jens Kockskämper

Tag der mündlichen Prüfung am _____

Table of content

Abbreviations

A_{2A}-AdoR	A_{2A}-adenosine receptor
AC	adenylyl cyclase
ACh	acetylcholine (agonist for muscarinic acetylcholine receptors)
AKAP	A-kinase anchoring protein
ATP	adenosine triphosphate
α_{2A}-AR	α_{2A}-adrenoceptor
β-AR	β-adrenoceptor (type 1 or 2)
cAMP	cyclic adenosine monophosphate
Cer	Cerulean (a variant of eCFP)
CFP	cyan fluorescent protein (eCFP: enhanced CFP)
CHO	chinese hamster ovary (cell line)
DMEM	Dulbecco's Modified Eagle's Medium
EC_{50}	half-maximal effective concentration (concentration-response curves)
Epac	exchange protein directly activated by cAMP
Epac1-camps	FRET-based cAMP sensor, which contains the Epac1-domain
FCS	fetal calf serum
FRAP	Fluorescence Recovery After Photobleaching
FRET	Förster/Fluorescence Resonance Energy Transfer
FSK	forskolin
GFP	green fluorescent protein
GIRK channel	G-protein-gated inwardly rectifying K^+ channel
GPCR	G-protein-coupled receptor
G-protein	guanine nucleotide binding protein (s: stimulatory; i: inhibitory)
Gαi/AC5-FRET	FRET-assay, the labelled proteins are $G\alpha_{i1}$-CFP and YFP-AC5
Gαi/Gβγ-FRET	FRET-assay, the labelled proteins are $G\alpha_{i1}$-YFP and CFP-$G\gamma_2$
HEK	human endothelial kidney (cell line; used in this study: HEK293T)
HRP	horse radish peroxidase
Iso	isoprenaline (agonist for β-AR)
kDa	kilo Dalton
M_2-AChR	type 2 muscarinic acetylcholine receptor (also other types)
NE	norepinephrine (agonist for α_{2A}-AR and β-AR)
PAGE	polyacrylamide gel electrophoresis

PBS	phosphate buffered sodium (buffer)
PCR	polymerase chain reaction
PDE	phosphodiesterase
PKA	protein kinase A
PLC	phospholipase C
RGS4	regulator of G-protein signalling type 4
S.E.M.	standard error of the mean
SDS	Na^+ dodecyl sulphate
$t_{0.5}$	time to half-maximal stimulation or recovery (in FRET recordings)
wt	wild-type
YFP	yellow fluorescent protein
[cAMP]	cAMP concentration (also used with other substances)

About G-proteins:

In the following sections G-protein names without index, e.g. Gs-protein or Gi1-protein, are used for the respective heterotrimeric G-proteins. Indices are used for specific subunits, e.g. $G\alpha_s$ or $G\alpha_{i1}$. If the text refers to "$G\beta\gamma$-subunit", this means the combination of $G\beta_1$ and $G\gamma_2$. No other combination of Gβ- and Gγ-subunits was investigated during this study.

1 Introduction

The signalling pathway from G-protein-coupled receptors (GPCRs) to the regulation of cytosolic levels of cAMP (cyclic adenosine monophosphate) is present in virtually all cells. These receptors, being membrane spanning proteins, are the largest family of drug targets. Many drugs, including important classes like "β-blockers" (β_1-adrenergic antagonists, e.g. metoprolol) and blockbusters such as β_2-sympathomimetics (e.g. salmeterol), exert their pharmacological effect through the regulation of cellular cAMP levels. This second messenger mediates many important physiological functions like heart frequency, contraction and ultimately blood pressure, relaxation of smooth muscle cells or insulin secretion (Metrich et al., *Pflugers Arch.* 2010; Halls and Cooper, *Cold Spring Harb. Perspect. Biol.* 2011). β_1-adrenergic antagonists lower cAMP and thereby reduce heart rate, cardiac output and finally the blood pressure. β_2-adrenergic agonists are used to relieve patients suffering from asthmatic attacks, because they increase cellular cAMP which relaxes smooth muscle cells and thereby increases the diameter of the bronchi.

Cellular levels of cAMP are carefully regulated by three main mechanisms: A) stimulation or B) inhibition of the production and C) degradation (see Figure 1). A) Stimulation of the production is the result of the activation of GPCRs that couple to stimulatory G-proteins (Gs-proteins, guanine nucleotide-binding proteins) (Northup et al., *Proc. Natl. Acad. Sci. U. S. A.* 1980), which in turn increases the enzymatic activity of adenylyl cyclases (ACs). ACs are the family of enzymes, that actually catalyse the conversion of ATP (adenosine triphosphate) into cAMP. β_2-adrenergic agonists are important examples for this stimulation of AC activity and the increase in cellular cAMP levels. β_1-adrenergic antagonists prevent the activation of the stimulatory pathway, which ultimately lowers cellular cAMP levels. B) Cellular levels of cAMP can also be lowered through the direct activation of inhibitory G-proteins (Gi-proteins) (Bokoch et al., *J. Biol. Chem.* 1983). These inhibit cAMP production and the cAMP-degrading members of the PDE-superfamily (phosphodiesterases) (Essayan, *J. Allergy Clin. Immunol.* 2001) will further decrease the second messenger levels. The activation of Gi-coupled receptors is the cellular mode of action of morphine, a very potent analgesic. C) Interference with cAMP degradation by PDEs can further regulate cellular cAMP concentration. Theophylline, used against asthma as the β_2-adrenergic agonists, elevates cAMP by inhibiting the degradation through PDEs.

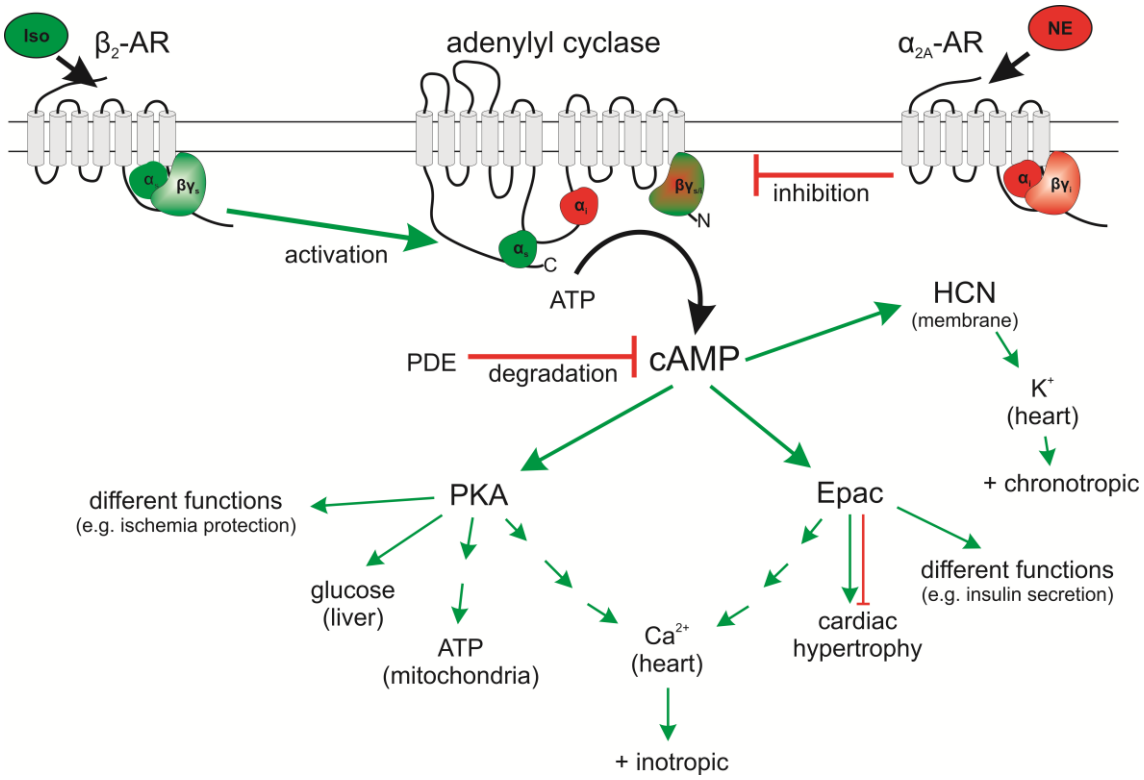

Figure 1: Stimulatory and inhibitory signalling from GPCRs via G-proteins and ACs to the second messenger cAMP

GPCRs activate their respective G-proteins, which will subsequently stimulate or inhibit ACs. This regulates the generation of the second messenger cAMP. cAMP can elicit several functions, some of them depicted in this scheme. Degradation of cAMP by PDEs will influence the cellular amount of cAMP and the according signalling pathways. Further details are provided in the text. Please note, that the AC is displayed with its N-terminus to the right to allow for better schematic display of the interaction with G-protein subunits.

According to the abundance of the above signalling cascade, detailed knowledge about the interaction between the partners involved is essential for the understanding of cellular processes as well as the generation and optimisation of therapeutic drugs. Biochemical research has provided detailed knowledge about the interaction between G-proteins and ACs (Sunahara et al., *Annu. Rev. Pharmacol. Toxicol.* 1996; Tesmer and Sprang, *Curr. Opin. Struct. Biol.* 1998). In addition, the development of new microscopic methods revealed many of the dynamics of the signalling pathway (see (Lohse et al., *Trends Pharmacol. Sci.* 2008) and (Lohse et al., *Pharmacol. Rev.* 2012) for recent reviews). However, some questions remained open, especially concerning the dynamics of AC regulation.

In the following, the individual partners of this signalling cascade will be introduced separately from the receptor via the G-proteins to ACs and finally the second messenger cAMP.

1.1 G-protein-coupled receptors (GPCRs)

Most prominently, GPCRs consist of seven membrane-spanning helices and are also referred to as 7TM-receptors (7 transmembrane), accordingly.

While most of the receptors will bind their ligands in a binding pocket inside the TM-bundle, some receptors also have ligand binding domains on their N-termini (Baldwin, *Curr. Opin. Cell Biol.* 1994; Fredriksson et al., *Mol. Pharmacol.* 2003). These receptors will usually bind peptides like the luteinising hormone (LH) or thyroid-stimulating hormone (TSH).

In the past few years, much insight was gained into the structure of GPCRs. Rhodopsin, the light-receptor of the visual system, had been crystallised about 13 years ago (Palczewski et al., *Science* 2000), but it took until 2007 to crystallise another human receptor, the β_2-adrenoceptor (Rasmussen et al., *Nature* 2007).

The third intracellular loop together with the C-terminus is a major interaction site for heterotrimeric G-proteins (Holthoff et al., *Circ. Res.* 2012). Upon ligand binding to the receptor several helices will undergo conformational changes. The most prominent change is the opening of a cleft on the intracellular side of the receptor through rearrangement of the helices 5 and 6 (Deupi and Standfuss, *Curr. Opin. Struct. Biol.* 2011). This cleft provides the binding moiety for the C-terminus of the G-protein α-subunit (Rasmussen et al., *Nature* 2011).

Although there are about 700 genes for GPCRs of the Rhodopsin family (Fredriksson et al., *Mol. Pharmacol.* 2003), there are only four major classes of G-proteins the receptors will interact with. They can therefore be divided into Gs-, Gi/o-, Gq/11- and G12/13-coupled receptors. According to the G-protein family it couples to, each receptor will stimulate distinct pathways.

There are some other types of GPCR-signalling apart from the activation of G-proteins. These pathways are referred to as non-canonical and include the activation of and signalling via GRKs (G-protein-coupled receptor kinase), arrestins and other molecules, such as RhoA, MAP kinase and NF-κB (Zhang and Eggert, *Mol. Biosyst.* 2013). These

signalling events do not elicit the interaction between G-proteins and ACs and therefore have not been investigated in this study.

1.1.1 β_2-adrenoceptor

In these studies the pharmacological relevant β_2-adrenoceptor (β_2-AR) was used as a model receptor to activate stimulatory G-proteins (Gs-proteins). This receptor is endogenously expressed in many cell types and tissues (Uhlen et al., *Nat. Biotechnol.* 2010), including the HEK293T cell line used in this study. This enabled stimulation of the Gs-signalling pathway without additional transfection of the receptor, which was important for some functional experiments.

Closely related to the β_2-AR is the β_1-AR, which is mainly expressed in the heart. The β_2-AR is also expressed in the heart, but it seems to be of less importance when it comes to the mediation of adrenergic response (Chruscinski et al., *J. Biol. Chem.* 1999). However, it is widely distributed throughout muscle tissues, especially smooth muscles in the uterus, gut, endothelium and bronchi. Agonists of the β_2-AR are, for example, used in the treatment of asthma and COPD (chronic obstructive pulmonary disease), where they relax the bronchi and thereby increase airway-diameter. Activation of β_2-ARs in blood vessels has hypotensive effects, because the vessel diameter is increased. However, this principle is currently not used in therapy of hypertension, at least not on its own. Due to its expression in the uterus, β_2-AR agonists can also be used to prevent labour and have been tested for treating dysmenorrhoea. However, the drugs also activate the β_1-AR and adverse effects limit their safety and use (Fedorowicz et al., *Cochrane Database Syst. Rev.* 2012). To prevent adverse cardiac effects like tachycardia, β_2-AR agonists are designed to preferentially activate β_2-AR over β_1-AR. Another option to reduce adverse effects is to apply the substances locally. In the eye, β_2-ARs control the production of the intraocular fluid and local application of β_2-AR antagonists is used to treat glaucoma, mainly by inhibiting new liquid production. The endogenous ligands for this receptor are epinephrine and with less potency norepinephrine (NE) (Sharman et al., *Nucleic Acids Res.*). The pharmacological tool compound isoprenaline (Iso) is structurally closely related to epinephrine and equally potent. In the present study Iso was used to selectively stimulate β_2-adrenoceptors.

The β_2-AR has been shown to dimerise (Hebert et al., *J. Biol. Chem.* 1996; Dorsch et al., *Nat. Methods* 2009). Receptor-dimerisation is a model with steady growing

evidence (see (Milligan, *Mol. Pharmacol.* 2013) for a recent review). Homodimerisation of the β_2-AR has been shown to be necessary for proper membrane targeting (Salahpour et al., *J. Biol. Chem.* 2004) as well as receptor activation and signalling (Hebert et al., *J. Biol. Chem.* 1996). However, the functional relevance of GPCR-dimers remains unsolved.

1.1.2 α_{2A}-adrenoceptor

The α_{2A}-adrenoceptor (α_{2A}-AR) was used to activate the inhibitory G-proteins (Gi-proteins) in this study. The α_{2A}-AR is predominately expressed in the brain where it is involved in synaptic function. It controls the release of neurotransmitters, especially by a negative feedback mechanism (Hein et al., *Nature* 1999). Pharmacological activation of this receptor, e.g. by clonidine, is used to treat hypertension. Clonidine activates the α_{2A}-AR and thereby reduces catecholamine-release, which results in decreased blood pressure and cardiac activity. In addition clonidine binds to imidazoline receptors of the medulla oblongata, which adds to the hypotensive effect (Bousquet et al., *J. Pharmacol. Exp. Ther.* 1984). Because of the presence of the α_{2A}-AR in the central nervous system it seems to be related to further CNS effects. Clonidine is discussed to be effective in addition to morphine treatment (Engelman and Marsala, *Br. J. Anaesth.* 2013) and attention-deficit/hyperactivity disorder (Childress and Sallee, *Drugs Today (Barc)* 2012).

Like other adrenoceptors, the α_{2A}-AR is endogenously activated by epinephrine and norepinephrine. The latter was used to activate the signalling pathway. Upon activation of the receptor and subsequently the Gi-protein, ACs will be inhibited and cellular cAMP levels will be decreased. This effect is mainly mediated by the $G\alpha_i$-subunit. $G\beta\gamma$-subunits derived from Gi-proteins can directly activate G-protein-gated inwardly rectifying K^+ channels (GIRK channel) as well as inhibit N-type Ca^{2+} channels. The latter is an important mediator of the presynaptic inhibition of neurotransmitter release (Currie, *Channels (Austin)* 2010).

The α_{2A}-AR has recently been shown to be voltage-dependent in the presence of agonist (Rinne et al., *Proc. Natl. Acad. Sci. U. S. A.* 2013). Physiological membrane potentials promote the activation of the receptor, whereas depolarisation deactivates the receptor, obviously by reducing ligand binding. As the receptor is localised in neurons and will

therefore be exposed to changes in the membrane potential quite frequently, the voltage sensitivity might provide a potent and fast regulation mechanism for this receptor.

1.2 G-proteins

G-proteins were initially identified, because the researchers were trying to identify the regulatory subunit of adenylyl cyclases (Northup et al., *Proc. Natl. Acad. Sci. U. S. A.* 1980). Their name is derived and abbreviated from their ability to bind guanine nucleotides. G-proteins are heterotrimeric proteins, consisting of α-, β- and γ-subunits. β- and γ-subunits have a very high affinity towards each other and do not dissociate under normal conditions. As they act as a heterodimer, they will be referred to as Gβγ in the following. Currently 23 α-, 5 β- and 12 γ-subunits are known (McCudden et al., *Cell. Mol. Life Sci.* 2005). The α-subunit contains the binding site for the nucleotide. It is also the subunit that defines the G-protein's state of activity. If GDP is bound, the G-protein is inactive, while the GTP-bound protein is active. Please refer to section 1.2.4 for a more detailed description of the G-protein cycle. There is also an intermediate state, where no nucleotide is bound to the α-subunit. This state is considered a high-affinity state for the interaction with an active GPCR.

According to common theory, the heterotrimeric G-protein will dissociate upon activation and the Gα- and Gβγ-subunits will interact with their individual effectors. This model might not properly reflect the endogenous situation in all G-protein types, though. Resonance energy transfer (RET)-based assays resolve protein/protein interactions and are used to investigate agonist-mediated G-protein activation. These assays should report a loss of RET upon protein dissociation. At least the Gi-protein is unlikely to fully dissociate, as the RET-signal increases under certain conditions (see section 1.5.1 for further details). This suggests subunit rearrangement rather than dissociation, at least in the absence of effector proteins.

1.2.1 Gα-subunits

As mentioned above, the G-proteins can be divided into four major classes (Gs, Gi/o, Gq/11 and G12/13), defined by their α-subunits. Their N-terminus is posttranslationally either myristinylated or palmitoylated to ensure membrane association (McCudden et al., *Cell. Mol. Life Sci.* 2005). Of the four, only $G\alpha_s$ and $G\alpha_i$ interact with adenylyl cyclases. $G\alpha_s$-subunits activate all nine membrane integrated AC isoforms (Pavan et al., *Drug Discov. Today* 2009) and thereby stimulate the production of cAMP. $G\alpha_i$-subunits will inhibit the production of cAMP, at least through the AC isoforms I, V and VI.

While $G\alpha_s$ is expressed abundantly, $G\alpha_{i1}$ is mostly expressed in the brain. $G\alpha_{i2}$ and $G\alpha_{i3}$ are important subunits in the immune system (Wiege et al., *J. Immunol.* 2013) and the heart (Hippe et al., *Naunyn-Schmiedeberg's Arch. Pharmacol.* 2013). Further details on the interaction with ACs and the subsequent effects of cAMP are introduced in sections 1.3ff.

The main effectors of Gq-proteins are phospholipases and their second messengers are DAG (diacyl-glycerol) and IP3 (inositol-trisphosphate) (Jensen et al., *J. Gen. Physiol.* 2009). Accordingly $G\alpha_q$ was used for control purposes in this study.

1.2.2 Gβγ-subunits

Gβ- and Gγ-subunits form constitutively heterodimers and do not dissociate under normal conditions. Gγ is C-terminally prenylated and thereby provides the membrane anchor for the dimer. Most combinations of the 5 Gβ- and 12 Gγ-subunits are functional. Some combinations seem to preferentially bind certain receptors or activate specific signalling pathways (McCudden et al., *Cell. Mol. Life Sci.* 2005). However, there is currently no evidence showing the preference of individual Gβγ-combinations towards certain Gα-subunits. In this work, only $G\beta_1\gamma_2$-subunits were investigated.

Like Gα, Gβγ-subunits can interact with effectors. Gi-derived Gβγ-subunits can interact with and stimulate the GIRK channel or inhibit N-type Ca^{2+} channels. Electrophysiological recording of the GIRK channel has classically been used to most directly monitor Gi-protein activity. ACs are also direct effectors of the Gβγ-subunits. AC isoforms II, IV and VII are activated by them, while type I AC is inhibited (Smrcka, *Cell. Mol. Life Sci.* 2008; Pavan et al., *Drug Discov. Today* 2009). There are conflicting reports on the regulation of type V AC (AC5) by Gβγ-subunits. While they have been stated to inhibit AC5 (Smrcka, *Cell. Mol. Life Sci.* 2008; Pavan et al., *Drug Discov. Today* 2009), they are also necessary for the activation of AC5 through $G\alpha_s$ (Gao et al., *J. Biol. Chem.* 2007) and have been shown to interfere with $G\alpha_i$-mediated inhibition of AC5 (Sadana et al., *Mol. Pharmacol.* 2009).

Most Gβγ-effectors are regulated by Gi-derived subunits – a quite elaborate list can be found in a review by Alan V. Smrcka (*Cell. Mol. Life Sci.* 2008). However, Gβγ and $G\alpha_s$ have been found to jointly interact with AC5 (Sadana et al., *Mol. Pharmacol.* 2009).

1.2.3 Different sensitivity of $G\alpha_i$- and Gi-derived $G\beta\gamma$-pathways

About 20 years ago an interesting effect of Gi-signalling was reported. AC5 is obviously very potently inhibited by Gi-proteins as observed by the specific regulation of it through D3 dopamine receptors (Robinson and Caron, *Mol. Pharmacol.* 1997). In addition, Li et al. discovered, that within the same cell type, there are several outcomes of the same receptor (*J. Gen. Physiol.* 1994). They reported that activation of type 2 muscarinic acetylcholine receptor (M_2-AChR) by low concentrations of agonist resulted in the inhibition of Ca^{2+} currents, while higher concentrations of ACh led to the activation of K^+ currents. The inhibition of Ca^{2+} currents was a cAMP-dependent effect, while the activation of K^+ currents was based on the G-protein activity-dependent activation of GIRK channels. These observations already hinted at a very specific interaction between Gi-proteins and ACs, especially AC5, a fact that also occurred in the course of this study.

1.2.4 G-protein cycle and RGS proteins

The G-proteins undergo an activation/deactivation-cycle as depicted in Figure 2.

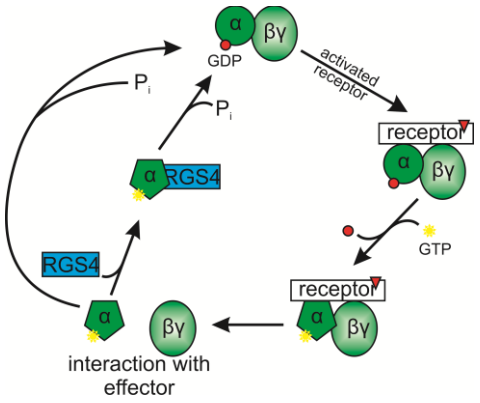

Figure 2: The G-protein cycle and the influence of RGS proteins

G-proteins cycle through activation and deactivation. Binding of a ligand-activated receptor will lead to the exchange of GDP for GTP and thereby render the G-protein active and able to interact with its effector(s). The endogenous GTPase activity will cleave GTP to GDP again. The subunits will subsequently reassemble to their inactive conformation and the cycle will come to its closure. RGS proteins can accelerate the deactivation by enhancing the GTPase activity.

In the G-protein's inactive conformation GDP is bound to the α-subunit. The activated receptor will bind the inactive G-protein, which releases the bound GDP. The now nucleotide-free G-protein is stabilised by the active receptor before the α-subunit binds GTP and the G-protein is rendered active. This step occurs very fast, because of the high cellular concentration of GTP. The now active G-protein can interact with its

effectors. The deactivation of the G-protein is initiated when the endogenous GTPase activity of the Gα-subunit cleaves the bound GTP to GDP. Subsequently the G-protein subunits will establish their inactive conformation again. This deactivation step can be accelerated by so-called GAPs (GTPase activating proteins), e.g. the regulators of G-protein signalling (RGS proteins). Of the vast number of RGS proteins and proteins containing RGS-domains, the RGS4 family is the largest and has the least complicated domain structure. Members of this family basically consist of only the RGS domain and nearly all of them regulate Gi/o- and Gq-proteins (Kimple et al., *Pharmacol. Rev.* 2011). RGS2 has been reported to reduce the activity of AC3 in olfactory neurons (Sinnarajah et al., *Nature* 2001), which hinted at regulation of Gs-proteins. Later work revealed that RGS2 directly binds to several AC isoforms (Salim et al., *J. Biol. Chem.* 2003; Xie et al., *Sci. Signal.* 2012) and thereby directly reduces AC activity. Currently no RGS proteins are known that regulate Gs-protein and neither have Gs-protein GAPs been reported. When tested *in vitro*, RGS proteins increase the endogenous GTPase activity of the Gα-subunits (Watson et al., *Nature* 1996). This leads to an accelerated G-protein deactivation *in vivo* (Doupnik et al., *Proc. Natl. Acad. Sci. U. S. A.* 1997), which was identified by GIRK current measurements. In the current study, RGS4 was used in kinetic experiments to selectively accelerate Gi-protein deactivation and thereby alter kinetics of the G-protein cycle.

Among the GTPase activating proteins, there are also G-protein effectors. PLC-β, for example, is an effector and GAP of the Gq-protein (Ross, *Sci. Signal.* 2011). So far no such functionality has been reported for ACs and this study also aimed to investigate potential G-protein regulation by this effector.

1.3 Adenylyl cyclases

The main function of adenylyl cyclases (ACs) is the production of the second messenger cAMP (cyclic adenosine-mono-phosphate) from ATP. Currently ten AC isoforms are known, nine of them being membrane-integrated. Type 10 AC is not a transmembrane protein and also referred to as soluble AC (sAC) (Gancedo, *Biol. Rev. Camb. Philos. Soc.* 2013).

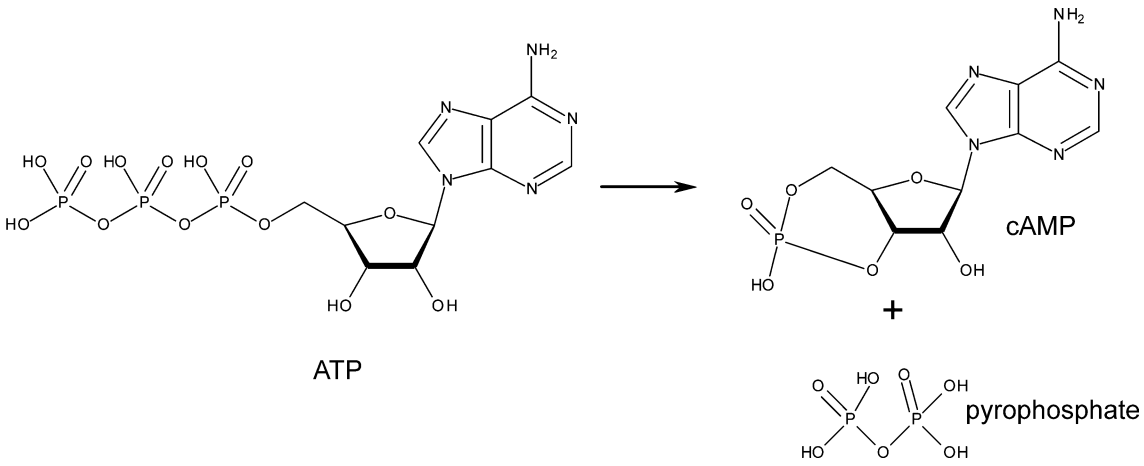

Figure 3: Catalytic conversion of ATP to cAMP

cAMP is generated from ATP by the cleavage of pyrophosphate and ring-closure between the oxygen of the ribose residue and the remaining phosphate.

Biochemical research of the ACs revealed important structural information (for comparison see Figure 4). The mammalian membrane-integrated ACs consist of 12 transmembrane helices, grouped into two bundles of six (Linder, *Cell. Mol. Life Sci.* 2006). These two bundles are separated by a large intracellular loop, which is referred to as C1-domain, as it contains parts of the catalytic site. The C-terminus – after the second set of transmembrane helices – contains the second part of the catalytic domain and is therefore referred to as C2. Both catalytic domains are further subdivided into two parts (C1a and b; C2a and b). The N-terminus is implicated to be involved in self-regulation of the AC, at least of AC5 (Sadana et al., *Mol. Pharmacol.* 2009). The whole enzyme is yet to be crystallised, but crystal structures exist for the catalytic domains. These were derived from a soluble chimeric heterodimer consisting of the C1-domain of AC5 and the C2-domain of AC2. The structures revealed the binding sites for the nucleotide (Tesmer et al., *Science* 1997), catalytically necessary cations like Mg^{2+} (Tesmer et al., *Science* 1999), forskolin (Zhang et al., *Nature* 1997) and its analogues (Pinto et al., *Biochem. Pharmacol.* 2009). Furthermore, the interaction with $G\alpha_s$ was revealed (Tesmer et al., *Science* 1997) and the mode of inhibition of AC5 through Ca^{2+} (Mou et al., *Biochemistry (Mosc.)* 2009). Biochemical approaches, including mutational studies, immunological and microscopic approaches, mapped the binding sites for different G-protein subunits (Sunahara et al., *J. Biol. Chem.* 1997; Dessauer et al., *J. Biol. Chem.* 1998; Wittpoth et al., *Proc. Natl. Acad. Sci. U. S. A.* 1999; Dessauer et al., *J. Biol. Chem.* 2002; Sadana et al., *Mol. Pharmacol.* 2009).

1.3.1 Type 5 adenylyl cyclase

Summarising the research mentioned above, the following is known about the activation of ACs in general and the regulation of AC5, specifically (refer to Figure 4 for a scheme of the individual domains). Forskolin and $G\alpha_s$-GTP bind to the C2-domain. This enhances the affinity of C2 to C1 about 100-fold and activates ACs by facilitating the formation of the catalytic subunit (closed conformation of C1 and C2) and presumably further conformational changes. The nucleotide binds within this domain dimer, as well as the metal ion (Mg^{2+} in AC5), which establishes complex bonds to the pyrophosphate residue of the nucleotide (Tesmer and Sprang, *Curr. Opin. Struct. Biol.* 1998). Ca^{2+} obviously competes with and displaces Mg^{2+}, which results in the inhibition of AC5 and AC6, the most closely related isoform (Pavan et al., *Drug Discov. Today* 2009). $G\alpha_{i1}$ binds to the C1-domain opposite of $G\alpha_s$-GTP on C2 and thereby interferes with catalytic core formation. The N-terminus of AC5 has several functions. It interacts with the C1-domain, thereby regulating $G\alpha_i$-mediated inhibition of AC5 and also $G\alpha_s$-mediated activation. The amino acids 60-129 have been mapped as the interaction site for $G\beta\gamma$-subunits and $G\alpha_s$-GDP. However, the actual transition from the inactive complex to the active conformation remains elusive. As the N-terminus is less conserved between AC5 and AC6, it might be the cause for regulatory differences between these otherwise closely related isoforms (Chen-Goodspeed et al., *J. Biol. Chem.* 2005).

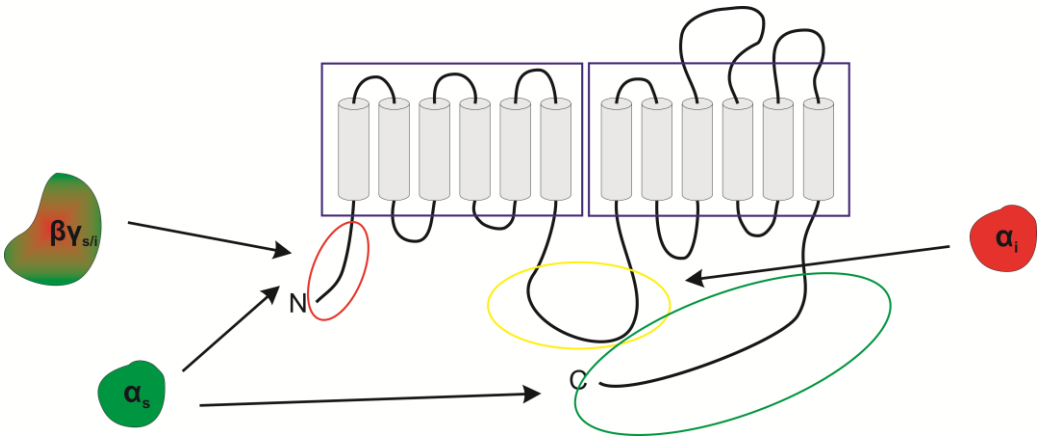

Figure 4: Domains of AC5

AC5 consists of two bundles of each six transmembrane helices (blue). The N-terminus (red) contains binding sites for $G\beta\gamma$ and inactive $G\alpha_s$. $G\alpha_i$ will bind within the C1-domain (yellow) and interfere with the formation of the catalytic core consisting of C1 and C2. The C2-domain is located on the C-terminus of AC5 (green) and also contains putative binding sites for active $G\alpha_s$ and forskolin.

AC5 mRNA is ubiquitously expressed (Wu et al., *Genome Biol.* 2009). AC5 is an important isoform in the heart, but hardly distinguishable from AC6 (Gottle et al., *J. Pharmacol. Exp. Ther.* 2009). Several physiological and pathophysiological functions have been linked to AC5, not least through the availability of AC5-knock-out mice. The central nervous system relies on AC5 in learning and memory (Kheirbek et al., *J. Neurosci.* 2009; Kheirbek et al., *Learn. Mem.* 2010). Furthermore, AC5 plays a relevant role in alcoholism (Kim et al., *Psychopharmacology (Berl.)* 2011) and further mediates morphine action (Kim et al., *Proc. Natl. Acad. Sci. U. S. A.* 2006). AC5 has also been identified as being involved in morphine withdrawal symptoms as it is hyperactivated after morphine treatment (Fan et al., *Mol. Pharmacol.* 2009). Deletion of AC5 protects the heart from cardiomyopathies (Yan et al., *Cell* 2007; Vatner et al., *Circ. J.* 2009), but overexpression is associated with hypertrophy. AC5-knock-out is also related to longevity, presumably through mechanisms closely related to metabolic changes in response to calorie restriction (Vatner et al., *Aging (Albany NY)* 2012).

It is controversially discussed whether AC5-downregulation (potentially achieved through selective pharmacological inhibition) is generally beneficial. Although AC5 and AC6 are closely related enzymes, their physiological function is distinct. Hypertrophy leads to an upregulation of AC5, while AC6 is downregulated and AC5-overexpression seems to be predisposing for hypertrophy. This may be caused by the selective anchoring and subcellular localisation of AC5 by mAKAP (muscle protein A-kinase anchoring protein), a protein that does not bind AC6. Controversially to these observations, beneficial effects of AC5-overexpression have been found whenever cardiomyopathies have been associated to Gq-protein overexpression. These myopathies obviously result in a reduced expression of AC5, which explains why AC5-overexpression could be beneficial (Vatner et al., *Am. J. Physiol. Heart Circ.Physiol.* 2013).

1.4 cyclic AMP (cAMP)

cAMP was identified in 1957 as a “heat-stable factor (formed by particulate fractions of liver homogenates in the presence of ATP, Mg^{++}, and epinephrine or glucagon)” (Sutherland and Rall, *J. Am. Chem. Soc.* 1957). Soon it became evident that cAMP was present in virtually all cells and tissues (Sutherland and Robison, *Pharmacol. Rev.* 1966). To establish the concept of cAMP being a second messenger, further regulatory mechanisms still had to be identified (Blumenthal, *Perspect. Biol. Med.* 2012). Today, a

wide variety of disease-treatment manipulates cellular levels of this second messenger (Pierre et al., *Nat. Rev. Drug Discov.* 2009). Meanwhile, cAMP effects have been identified in many organisms (Gancedo, *Biol. Rev. Camb. Philos. Soc.* 2013). Accordingly, it comes as no surprise, that even some bacterial toxins exert their effects via the alteration of cAMP, e.g. the edema factor of *B. anthraxis*, which elevates cAMP through its own adenylyl cyclase activity (Tang and Guo, *Mol. Aspects Med.* 2009).

Cellular amounts of cAMP are controlled through its generation by adenylyl cyclases (ACs) and the degradation by phosphodiesterases (PDEs), respectively. Accordingly, cAMP levels are highly dynamic and the temporal patterns of cAMP are critical regulators of cell function as shown for example in pancreatic cells (Willoughby and Cooper, *J. Cell Sci.* 2006; Willoughby et al., *J. Biol. Chem.* 2010; Halls and Cooper, *Cold Spring Harb. Perspect. Biol.* 2011).

cAMP itself can elicit a wide variety of cellular responses, which are mainly dependent on the cell-type (see Figure 1). Most prominently cAMP leads to the activation of PKA (protein kinase A) where it binds to specific binding domains. In heart muscle cells this can result in the phosphorylation and activation of Ca^{2+} channels, which in turn will result in higher intracellular [Ca^{2+}] and increased myocyte contraction (positive inotropy). PKA-dependent phosphorylation of the small heat-shock protein Hsp20 protects the heart from damage caused by ischemia (Edwards et al., *Biochem. Soc. Trans.* 2012). PKA can also phosphorylate Complex I of the respiratory chain of the mitochondria (Papa et al., *FEBS Lett.* 2012) and thereby regulate oxidative energy production. In the liver, PKA-phosphorylation will subsequently activate a phosphorylase and thereby increase the conversion of glucagon into glucose (Sutherland and Robison, *Pharmacol. Rev.* 1966; Gancedo, *Biol. Rev. Camb. Philos. Soc.* 2013).

Apart from the activation of PKA cAMP can also directly activate HCN-channels (hyperpolarisation-activated cyclic-nucleotide-modulated channels), which in the heart will result in positive chronotropy (Ludwig et al., *Nature* 1998; Santoro et al., *Cell* 1998). Activation of these channels by cAMP leads to a faster diastolic depolarisation of the membrane potential, subsequently decreasing the time to the next action potential. Furthermore, cAMP signalling is part of the circadian rhythm which, among others, influences pancreatic islet insulin release (Peschke, *J. Pineal Res.* 2008). This effect is regulated through melatonin, whose receptor couples Gi-proteins.

Another effector of cAMP is Epac (exchange protein directly activated by cAMP, official name RAPGEF3). It mediates cAMP effects independent of PKA-phosphorylation and ion channels. It is alternatively referred to as cAMP-regulated guanine nucleotide exchange factor (cAMPGEF) (Holz et al., *J. Physiol.* 2006). Two isoforms have been identified so far: Epac1 and Epac2, named after their respective number of cAMP binding domains. A main effector of Epac is Rap (small molecular weight GTPase), whose activation triggers further downstream events. In the heart, Epac is necessary for the full effect of β-adrenergic stimulation, as it will activate Rap, which in turn activates CaMKII (Ca^{2+}/calmodulin-dependent protein kinase II) via PLCε and PKCε (phospholipase C and protein kinase C, respectively). This will ultimately result in the phosphorylation of the Ryr2 (Ryanodin receptor type II) and PLB (phospholamban), thereby increase Ca^{2+} release from the SR and add to the Ca^{2+}-induced Ca^{2+} release (CICR), which is the main mediator of excitation-contraction coupling (Gloerich and Bos, *Annu. Rev. Pharmacol. Toxicol.* 2010). In case of chronic β-adrenergic stimulation, the heart will undergo remodelling and hypertrophy. This can also be linked to Epac via calcineurin and CaMKII (Gloerich and Bos, *Annu. Rev. Pharmacol. Toxicol.* 2010; Metrich et al., *Pflugers Arch.* 2010). On the other hand, Epac can be protective against hypertrophy by inhibiting ERK5-induced (extracellular signal-regulated kinase 5) hypertrophic changes (Gloerich and Bos, *Annu. Rev. Pharmacol. Toxicol.* 2010).

Apart from its function in the heart Epac has been reported to attribute to the secretion of insulin and neurotransmitters (Gloerich and Bos, *Annu. Rev. Pharmacol. Toxicol.* 2010), as well as the regulation of the endothelial barrier function, which in turn might control excessive migration of leukocytes in inflammatory diseases (Metrich et al., *Pflugers Arch.* 2010). Furthermore, there is growing evidence for Epac being involved in kidney diseases (Patschan et al., *Am. J. Physiol. Renal Physiol.* 2010).

1.4.1 Compartmentalisation of cAMP

One could assume cAMP to diffuse freely within the cell, because of its rather small size and hydrophilicity. However, there is growing evidence for different cAMP compartments in which the individual pathways are organised. In cardiac myocytes β_1-AR results in a cAMP increase throughout the whole cell, while the closely related β_2-AR only triggers localised cAMP generation (Nikolaev et al., *Circ. Res.* 2006). ACs can be targeted to raft and non-raft membrane domains (Cooper, *Biochem. Soc. Trans.*

2005), which could also enhance the interaction with other proteins of the signalling pathway and thereby reduce the diffusion of cAMP. Lately, AC5 was shown to be mainly located in T-tubules of myocytes, whereas the closely related AC6 is localised more globally (Timofeyev et al., *Circ. Res.* 2013). Last, but not least, AKAPs (A-kinase anchoring proteins) can bind a wide variety of proteins and thereby integrate different proteins into signalling complexes (Kritzer et al., *J. Mol. Cell. Cardiol.* 2012). The recruitment of PKA, PDEs, Epac and maybe further proteins to these complexes would ensure close proximity of the signalling partners and the presence of PDEs could avoid activation of adjacent complexes through the immediate degradation of otherwise freely diffusible cAMP (Edwards et al., *Semin. Cell Dev. Biol.* 2012). The compartmentalisation of cAMP is presumably a potent mechanism to spatially and temporally confine the signalling cascades.

1.5 Real-time measurements using Förster Resonance Energy Transfer (FRET)

Biochemical studies have revealed a lot of important information about adenylyl cyclases, their structure and interaction with G-proteins. However, these studies are mostly based on *in vitro* methods and thereby restricted to steady-state interactions. The present study aimed to investigate dynamic changes in the G-protein/AC-interaction in living cells. FRET-microscopy has been used to investigate protein/protein-interaction in cells and therefore provided a promising tool. The development of an *in vivo* technique would further provide new options for the research on ACs in settings closer to the physiological environment of the investigated partners.

Förster or Fluorescence Resonance Energy Transfer is the radiation-free transfer of energy from an excited donor fluorophore to a non-excited acceptor fluorophore. The German scientist Theodor Förster described and calculated this phenomenon in 1948 (Förster, *Annalen der Physik* 1948). Based on his calculations, the FRET-efficiency E is dependent to the sixth power of the distance between the fluorophores r and the so-called Förster radius R_0:

$$E \sim \frac{1}{1 + \left(\frac{r}{R_0}\right)^6}$$

The Förster radius R_0 describes the distance between the two fluorophores where the FRET efficiency is half-maximal.

Apart from the distance between the two interacting fluorophores, two other aspects are crucial for the energy transfer. Firstly, efficient FRET needs a certain spectral overlap of the donor emission and acceptor excitation spectra. Secondly, the fluorophores' orientation should align the actual fluorescent planes (if existent). The second aspect is important for FRET between derivatives of GFP, the green fluorescent protein (Shimomura et al., *J. Cell. Comp. Physiol.* 1962; Tsien, *Annu. Rev. Biochem.* 1998), as these have a distinct fluorophore plane inside their β-barrel. For a long time cyan- and yellow-fluorescent mutations of GFP (CFP and YFP, respectively) have been used, because of the efficient FRET. In order to increase the fluorophores' brightness, several variants have been cloned. In this study, enhanced CFP (eCFP; abbreviated as CFP hereafter) and Cerulean (Cer) were used as FRET-donors. The FRET-acceptor used was a variant of enhanced YFP, which had been mutated to increase its brightness (eYFP F46L/L68V; abbreviated as YFP in the following).

Typically FRET is determined by either acceptor bleaching, sensitised emission, fluorescence lifetime or fluorescence anisotropy (Ishikawa-Ankerhold et al., *Molecules* 2012).

For fluorescence lifetime measurements (FLIM, fluorescence lifetime imaging microscopy) the exponential decay of the donor fluorescence is determined. This is influenced by the chemical environment of the fluorophores, but not by their concentration (Becker, *J. Microsc.* 2012). The presence of a FRET-acceptor changes the donor's environment and reduces the fluorescence lifetime. FRET-detection by means of fluorescence anisotropy relies on polarisation of excitation and emission light. Fluorophores within the plane of the polarised light can be excited, but only emission of properly aligned FRET-acceptors can be recorded (Ishikawa-Ankerhold et al., *Molecules* 2012).

Acceptor photobleaching was used in these studies to determine FRET under non-stimulated conditions. Direct excitation of the acceptor fluorophore with high-intensity light irreversibly bleaches the fluorescent protein and thereby destroys the FRET-pair. Subsequently the donor fluorophore can no longer transfer energy to the acceptor and its fluorescence intensity will increase if FRET occurred before the bleaching. This method is only applicable for steady-state experiments. To dynamically investigate the

interaction between fluorescently labelled proteins, a method closely related to sensitised emission was applied.

During sensitised emission the donor is excited and the fluorescence of the acceptor is monitored, as it will only occur – under ideal conditions –, if there is FRET between donor and acceptor. In reality, one always has to consider the spectral cross-talk between the fluorophores. The donor fluorescence spectrum will usually "tail" and therefore reach into the acceptor's emission channel, a phenomenon that is referred to as "bleed-through". In addition, the acceptor can often be excited by the donor excitation light. This is referred to as "false excitation" (refer to methods section for further details on spectra and correction factors). During the actual experiments CFP was excited, the CFP- and YFP-fluorescence were recorded simultaneously and the according ratio of YFP- over CFP-fluorescence was calculated. Low FRET would result in strong fluorescence of CFP and weak emission of YFP. Accordingly, a low FRET-ratio would be observed. In case of high FRET, the fluorescence of YFP would increase, while CFP-emission would decrease, resulting in an increase of the FRET-ratio (Figure 5).

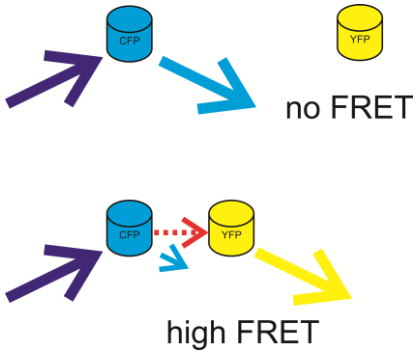

Figure 5: FRET-changes during sensitised emission

The sketch illustrates, that FRET only occurs if the acceptor (YFP) is close enough to the donor (CFP).

Using the methods based on sensitised emission, major parts of the signalling pathway from GPCR activation to the generation of second messengers have been investigated (see Lohse et al. (*Pharmacol. Rev.* 2012) for a recent review). The following sections only list the investigations and assays relevant for this study.

1.5.1 Real-time detection of G-protein activity

According to older textbook knowledge, activation of the G-protein will result in the dissociation of the α- from the βγ-subunit. If there is FRET between the subunits prior to stimulation, this should be decreased if not totally lost upon activation and

subsequent dissociation of the G-protein. All the G-protein-assays available show FRET under non-stimulated conditions.

Upon activation of the Gs-protein, the FRET-signal decreases (Hein et al., *J. Biol. Chem.* 2006), within less than one second. The decrease in the FRET-signal could represent the dissociation of the Gα- and Gβγ-subunits. However, the loss in FRET could also be due to an activity-dependent conformational change, that results in an increased fluorophore distance or orientation that does not favour FRET. Contrastingly, activation of the Gi1-protein will result in an increase in FRET between the subunits (Bünemann et al., *Proc. Natl. Acad. Sci. U. S. A.* 2003). This argues against the hypothesis that the subunits will completely separate upon activation. The activation of Gi-proteins also occurs fast, the according time course being in the same range as Gs-protein activation.

1.5.2 Real-time detection of cAMP

The development of FRET-based sensors like Epac1-camps allowed for the dynamic measurement of cAMP in single living cells (Nikolaev et al., *J. Biol. Chem.* 2004). This sensor consists of a cAMP binding domain from Epac (exchange protein directly activated by cAMP; official name RAPGEF3), which is coupled to YFP and CFP. In the inactive, i.e. non-cAMP-bound state, the sensor has a closed conformation where the fluorophores are in close proximity and accordingly high FRET is observed. FRET decreases upon generation of cAMP. Presumably, the hinge region of the Epac1 fragment opens upon binding of cAMP and the distance between CFP and YFP increases (Figure 6).

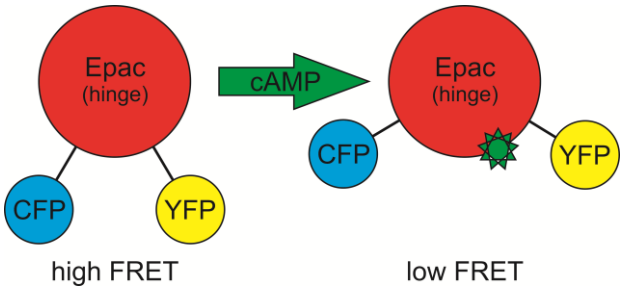

Figure 6: Presumed mode of action of the FRET-based cAMP sensor Epac1-camps

If no cAMP is bound, the sensor will show a closed conformation. The fluorophores are in close proximity and high FRET will be observed. Binding of cAMP to the sensor's hinge region will open the sensor and thereby increase the distance between CFP and YFP. Accordingly, the sensor will now yield low FRET.

Prior to the development of sensors like this, the detection of cAMP mainly relied on radioactive or biochemical methods (Dessauer, *Methods Enzymol.* 2002). These assays are suitable for steady-state experiments, as the cells are usually lysed for the detection. It was not possible to determine dynamic changes of cAMP, especially not in tissues. The use of Epac1-camps revealed a half-time of about 30 s for the generation of cAMP (Nikolaev et al., *J. Biol. Chem.* 2004). This is a rather slow process, compared to the previously described steps (receptor activation below 100 ms, G-protein activation below 1 s). Whether the interaction between the G-proteins and ACs or the generation of cAMP by the ACs is the limiting step in this pathway remained unclear.

The pharmaceutical industry has used bioluminescence-based cAMP assays in uHTS-applications (ultra high-throughput screening) (Wunder et al., *Mol. Pharmacol.* 2008). These assays show very high sensitivity in comparison to the classical cAMP detection methods and also allow kinetic investigation of cAMP levels. Being screening assays, they do not allow observation in single cells, though. During these studies, collaboration with Dr. Frank Wunder (Bayer Research Center, Wuppertal) was established, as these assays provided tools for the fast characterisation of the AC-constructs.

1.6 Aim of this study

Most parts of the signalling pathway from GPCRs to cAMP regulation had already been investigated with high temporal resolution. However, the direct interaction between G-proteins and their effectors has not been studied in such detail. Research on ACs has been limited to steady-state assays and interaction dynamics of G-proteins and ACs remained elusive. This study was designed to develop a FRET-based assay to dynamically investigate the interaction between AC5 and different G-protein subunits in living cells. The FRET-technique was chosen, because it combined high temporal resolution with the possibility to measure the interaction in living cells. This allows biochemical investigation of the G-protein/AC-interaction *in vivo* and also complements the already available microscopic methods for the signalling pathway from GPCR to second messenger. Most available assays to analyse cAMP generation cannot properly resolve Gi-protein-dependent regulation of ACs. The new assay was therefore especially intended to investigate Gi-protein/AC-interaction in combination with existing FRET-based cAMP-assays. There were also previous unexplained reports on the high sensitivity of cAMP-dependent over Gi-protein-dependent pathways (Li et al., *J. Gen. Physiol.* 1994). Furthermore, AC5 had been reported to be selectively regulated through dopamine D3 receptors (Robinson and Caron, *Mol. Pharmacol.* 1997). In combination, both effects hinted at a high sensitivity of ACs towards Gi-protein-mediated inhibition. However, these investigations had been based on readouts downstream of Gi-protein and AC5. Using the new assay, this study aimed to reveal potential mechanisms underlying the high sensitivity through investigating the molecular interaction of the two signalling partners.

2 Material and Methods

The sections 2.2.4, 2.2.5, 2.2.6 and 2.2.7 of this chapter are also part of the author's own manuscript, which is under revision at the *Biochemical Journal* (BJ2013/0554) at the time of this publication.

2.1 Material

2.1.1 Enzymes

Enzymes for the Gateway cloning system were purchased from Invitrogen. Restriction enzymes and ligase were purchased from NEB (New England Biolabs) or Fermentas, as well as the polymerases Vent, Pfu and Taq. Further polymerases were purchased from Biozyme (Phusion) or Peqlab (Kappa-HiFi).

2.1.2 Antibodies (Western-Blot and immunofluorescence)

antibody	supplier	target	clonality	dilution	experiment	antibody species
A cyclase V/VI (C-17)	Santa Cruz (SC-590)	AC5	poly	1:100-1:500	WB/IF	rabbit
A cyclase V (P-20)	Santa Cruz (SC-74301)	AC5	poly	1:100	WB	goat
HA.11 Clone 16B12	Covance (MMS-101P)	HA-tag	mono	1:500	WB/IF	mouse
anti-actin clone C4	Merck Millipore (MAB1501)	actin	mono	1:100,000	WB	mouse
anti-GFP	Rockland (600-101-215)	GFP	poly	1:200	WB	goat
HRP-linked anti-mouse	Vector Laboratories (PI-2000)	primary AB (anti-mouse)	poly	1:4,000	WB	horse
HRP-linked anti-rabbit	Vector Laboratories (PI-1000)	primary AB (anti-rabbit)	poly	1:4,000	WB	goat
HRP-linked anti-goat	Vector Laboratories (PI-9500)	primary AB (anti-goat)	poly	1:4,000	WB	horse
DyLight 650 linked anti-mouse	Thermo Scientific (84545)	primary AB (anti-mouse)	poly	1:200	IF	goat
DyLight 650 linked anti-rabbit	Thermo Scientific (84546)	primary AB (anti-rabbit)	poly	1:200	IF	goat

Table 1: Antibodies used in this studies

2.1.3 Oligonucleotides

Oligonucleotides ("primers") for the Gateway-Cloning System were designed according to the manufacturer's protocol and with the help of Invitrogen's Vector NTI Software Suite (at the time of the primer design the software was free for academic users).

2.1.4 Plasmids

The following plasmids were either already published and available in the lab or were bought from the specified manufacturer.

plasmid	species[1]	origin or published	vector
YFP-hAC5	human	Carmen W. Dessauer (University of Texas, Houston, Texas)	pcDNA3
AC2	rat	Viacheslav O. Nikolaev (Würzburg)	pcDNA3
AC4	mouse	Viacheslav O. Nikolaev	pcDNA3
AC6-CFP	dog	Viacheslav O. Nikolaev	pcDNA3
Epac1-camps	human	Viacheslav O. Nikolaev (Nikolaev et al., *J. Biol. Chem.* 2004)	pcDNA3
pcDNA3		Invitrogen	pcDNA3
$G\alpha_{i1}$ C351I	rat	(Wise et al., *Biochem. J.* 1997)	pcDNA3
$G\alpha_{i1}$-YFP C351I	rat	(Bünemann et al., *Proc. Natl. Acad. Sci. U. S. A.* 2003)	pcDNA3
$G\alpha_{i1}$-CFP C351I	rat	Cloned analogous to $G\alpha_{i1}$-YFP	pcDNA3
$G\beta_1$	human	(Bünemann et al., *Proc. Natl. Acad. Sci. U. S. A.* 2003)	pcDNA3
$G\beta_1$-Cer	human	(Frank et al., *J. Biol. Chem.* 2005)	pcDNA3
$G\gamma_2$	bovine	(Bünemann et al., *Proc. Natl. Acad. Sci. U. S. A.* 2003)	pcDNA3
$G\gamma_2$-CFP	bovine	(Bünemann et al., *Proc. Natl. Acad. Sci. U. S. A.* 2003)	N1-eCFP (Clontech)
$G\alpha_s$	rat	(Hein et al., *J. Biol. Chem.* 2006)	pcDNA1, subcloned to pcDNA3
$G\alpha_s$-YFP	human	(Hein et al., *J. Biol. Chem.* 2006)	pcDNA1, subcloned to pcDNA3
$G\alpha_s$-Cer	human	Cloned analogous to $G\alpha_s$-YFP	pcDNA1, subcloned to pcDNA3
$G\alpha_q$	mouse	(Hughes et al., *J. Biol. Chem.* 2001)	pcDNA3
$G\alpha_q$-YFP	mouse	(Hughes et al., *J. Biol. Chem.* 2001)	pcDNA3
$G\alpha_q$-CFP	mouse	Cloned analogous to $G\alpha_q$-YFP	pcDNA3
$G\alpha_0$-YFP	rat	(Hommers et al., *J. Biol. Chem.* 2010)	pcDNA3
α_{2A}-AR (HA-tagged)	mouse	(Bünemann et al., *Proc. Natl. Acad. Sci. U. S. A.* 2003)	pcDNA3
α_{2A}-AR-YFP	mouse	(Krasel et al., *J. Biol. Chem.* 2005)	pcDNA3
β_2-AR[2]	human	(Krasel et al., *J. Biol. Chem.* 2005)	pcDNA3
M_2-AChR	human	(Roseberry et al., *Mol. Pharmacol.* 2001)	pGES

M_3-AChR	human	Obtained from Missouri S&T cDNA Ressource Center (www.cdna.org)	pcDNA3
A_{2A}-AdoR	human	(Hein et al., *J. Biol. Chem.* 2006)	pcDNA3
RGS4 (HA-tagged)	rat	Moritz Bünemann derived from (Doupnik et al., *Proc. Natl. Acad. Sci. U. S. A.* 1997)	pcDNA3
mGFP-10-sREACh-N3		addgene.org (#21947) (Murakoshi et al., *Brain Cell Biol.* 2008)	mGFP-C1 (Clontech)
YFP*-β_2-AR-CFP(2)	human	Sandra Dorsch (Dorsch et al., *Nat. Methods* 2009)	pcDNA3
CD86-YFP	human	(Dorsch et al., *Nat. Methods* 2009)	pcDNA3
membrane associated YFP(3)		(Hein et al., *EMBO J.* 2005)	pcDNA3
membrane associated CFP(3)		cloned analogous to membrane associated YFP	pcDNA3
TurboFP635 ("Katushka")(4)		Evrogen FP722 (Shcherbo et al., *Nat Methods*)	Clontech-N-like

Table 2: Plasmids used during this study

(*1*) No species is indicated for fluorescent proteins and empty vector. (*2*) Plasmid contains polymorphisms 16-Arg, 27-Gln and 164-Thr. (*3*) Membrane anchor sequence: MGCINSKRKD. (*4*) "Katushka" is not derived from GFP and will not be detected by antibodies against GFP.

2.1.5 Cell culture media

Cell culture media and supplements were obtained from PAA (Pasching, Austria). The normal culturing medium was Dulbecco's Modified Eagle Medium (DMEM) with 4.5 g/L glucose, 10 % (v/v) fetal calf serum, 2 mM L-glutamine, 100 U/mL penicillin and 0.1 mg/mL streptomycin.

2.1.6 Software

The following software was used for the assigned purposes:

- Plasmid sequences, alignments
  - VectorNTI (Invitrogen)
  - ApE – A plasmid Editor (http://biologylabs.utah.edu/jorgensen/wayned/ape/)
  - Serial Cloner (http://serialbasics.free.fr/Serial_Cloner.html)
- Data analysis and statistics
  - Microsoft Excel 2007 or newer
  - GraphPad Prism 5
  - OriginLabs OriginPro 8 and 9
- Picture/Image analysis and modification (cropping, range-adjusting, overlay)
  - ImageJ 1.46r (http://imagej.nih.gov/ij/)
  - Corel Photo-Paint X4
- Figure optimisation for publishing

- CorelDraw X4

Image acquisition on microscopes and the ChemiDoc (imaging-system for gels) was performed with the supplied software on the individual setups. Images were saved as Tiff or JPG to allow further analysis with ImageJ or Photo-Paint.

2.2 Methods

All buffers used in the following protocols are listed in section 2.2.8.

2.2.1 Molecular biology

2.2.1.1 Generation of competent E. coli

Competent *E. coli* for plasmid production were prepared following a protocol modified from that published by Chung et al. (Chung et al., *Proc. Natl. Acad. Sci. U. S. A.* 1989).

1. Plate bacteria on LB-agar and incubate overnight
2. Pick a colony and grow bacteria in 10 mL LB-broth overnight (50 mL Falcon tube)
3. Give 5-10 mL of suspension into a final volume of 250 mL LB-broth and grow to an OD600 of 0.3-0.6. This will typically take 1.5 to 4 h.
4. Harvest bacteria by centrifugation at 5000 rpm and 4 °C for 10 min; resuspend gently in 25 mL ice-cold TSB
5. Incubate for 1-2 h on ice
6. Aliquot, freeze in liquid nitrogen and store at -80 °C

2.2.1.2 Transformation of E. coli

1. Thaw bacteria on ice. When completely thawed, mix

amount	ingredient
20 µL	5x KCM-buffer
80 µL	water
2 µL	DNA
100 µL	competent cells

2. Incubate 20 min on ice
3. Incubate 10 min at RT
4. Add 1 mL LB-broth
5. Incubate 50 min shaking at 37 °C
6. Optional: centrifugate for 30-60 s and resuspend in 50-200 µL LB-broth
7. Plate 60-100 µL of 5. on ampicillin-containing LB-agar and incubate overnight

2.2.1.3 Plasmid preparation

Medium-scale plasmid preparations ("Midi-Prep") were carried out using Qiagen's Plasmid Midi Kit according to manufacturer's protocol with 100 mL of bacteria-suspension grown overnight.

Small-scale plasmid preparations ("Mini-Prep") for control purposes were performed from 1.5 of 4 mL overnight suspension. The buffers P1, P2 and P3 from the Plamid Midi Kit (Qiagen) were used here as well. All centrifugation steps are performed in a desktop centrifuge for reaction tubes at maximum speed.

1. Centrifuge 1.5 mL suspension for 20 s to sediment the cells; discard the supernatant
2. Resuspend pellet in 300 µL buffer P1
3. Add 300 µL buffer P2, mix and incubate 5 min at room temperature (RT)
4. Add 300 µL buffer P3, mix well and centrifuge for 15 min at 4 °C
5. Transfer 800 µL supernatant to a new reaction tube, add 750 µL n-propanol, mix and centrifuge for 15 min at 4 °C
6. Remove supernatant carefully, dry the pellet and solve in 50 µL water

The resulting DNA might not be pure enough for some further cloning steps (esp. digestion with EcoRI). In that case the plasmid-DNA should be cleaned further using a small column (e.g. from Qiagen's QIAquick Gel Extraction Kit).

2.2.1.4 Polymerase chain reaction (PCR)

amount	ingredient
x µL	template (1-5 ng)
2 µL	buffer 10x
2 µL	dNTP mix (2 mM each)
1 µL	forward primer (10 µM)
1 µL	reverse primer (10 µM)
ad 20 µL	water
0.5-1 µL	polymerase (Phu, Vent, Taq, Phusion, Kapa-HiFi)

- The actual programming of the thermocycler needs to be adapted to the primers, template-size and the polymerase (according to manufacturer's protocol).

2.2.1.5 Agarose gel electrophoresis

In this study only gels of 1 % (m/v) agarose in TAE buffer were used. The agarose can only be dissolved, if the buffer is warmed. To allow UV-light detection of the DNA, ethidiumbromide (2 µL of a 10 mg/mL solution, Promega) was pipetted into the chamber immediately before pouring the warm gel-solution into the chamber.

2.2.1.6 Cloning of plasmids

2.2.1.6.1 xFP-labelled adenylyl cyclases

The 3-fragment MultiSite Gateway Pro system (Invitrogen) was used to clone fluorescently labelled ACs. Using the ACs as the insert for the second/middle fragment, it was possible to easily add different fluorophores to either terminus. Primer-design was carried out according to the manufacturer's protocol with the help of the software Vector NTI (Invitrogen, at that time free for academic users). To increase the linkers flexibility, four additional aminoacids were added. All the reactions were carried out according to the manufacturer's manual, but the size of each reaction was reduced by 50 % to save enzymes. Several so-called entry-clones were generated or provided (Table 3). Some entry clones and the empty vectors were provided by Sabine Merkle and Prof. Dr. Stefan Engelhardt. Further fluorescent entry clones were cloned. The final construct was recombined from the entry clones into the expression vector pT-RExT-DEST30. The amino acid sequence linking YFP and the ACs is AGAGHPTFLYKVA. The C-terminal linker contains the Stop-codon and has the amino acid sequence TTLYNKVV*.

name	insert[1]	fragment	cloned by
Entry 5.11	AC5	2/middle	me
Entry 2.6	AC2	2/middle	me
Entry 4 #5	AC4	2/middle	me
Entry 6 #7	AC6	2/middle	me
	Katushka	1/N-term.	me
Entry DY.2	sREACh	1/N-term.	me
Entry YFP 1/4	YFP*[2]	1/N-term.	Monika Frank
Entry CFP 1/4	CFP	1/N-term.	Monika Frank
Entry Cer 1/4	Cer	1/N-term.	Monika Frank
Entry YFP 3/2	YFP*	3/C-term.	Monika Frank
Entry CFP 3/2	CFP	3/C-term.	Monika Frank
Entry Cer 3/2	Cer	3/C-term.	Monika Frank
Spacer 1-4	none[3]	1/N-term.	Sabine Merkle, Stefan Engelhardt
Spacer 3-2	none[4]	3/C-term.	Sabine Merkle, Stefan Engelhardt

Table 3: Entry-Clones generated or used in the Gateway cloning system

The table lists all the fragments generated or used during the cloning of fluorescent AC-constructs. The numbers in the names refer to the flanking recombination sites, which show the order 1-4-3-2. Accordingly the second or middle fragment is flanked by the sites 4 (N-terminus) and 3 (C-terminus). (*1*) N-terminal and middle fragments do not contain a Stop-codon. All the middle constructs contain a Start-Codon, though. (*2*) YFP* is an eYFP-variant: eYFP(F46L/L68V) (Start-codon not counted!). (*3*) This fragment does not contain any coding sequence. The Start-codon of the second fragment is used to start translation in this case. (*4*) This fragment only codes for a Stop-codon, positioned directly after the recombination site no. 3.

The constructs generated using this system are listed in the results section (Table 5).

2.2.1.6.2 wild-type human AC5 in pcDNA3

Dr. Carmen W. Dessauer (University of Texas, Houston) had kindly provided pcDNA3-YFP-hAC5. From this construct pcDNA3-hAC5 was cloned by standard restriction and ligation protocols (see below). The sites used were BamHI, NotI and XbaI.

2.2.1.7 Basic protocols for restriction and ligation

2.2.1.7.1 Restriction

amount	ingredient
1-2 µg	plasmid
0.5 µL	per enzyme
2 µL	buffer 10x (according to enzyme)
0.2 µL	BSA 100x (according to enzyme)
ad 20 µL	water

- Incubate for 60 min at 37 °C
- Separate with agarose gel electrophoresis
- Optional: clean plasmid fragment from gel using the Gel Extraction Kit (Qiagen)

2.2.1.7.2 Ligation

amount	ingredient
0,5-1 µL	ligase
1 µL	buffer 10x
	vector*
	insert*
ad 10 µL	water

*The amounts used vary depending on the size of vector and insert, the concentration of the respective solutions and the backbone/insert-ratio.

- Incubate for 1-2 h at RT or at 14-16 °C over night
- Transform into competent bacteria

2.2.2 Biochemical approaches

2.2.2.1 Western-Blotting

The following protocol was derived from a general protocol available in the lab. The initial source remains unknown, though. The actually used antibodies are described in the results section at the according blots.

HEK293T cells were transiently transfected as described in section 2.2.3 but instead of splitting the cells onto cover slips they were transferred to 10 cm culture dishes and incubated for another 24 h. The medium was removed and the dishes immediately frozen at -80 °C.

2.2.2.1.1 Lysate preparation (whole-cell lysates)

1. Thaw dishes on ice, add 1 mL of lysis buffer
2. Scrap cells, resuspend in the buffer and transfer to reaction tube
3. Homogenise suspension for 30 s with the Ultra-Turrax (Model IKA T10 basic)
4. Determine the amount of protein with Bradford's reagent
    a. Optional: adjust the samples with lysis buffer to equal amounts of protein
5. Add 5x sample buffer
6. Heat samples to 95 °C for 15 minutes

These lysates can be stored in the fridge for a few days.

2.2.2.1.2 Lysate separation, blotting and detection

1. Separate the lysates on 10 % SDS-PAGE (topped with a 3.5 % collection gel)
    a. 30 min at 60 V, then 100-120 V
2. Wet PVDF membrane (Roche) in methanol, store in transfer buffer until sandwich with gel is built
3. Transfer the proteins to PVDF membrane with either wet or semi-dry blotting. Wet blotting tends to transfer the proteins better to the membrane, especially larger proteins
    a. Caution: The stacking order is different for both methods, the transfer buffers contain different amounts of methanol
    b. Semi-dry: 60 min at 15 V; performed at RT
    c. Wet: 2 h at 200 mA, then 18 h at 20 mA; performed at 4 °C

The following steps are performed on desktop shakers.

4. Incubate with "milk" for 1 h at RT to block the membrane
    a. Some antibodies might need special sera to be incubated in. In this case the membrane is blocked with the same solution as used to dilute and incubate the antibody.
5. Incubate with primary antibody (diluted in "milk") over night at 4 °C
6. Incubate 1 h at RT
7. Wash with TBST (3x 5 min)
8. Incubate with secondary HRP-labelled antibody (diluted in "milk") for 1 h
9. Wash with TBST (3x 15 min)
10. Incubate in HRP detection solution (e.g. HRP-Juice PLUS, PJK) and detect bioluminescence with the Chemidoc system (BioRad).

The membrane can be stripped and used for another antibody-detection. This procedure does not completely remove the already used primary antibodies, though. These steps are also performed on a shaker.

11. Optional: Wash membrane with water (5 min)
12. Incubate with stripping buffer for 5-15 min

13. Wash with PBS (purchased from PAA) and TBST (5 min each)
14. Continue from point 4. (blocking)

2.2.2.2 Immunofluorescence

1. HEK293T cells were transfected and transferred to cover slips as described in section 2.2.3.
2. Remove medium
3. Wash cover slips with PBS (2x)
4. Incubate with paraformaldehyde (4 % in PBS) for 30 min at RT
5. Wash with PBS (3x)
6. Block for 1 h (5 % FCS in PBS)
7. Wash with PBS
8. Incubate with primary antibody (diluted in blocking solution, see above)
9. Wash with PBS (3x 5 min)
10. Incubate with secondary antibody (fluorescently labelled) for 1 h (diluted in blocking solution)
11. Wash with PBS (3x 5 min)

2.2.3 Cell culture and transfections

HEK293T cells were passaged every 2-3 days and cultured on 10 cm dishes. HEK293T cells were transfected using Effectene transfection reagent (Qiagen) according to the manufacturer's protocol. In general two different transfection procedures were used. Initially a 3-day protocol (mainly in the experiments involving Gs-proteins) was applied, but was switched to a 4-day protocol in the later experiments. It was observed that the cells transfected with Gs-proteins become round and die, possibly because of some endogenous activity of the pathway. Performing transfections according to the 3-day protocol reduced this effect. In contrast to this, the cells transfected with Gi-protein-involving pathways tolerate the 4-day protocol and show better membrane expression of YFP-AC5. The 4-days protocol also improved RGS4 expression in the later experiments.

3-day protocol	
day	step
1, morning	passage cells from 10 cm to 6 cm dish (usually 0.75-1.0 mL of 10 mL suspension)
1, evening	replace medium and transfect cells
2, morning	stop transfection (i.e. change medium)
2, evening	split cells onto cover slips(2)
3	measurement

4-day protocol	
day	step
1, morning	passage cells from 10 cm to 6 cm dish (usually 0.3-0.5 mL of 10 mL suspension)
2, morning	replace medium and transfect cells
2, evening	stop transfection (i.e. change medium)(1)
3, evening	split cells onto cover slips
4	measurement

Table 4: Transfection protocols

The 10 cm dish used on day 1 was about 80 % confluently grown with cells. (*1*) To prevent serum-derived stimulation of α_{2A}-AR yohimbine (100 nM) was added to the medium from this point onwards. (*2*) Cover slips should be coated with poly-L-lysine to increase adherence of the cells.

2.2.4 Fluorescence microscopy

2.2.4.1 FRET-microscopy in single living cells

FRET-measurements of transiently transfected HEK293T cells were performed about 48-54 h after transfection at room temperature using an inverted microscope (eclipse Ti, Nikon) equipped with a 100x oil immersion objective (Plan Apo VC 100x/1.40 Oil ∞/0.17 Dic N2, Nikon). A fast switching, xenon arc-based illumination system (Lambda DG-4, Sutter Instrument) was used as light source. The following filters (all Chroma) were used: ET 430/24x (CFP excitation) or ET 500/20x (YFP excitation), T455LP (long-pass beamsplitter to collect combined fluorescence of CFP and YFP) or CFP/YFP-beamsplitter plus CFP/YFP emission filter (Cat.No. 59017bs and 59017m), z488/800-1064rpc (beamsplitter to separate CFP and YFP emission), ET 480/40 (CFP emission) and HC 534/20 (YFP emission). The last three components were set in an Optosplit II (Cairn Research) to simultaneously record CFP and YFP fluorescence using a fast CCD camera (Evolve512, Roper Scientific). Microscope, camera and DG-4 were controlled using NIS-Elements AR (laboratory Imaging). In order to synchronise camera and lamp an additional trigger-box was supplied by Nikon. Cells were continuously superfused with buffer (see section 2.2.8.1) or buffer containing agonist in

different concentrations using a fast-switching 8 channel valve-controlled pressurised perfusion system with solenoid valves (Ala-VC³-8SP, Ala Scientific Instruments). For FRET-measurements CFP and YFP emission were recorded simultaneously while cells where excited with 430 nm. Depending on the fluorescence intensity, the illumination time was set to 20-40 ms at an interval of 500 ms or 2 s in the Epac1-camps experiments. Some of the kinetic experiments were performed at a sampling rate of 33 Hz. This is indicated in the respective figures. The lamp was set to lowest intensity to prevent bleaching. Cell fluorescence was recorded at 488 ± 20 nm (F_{488} for CFP) and 534 ± 10 nm (F_{534} for YFP) and corrected for background fluorescence, resulting in F_{CFP} and F_{YFP}. To determine FRET, F_{YFP} was additionally corrected for bleed-through of CFP fluorescence into the F_{534}-channel and direct excitation of YFP at 430 ± 12 nm excitation was subtracted (refer to section 2.2.4.5 for a detailed description of this). The resulting fluorescence was divided by F_{CFP} and $\frac{F_{YFP}}{F_{CFP}}$ is referred to as "FRET-ratio". In the course of this work, ratio-traces will usually be presented by themselves, but it was verified that all changes in FRET-ratio were accompanied by opposing movements of the individual fluorescence traces.

2.2.4.2 Donor recovery after acceptor photobleaching

Cells were kept in buffer without agonist during the bleaching process. Making use of the CFP/YFP-filters described above we collected CFP fluorescence during a 6 minute bleaching process for YFP. Fluorescence was recorded every 5 s. Between recordings the lamp was set to permanent YFP excitation (500 ± 10 nm) at the highest possible intensity to bleach the FRET-acceptor. The relative F_{CFP} change before ($F_{CFP,0}$) and after bleaching (F_{CFP}) was evaluated as $\frac{F_{CFP}-F_{CFP,0}}{F_{CFP,0}}$.

2.2.4.3 Quantification of relative expression levels by means of fluorescence

We used the previously published construct YFP-β_2-AR-CFP (Dorsch et al., *Nat. Methods* 2009) for calibration of the stoichiometry of relative expression levels of CFP and YFP. This construct bears the same fluorophores used in YFP-AC5 and $G\alpha_{i1}$-CFP, which allows for fluorescence comparison. The fluorescence intensities for both fluorophores, individually excited, were recorded and corrected for background fluorescence. F_{CFP} was divided by F_{YFP} to calculate the calibration factor. To calculate the individual expression ratio, the F_{CFP}/F_{YFP}-ratio of the Gαi/AC5-FRET cells was

measured similarly and was divided by the calibration factor to determine the amount of $G\alpha_{i1}$-CFP overexpression over YFP-AC5.

2.2.4.4 Immunofluorescence and confocal microscopy

Immunofluorescently labelled cells were imaged using an epifluorescence microscope (Leica DMI 6000B with a Leica DFC360 FX camera). Confocal pictures were acquired with a Leica SP5 confocal microscope using excitation wavelength of 405 nm (laser diode) and 514 nm (Ar-laser).

2.2.4.5 Correction factors

As mentioned in the introduction, FRET will only occur, if the excitation spectrum of the acceptor fluorophore will overlap with the donor's emission spectrum. The spectra usually do not follow Gaussian curves and therefore spectral crosstalk between the fluorophores will be observed in varies degrees. "Tailing" of donor emission into the channel used to detect acceptor emission is referred to as "bleed-through". Furthermore, acceptor excitation by wavelengths intended to excite the FRET-donor is termed "false excitation", because in this case the acceptor's fluorescence is not occurring through FRET from the donor. Figure 7 depicts the excitation and emission spectra of CFP and YFP, respectively.

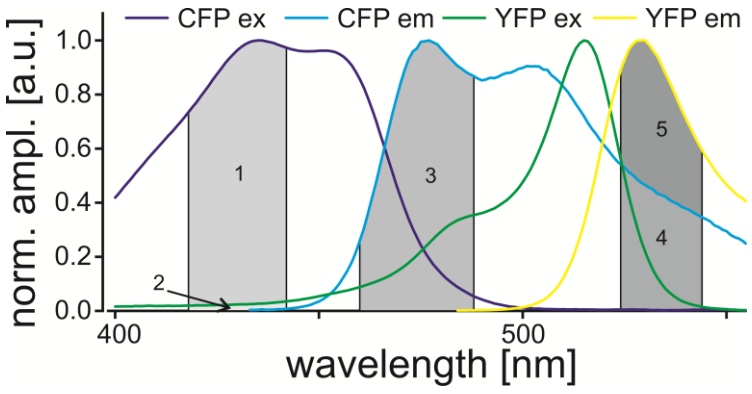

Figure 7: Excitation and emission spectra of fluorescent proteins

This shows the normalised excitation (ex) and emission (em) spectra for the cyan and yellow fluorescent protein, respectively. The grey fields indicate (*1*) CFP excitation, (*2*) YFP false excitation and (*3*) CFP emission recorded. The recorded YFP emission consists of (*4*) CFP bleed-through into the channel intended to record YFP fluorescence and (*5*) YFP fluorescence induced by FRET. (All fields are indicated according to the filters installed on the Nikon microscope; refer to section 2.2.4.1 for further details).

To allow for the correction of the spectral cross-talk, the following factors have to be measured. Because they are influenced by the spectrum of the light-source, as well as

e.g. filters and lenses, they have to be determined, if the bulb or any other components in the light-path have been changed.

2.2.4.5.1 CFP fluorescence bleed-through into F_{534}-channel

HEK293T cells are transiently transfected with only one CFP-containing plasmid (e.g. membrane associated CFP). Cells are measured on the microscope as described in section 2.2.4.1 for the actual FRET experiments. F_{488} and F_{534} are recorded and corrected for background fluorescence. The correction factor for bleed-through is calculated by dividing F_{534} by F_{488}. At the time of this study, this factor was about 0.4 (Nikon-Setup with DG4).

2.2.4.5.2 False excitation of YFP at 430 ± 12 nm

HEK293T cells are transfected with an YFP-containing plasmid. The fluorescence F_{534} is recorded for excitation at 430 ± 12 nm (filter setting 455LP) and 500 ± 10 nm (filter setting CFP/YFP dual band filter). Both F-values are corrected for background and $F_{534(430)}$ is divided by $F_{534(500)}$. The according value was in the range of 0.05 at the time of this study.

2.2.5 Electrophysiology

The according experiments were performed by Dr. Andreas Rinne in a collaborative effort.

Patch pipettes (resistance 2 MΩ to 5 MΩ) were manufactured using borosilicate glass capillaries (GL150F-10, Havard Apparatus) with a horizontal pipette puller (P87, Sutter Instruments). During experiments, cells were continuously superfused with extracellular buffer consisting of (in mM): KCl 20, NaCl 122, $MgCl_2$ 1, $CaCl_2$ 0.5 and HEPES 10 (pH 7.4 with NaOH). The intracellular solution was composed of (in mM): K^+-aspartate 100, KCl 40, NaCl 5, $MgCl_2$ 7, EGTA 2, GTP 0.25, Na^+-ATP 5 and HEPES 20 (pH: 7.2 with NaOH). G-protein-activated inwardly rectifying K^+ (GIRK) channels of HEK293T cells expressing α_{2A}-AR and GIRK1/4-subunits were activated by application of NE-containing solutions. Corresponding whole-cell GIRK currents were recorded in the inward direction (V_{hold}: -90 mV, calculated EK: -48 mV) using an EPC 7 amplifier with an ITC-16 interface and Patchmaster software v2.52 (all HEKA). To identify GIRK currents, background-subtracted I/V-relationships were obtained by applying fast voltage ramps (-120 mV to +60 mV within 500 ms) in the absence and presence of NE.

2.2.6 Bioluminescence-based cAMP-assay

The assay has been described before (Wunder et al., *Mol. Pharmacol.* 2008) and was performed in a collaborative effort with Dr. Frank Wunder at Bayer Research Center in Wuppertal. In general, this assay uses aequorin with its cofactors coelenterazine and Ca^{2+} to generate bioluminescence. The activation of ACs results in an increase in cAMP, which in turn opens CNG-channels (cyclic nucleotide-gated channels). Subsequently Ca^{2+} can enter the cells, which are kept for a brief period in Ca^{2+}-free tyrode. The CNG-channel is opened according to the amount of generated cAMP, hence increasing amounts of cAMP will result in a higher portion of open channels, which in turn increases the Ca^{2+}-influx and yields higher bioluminescence.

2.2.7 Data analysis and statistics

All FRET-recordings were corrected for photobleaching by subtracting a monoexponential baseline using OriginPro (OriginLab), unless stated otherwise. Signal amplitudes were calculated as agonist-induced alteration of the FRET-signal ($\Delta(F_{YFP}/F_{CFP})$). As the Gαi/AC5-FRET recordings could not be fitted properly to simple exponential equations, we determined $t_{0.5}$-values directly from the traces. In all cases $t_{0.5}$ was determined as the time to reach half of the maximally evoked FRET-amplitude after agonist exposure or withdrawal. Application of saturating concentrations of NE resulted in an additional increase in the FRET-ratio of the Gαi/AC5-FRET after agonist withdrawal before recovering to baseline as seen for example in Figures 18, 20 and 24. Interestingly, this transient increase resulted in a comparable amplitude as the FRET-change of the highest concentration that did not show this effect (usually a concentration below 10 nM NE). Increasing concentrations of NE reduced the actual amplitude of the agonist-induced FRET-increase, but did not affect the total amplitude of the transient (compare to Figure 24). We therefore hypothesised an inhibitory effect of the receptor as previously reported (Hommers et al., *J. Biol. Chem.* 2010). In order to avoid contribution of this unknown inhibitory component in the concentration-response experiments, we measured the peak value of this transient as the total amplitude of the agonist-induced FRET-change at the given concentration. Most likely because of desensitisation effects we sometimes observed an additional reduction of the total amplitude for 1 µM NE in the Gαi/AC5-FRET, resulting in bell-shaped concentration-response curves (Figure 24). In those experiments we normalised to the next lower concentration and omitted the 1 µM NE-value during sigmoidal fitting.

To quantify Western-Blots Tiff-images acquired with the ChemiDoc were analysed using ImageJ (1.46r; http://imagej.nih.gov/ij/). A rectangular-shaped region of interest was placed on each band and raw intensities were measured. An additional region of interest of the same size was placed over an empty part of each band to allow for background correction. The obtained intensity values were analysed with Excel 2010 (Microsoft Corporation).

Statistics were obtained using GraphPad Prism and OriginPro by t-test or ANOVA with post-hoc tests as indicated in the individual figure legends.

2.2.8 Buffers

Where buffers were prepared in water, ultra-filtered water (Ultra Clear UV plus, Reinstwassersystem; SG Wasseraufbereitung, Barsbüttel, Germany) was used, as this was the highest quality available in the lab. The quality is comparable to double distilled water.

PBS was purchased from PAA.

This section lists x-fold stock solutions for some buffers. Unless otherwise specified, the according working solutions (1x solutions) were used in the actual experiments.

2.2.8.1 "FRET" buffer

amount	ingredient
137 mM	NaCl
5.4 mM	KCl
10 mM	HEPES
2 mM	$CaCl_2$
1 mM	$MgCl_2$
	water

– adjust pH to 7.4!

2.2.8.2 LB-broth and LB-agar (bacterial media)

amount	ingredient
1.0 %	Peptone
0.5 %	yeast extract
1 %	NaCl
	water

- for agar-preparation add 1.5 % agar
- autoclave medium
- The powdered ingredients can be purchased as premixed bulk (e.g. from AppliChem). The mix is often cheaper than the individual ingredients.

2.2.8.3 TSB (transformation and storage buffer) for competent bacteria

amount	ingredient
10 % (m/v)	PEG 3000
5 % (v/v)	DMSO
20 mM	$MgSO_4$ or $MgCl_2$
	LB-broth

- filter sterile
- if desired store at -20 °C

2.2.8.4 5x KCM buffer (for transformation of competent bacteria)

amount	ingredient
500 mM	KCl
150 mM	$CaCl_2$
250 mM	$MgCl_2$
	water

2.2.8.5 50x TAE buffer (agarose gel electrophoresis)

amount	ingredient
242 g	Tris (base)
57.1 mL	glacial acetic acid
10 mL	EDTA (0.5 M, pH 8) (see below)
ad 1 L	water

2.2.8.6 0.5 M EDTA

amount	ingredient
35 g	EDTA (water-free)
~4 g	NaOH
ad 200 mL	water

- adjust pH to 8.0 with NaOH
- EDTA will not dissolve until the pH is in the range of 8.0

2.2.8.7 10x Agarose gel loading buffer (by Dr. Joachim Schmitt)

amount	ingredient
40 % (m/v)	glycerol
10 mM	EDTA
10 mM	Tris
0.25 % (m/v)	Orange G
	water

2.2.8.8 Lysis buffer for Western-Blot preparation

amount	ingredient
20 mM	Tris
2 mM	EDTA
1 tablet/10 mL buffer	proteinase inhibitor mix (cOmplete ULTRA Tablets Mini EDTA-free, Roche)
	water

2.2.8.9 Sample buffer (5x) for Western-Blot

amount	ingredient
50 % (m/v)	glycerine
312.5 mM	Tris-HCl
10 % (m/v)	SDS
25 % (m/v)	β-mercaptoethanol
0.1 % (m/v)	brome phenol blue
	water

- store at 4 °C

2.2.8.10 10x Running buffer for SDS-PAGE

amount	ingredient
144 g	glycine
30 g	Tris (base)
10 g	SDS
ad 1 L	water

2.2.8.11 3.5 % collection gel for SDS-PAGE

amount	ingredient
6.2 mL	H_2O
2.5 mL	0.5 M Tris pH: 6.8
0.1 mL	10 % SDS
1.2 mL	30 % Acryl/bis 30 %
0.05 mL	APS 10 %
0.01 mL	TEMED

2.2.8.12 10 % separation gel for SDS-PAGE

amount for 1 gel	ingredient
4 mL	H_2O
2.5 mL	1.5 M Tris pH: 8.8
0.1 mL	10 % SDS
3.3 mL	30 % Acryl/bis 30 %
0.05 mL	APS 10 %
0.01 mL	TEMED

2.2.8.13 Blocking milk for Western-Blot

amount	ingredient
5 % (m/v)	skim milk powder
	TBST

2.2.8.14 Blocking solution for immunofluorescence

amount	ingredient
5 % (v/v)	FCS
	PBS

2.2.8.15 10x TBS (and TBST)

amount	ingredient
292 g	NaCL
24.2 g	Tris (base)
ad 1 L	water

- adjust pH to 7.5

2.2.8.15.1 TBST

1x TBS supplemented with 0.05 % (v/v) Tween 20

2.2.8.16 10x Transfer buffers for wet and semi-dry blotting

amount	ingredient
30 g	Tris (base)
144 g	glycine
ad 1 L	water

- adjust pH to 8.3

1x transfer buffer for semi-dry blotting		1x transfer buffer for wet blotting	
100 mL	10x stock	100 mL	10x stock
100 mL	methanol	200 mL	methanol
ad 1 L	water	ad 1 L	water

2.2.8.17 Stripping buffer for membranes

amount	ingredient
15 g	glycine
1 g	SDS
10 mL	Tween 20
ad 1 L	water

2.2.8.18 Paraformaldehyde (for immune fluorescence)

1. Heat 100 mL PBS to about 70 °C
2. Add 4 g PFA
3. Stir until dissolved
4. Adjust volume back to 100 mL

Filter, store at 4 °C

3 Results

3.1 Generation of fluorescently labelled ACs

In order to investigate the interaction between ACs and G-protein subunits by means of FRET the ACs had to be fluorescently labelled. Lacking detailed structural information from protein crystals it could not be determined, whether intramolecular loops would be suitable for insertion of the fluorescent tags. Therefore the fluorophores were attached to the N- or C-terminus. To clone the fluorescently labelled ACs the 3-Fragment Multisite Gateway Technology (Invitrogen) was chosen. Being a recombination based technique it abolished the need for unique restriction sites and therefore allowed easy addition of the fluorescent proteins to either terminus of the ACs. However, those recombination sites encode for linkers of at least 10 amino acids, including a flexibility-reducing prolin. For compensation, four flexible amino acids were added (see methods section for further details)

Several labelled AC-constructs were generated as listed in Table 5. Functional and/or regulatory impairments of the labelled enzymes, especially of those with C-terminal labels, could not be excluded prior to cloning. The large variety of constructs was cloned to provide enough options for identifying functional ones.

As the constructs are generally built the same way, the representative plasmid maps shown in Figure 8 apply to the other constructs accordingly.

N-terminus	AC	C-terminus	clone name	published as
YFP*[1]	type V	spacer	Y5.9	YFP-AC5
Cerulean			Cer5	
CFP[2]			C5.11	
spacer	type V	YFP*	5Y.6	
		Cerulean	5Cer	
		CFP	5C.1	
TurboFP-635 (Katushka)	type V	spacer	Kat-AC5	
sREACh (“dark YFP”)	type V	spacer	D5.2	sREACh-AC5
YFP*	type VI	spacer	Y6.5	
CFP			C6.3	
spacer	type VI	YFP*	6Y.1	
		Cerulean	6Cer.3	
		CFP	6C.4	
YFP*	type II	spacer	Y2.6	
Cerulean			Cer2.3	
CFP			C2.4	
spacer	type II	Cerulean	2Cer.6	
		CFP	2C.2	
YFP*	type IV	spacer	Y4.2	
CFP			C4.1	
spacer	type IV	YFP*	4Y.1	
		Cerulean	4Cer.1	
		CFP	4C.6	
spacer[3]	all above	spacer	2.6; 4.3; 5.4; 6.2	

Table 5: Constructs cloned using Invitrogen Multisite Gateway Technology

The published constructs are YFP-AC5 (clone Y5.9) and sREACh-AC5 (clone D5.2). The final constructs were not completely sequenced, but all intermediate constructs were verified by sequencing. (*1*) YFP*: eYFP(F46L/L68V) cloned by J. P. Vilardaga. (*2*) CFP: enhanced CFP (eCFP) was used in this study. (*3*) ACs flanked by spacers were generated to obtain “wild-type-like” ACs that have the same additional linker on the C-terminus like the other constructs and are in the same vector backbone. However, these constructs were not used in these studies.

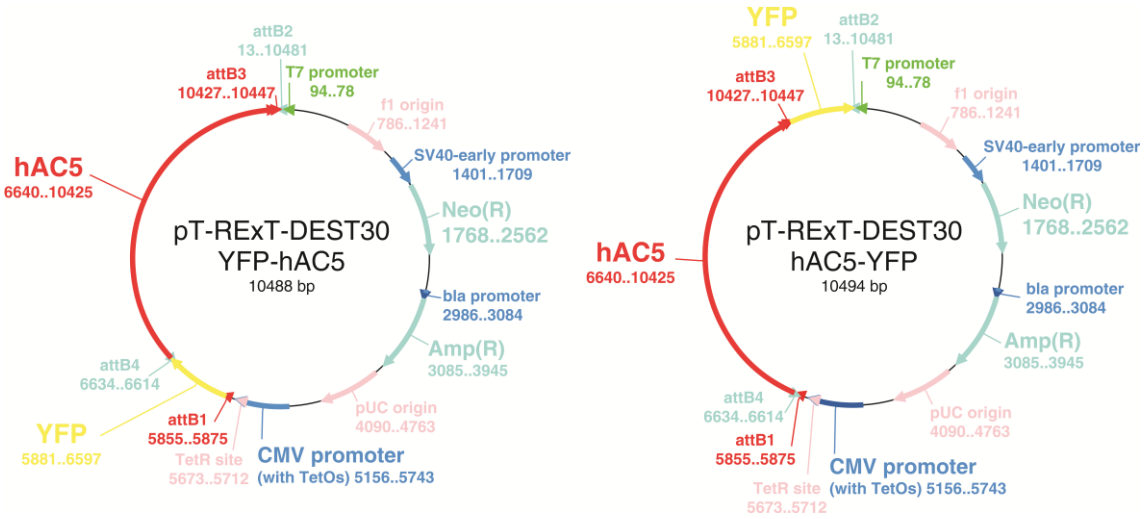

Figure 8: Representative plasmid maps

The maps show the plasmid of YFP-AC5 (left) and AC5-YFP (right). They are representative for the fluorescently labelled AC-constructs listed in Table 5.

In addition to the plasmids mentioned above, AC5-wt in pcDNA3 was cloned. This construct was obtained from the YFP-AC5-construct provided by Carmen W. Dessauer (University of Texas, Houston) and used for control purposes.

3.2 Expression of fluorescent AC-constructs in HEK293T cells

HEK293T cells can be easily transfected with the constructs. Even though transient overexpression of ACs is easy and obviously well tolerated by HEK293T cells, the constructs tend to predominantly localise to intracellular compartments – most likely membranes of the endoplasmic reticulum or Golgi apparatus – especially in cells expressing large amounts of protein. Optimisation of the transfection conditions enhanced cell membrane localisation of YFP-AC5. Cells that expressed lower amounts of tagged protein showed better membrane staining than bright cells expressing large quantities of YFP-AC5 (Figures 9A upper panel and 9B). Epifluorescence images are, however, not optimal to judge membrane localisation, especially if the expression is weak. Therefore, confocal images were acquired, which revealed that the construct localised well to the cell membrane (Figure 9C).

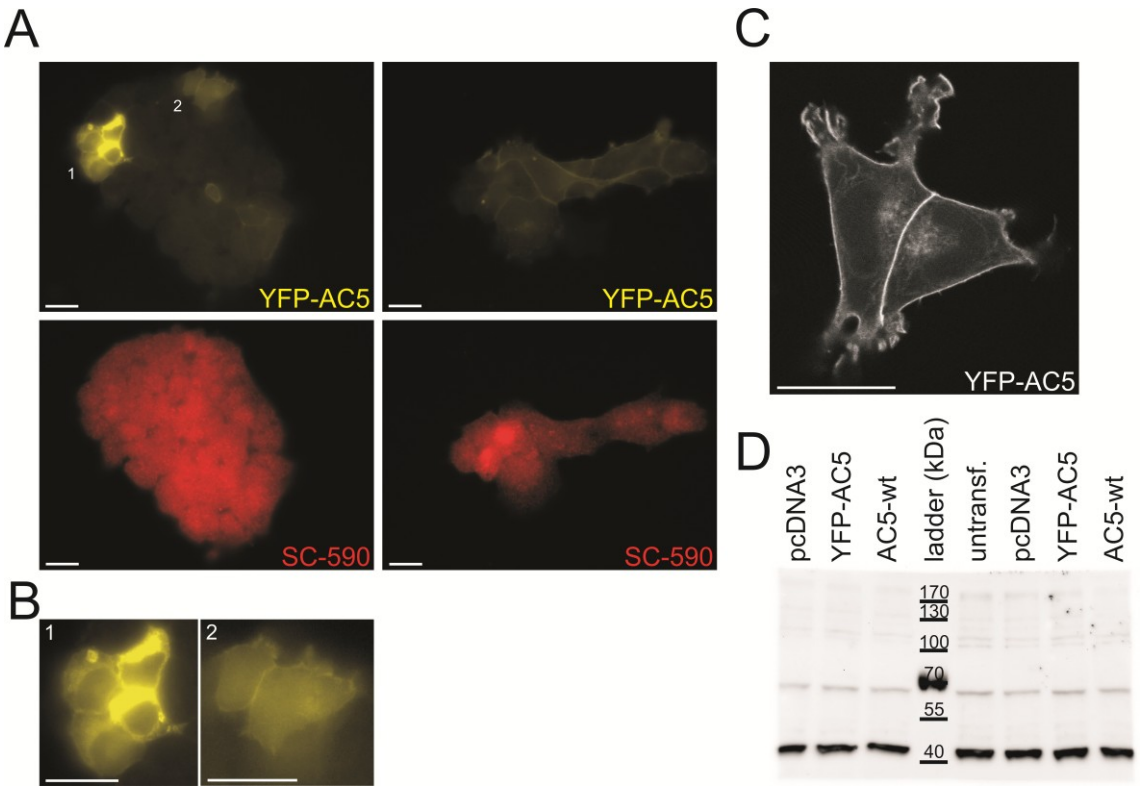

Figure 9: Subcellular localisation of YFP-AC5 and immunological detection of ACs

A to ***C)***: HEK293T cells were transiently transfected with YFP-AC5 and $G\alpha_{i1}$-CFP, as well as unlabelled α_{2A}-AR and $G\beta_1\gamma_2$-subunits. All scale-bars represent 20 µm. ***A)*** Cells were fixated, treated for immunofluorescence staining against ACs as detailed in the methods section and images were acquired with an epifluorescence microscope. YFP-AC5 was excited at 480 ± 20 nm and fluorescence recorded at 527 ± 15 nm (upper panel). The primary antibody against type V and VI ACs (SC-590) was detected using a red DyLight 650-conjugated secondary antibody (lower panel). This fluorophore was excited at 620 ± 30 nm and emission recorded at 700 ± 37 nm. SC-590 produced a uniform staining of all cells, regardless of the transfection state. ***B)*** Magnifications of the respective regions in ***A***. Cells strongly overexpressing YFP-AC5 showed major intracellular fluorescence (*1*), whereas weakly expressing cells showed better membrane localisation of YFP-AC5 (*2*). The contrast of magnification (*2*) was enhanced by reduction of the input range to 75 %. ***C)*** This confocal image, acquired from non-fixated cells, shows the membrane localisation of YFP-AC5 in a weakly expressing cell. YFP-fluorescence was excited using the 514 nm line of an Ar-laser. ***D)*** Western-Blot using the anti-AC5/6 antibody SC-590. Endogenous AC5 should be represented by a band at about 130 kDa, YFP-tagged AC5 at 160 kDa. For control purposes HEK293T cells were either not transfected at all (untransf.) or transfected with empty vector (pcDNA3). The other conditions contained YFP-AC5 or AC5-wt, respectively, cotransfected with $G\alpha_{i1}$-CFP, α_{2A}-AR and $G\beta\gamma$.

There is consensus in the scientific field about the poor specificity of antibodies against ACs (Gottle et al., *J. Pharmacol. Exp. Ther.* 2009). It was therefore not possible to determine the expression level of endogenous or transfected ACs or their subcellular distribution by means of immunofluorescence. In immunofluorescence experiments the

antibody produced a uniform staining in all cells, regardless of their transfection state or the cellular distribution of YFP-AC5 (Figure 9A lower panel). In Western-Blot experiments it produced a uniform prominent band at about 43 to 45 kDa, independent of the transfection of the cells (Figure 9D). This is only about 1/3 of the expected mass of AC5 (about 130 kDA, YFP-AC5 would be even heavier), but a very close match for the mass of actin. As no specific information about the subcellular distribution of endogenous ACs could be obtained from these experiments, it cannot be decided, whether YFP-labelled AC5 shows wild-type-like membrane targeting or not.

Among the generated constructs YFP-AC5 (Y5.9 in the author's lab journal) was the brightest and the one that localised best to the cell membrane. It was therefore further characterised and used in the FRET-experiments.

3.3 Characterisation of the newly generated YFP-AC5

Functional characterisation of fluorescent protein-labelled constructs is crucial. The newly cloned construct YFP-AC5 was compared to unlabelled AC5-wt with regard to forskolin activation, activation by Gs-proteins and regulation by Gi-proteins. Parts of these experiments were performed in collaboration with the workgroup of Dr. Frank Wunder at Bayer Healthcare Research Center in Wuppertal (Germany).

Using the bioluminescence-based cAMP-assays of Bayer Healthcare (Wunder et al., *Mol. Pharmacol.* 2008) the generation of cAMP was compared in CHO cells transfected with either AC5-wt, YFP-AC5 or mYFP for control purposes. Application of 10 µM forskolin or more resulted in a robust generation of cAMP in all three conditions, mainly due to endogenous ACs. Notably, cells transfected with either AC5-wt or YFP-AC5 showed elevated cAMP generation at forskolin concentrations between 30 nM and 3 µM. This resulted in biphasic concentration-response curves, suggesting the expression of additional, functional ACs apart from those endogenously present (Figure 10).

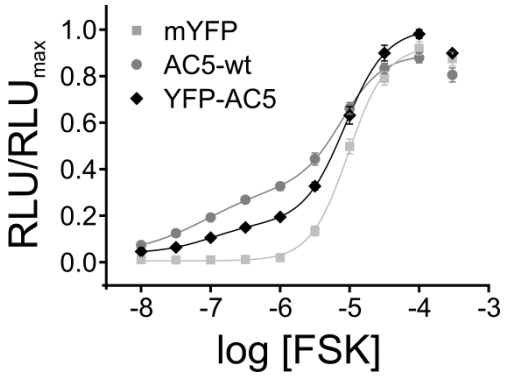

Figure 10: cAMP generation of AC5-constructs upon stimulation with forskolin

Average concentration-response curves to compare the forskolin-induced cAMP generation of AC5-wt and YFP-AC5 (mean ± S.E.M., n=5). The conditions were measured in parallel and normalised to the bioluminescence signal of YFP-AC5. cAMP generation was assessed using a bioluminescence-based cAMP reporter system in CHO cells. This assay reports changes in cellular [cAMP] through the cAMP-dependent activity of CNG-channels, which finally results in bioluminescence. Please refer to the methods section for further details. Application of forskolin (FSK) led to robust cAMP generation. 30 nM to 3 µM FSK resulted in biphasic concentration-responses in cells transfected with either YFP-AC5 or AC5-wt, as observed by the higher bioluminescence in this concentration range in comparison to control cells transfected with membrane-associated YFP (mYFP).

As forskolin is able to penetrate through the cell membrane and activate any AC, regardless of its localisation or nature (endogenous or transfected), a protocol to more selectively stimulate only transfected cells was worked out. The CHO cells used in the bioluminescence-assay don't express endogenous β_2-adrenergic receptors (β_2-AR). This receptor was therefore cotransfected together with the constructs mentioned above and cells were stimulated with isoprenaline (Iso). This experimental setup resulted in superimposable concentration-response curves for AC5-wt and YFP-AC5. Overexpression of the AC-constructs significantly increased the cAMP generation over control cells (Figure 11). These results verified wild-type-like Gs-signalling competence of the newly generated YFP-AC5.

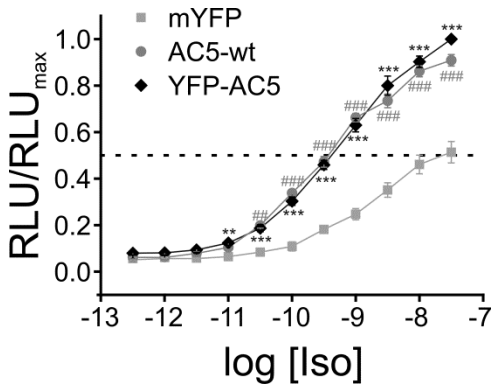

Figure 11: cAMP generation of AC5-constructs mediated by β_2-AR stimulation

Average concentration-response curves to compare Gs-signalling competence of AC5-wt and YFP-AC5 (mean ± S.E.M., n=5) using the same cAMP reporter system as in Figure 10. CHO cells were transfected with β_2-AR and the indicated constructs. The conditions were measured in parallel and normalised to the maximum bioluminescence signal of the YFP-AC5 transfection. Stimulation of the β_2-AR led to a stronger cAMP generation in cells that were transfected with the AC-constructs, than control cells (mYFP). Statistics were obtained with ANOVA and Dunnet's multiple comparison test (**/## $p<0.01$; ***/### $p<0.001$). Significant differences between mYFP and YFP-AC5 or mYFP and AC5-wt are represented by asterisks (*) or number signs (#), respectively.

So far cAMP-assays are limited in their detection of Gi-mediated changes of the second messenger. Therefore, the Gi-dependent regulation of YFP-AC5 could not be characterised using the CNG-channel-based bioluminescent assays. The FRET-based cAMP sensor Epac1-camps provides an alternative way to measure cAMP production in living cells. A protocol was established to measure Gs- and Gi-protein regulation of AC5. The expression of YFP-AC5 together with Epac1-camps would interfere with the sensor's signal/noise-ratio, though. To circumvent this impairment sREACh (non-fluorescent variant of YFP, "dark YFP") (Murakoshi et al., *Brain Cell Biol.* 2008) was cloned to the N-terminus of AC5, thereby generating a non-fluorescent construct of similar build as YFP-AC5. This construct was characterised in comparison to AC5-wt using the Epac1-camps and no difference between them was observed (see section 3.5.2.2.1 and Figure 29). From these experiments it was concluded, that sREACh-AC5 and likewise YFP-AC5 is under proper wt-like dual control of Gs- and Gi-proteins. The according experiments were performed in analogy to further functional studies that are presented later.

Having verified functionality and G-protein signalling competence of YFP-AC5 the receptor-induced FRET with G-protein subunits was investigated.

3.4 FRET-based detection of the interaction between YFP-AC5 and partners of the GPCR, G-protein signalling pathway

To investigate the interaction between the different G-protein subunits and AC5 a heterologous overexpression system was used. HEK293T cells were transiently transfected as described in the methods section. Unless stated otherwise, the indicated labelled partners were transfected together with the remaining unlabelled G-protein subunits and the according receptor. In most experiments YFP-AC5 was used as the FRET-acceptor. However, where CFP-labelled partner proteins were not available, Cer-labelled AC5 was used. This is indicated in the individual figures.

3.4.1 Basal interaction between the labelled partners

It has been reported that ACs and G-proteins interact under non-stimulated conditions and form signalling complexes (Rebois et al., *Cell. Signal.* 2012). Donor fluorescence recovery after acceptor photobleaching is a standard method to determine basal, non-stimulated interaction between FRET-pairs. It was used to investigate potential basal interaction between YFP-AC5 and CFP-labelled G-protein subunits. The difference in donor (CFP) fluorescence before and after bleaching of the acceptor (YFP) for 6 minutes was analysed. An increase in donor fluorescence reveals basal FRET between the fluorophores. The $G\alpha_{i1}/G\beta_1\gamma_2$-FRET assay (see section 3.5 for further details) provided a positive control, as the $G\alpha_{i1}$-YFP/$G\gamma_2$-CFP-pair shows FRET under non-stimulated conditions. Transfections containing CD86-YFP (Dorsch et al., *Nat. Methods* 2009), a T-cell receptor that does not interact with G-proteins, was used as a negative control. Additionally an acceptor-free transfection with AC5-wt allowed to control for donor-bleaching during the whole experimental procedure. The acceptor-free condition shows a loss in donor-fluorescence of about 3 % (-2.7 ± 1.4 %; n=12). A minor increase in donor-fluorescence of 1.4 ± 1.1 % (n=12) could be observed for the $G\alpha_s$-CFP/YFP-AC5-pair, which was not significantly different from the increase observed for the positive control, i.e. the $G\alpha_{i1}/G\beta_1\gamma_2$-FRET (5.1 ± 1.0 %; n=25). Furthermore, the according control condition ($G\alpha_s$-CFP/CD86-CFP) showed a similar increase (1.3 ± 2.0 %; n=4). In contrast to this, all other tested pairings showed on average a decrease in donor fluorescence. Statistic comparison against $G\alpha_{i1}/G\beta_1\gamma_2$-FRET revealed significant differences of those conditions as shown in Figure 12.

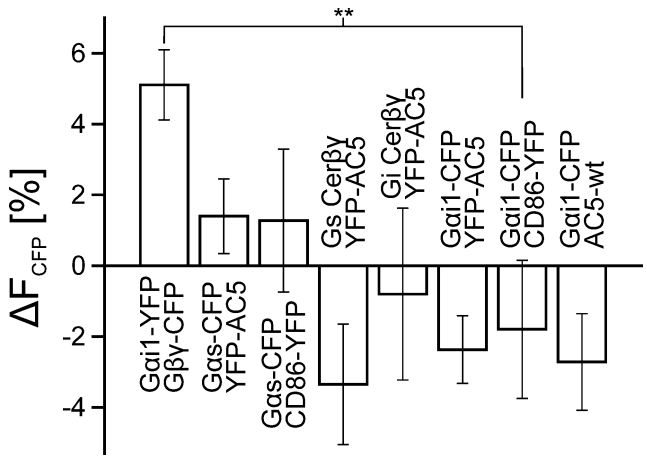

Figure 12: Donor fluorescence recovery after acceptor photobleaching

Depicted is the relative change of donor (CFP) fluorescence after 6 minutes of acceptor (YFP) photobleaching (mean ± S.E.M., n≥9). HEK cells were transfected with the indicated labelled proteins together with unlabelled G-protein subunits and receptors. The $G\alpha_{i1}$-YFP/$G\beta_1\gamma_2$-CFP pair shows FRET under non-stimulated conditions and was used as a positive control (left bar). The CD86 T-cell receptor does not interact with G-proteins and was used in combination with $G\alpha_{i1}$ as a negative control (second bar from right). The transfection with AC5-wt (right bar) did not contain any YFP-labelled construct and was used to monitor bleaching of CFP during the experiments. Statistics were obtained using ANOVA and Dunnett's multiple comparison test against the negative control condition $G\alpha_{i1}$-CFP/CD86-YFP (** p≤ 0.01, not significant differences are not indicated).

The results from the bleaching experiments did not hint at a basal interaction between AC5 and G-protein subunits.

3.4.2 Interaction between AC5 and a GPCR

For AC2 a complex of the AC with its regulating Gi-protein and the according receptor has been proposed previously (Rebois et al., *Cell. Signal.* 2012). The possibility of a similar signalling complex between AC5 and the α_{2A}-AR was therefore investigated by means of Förster Resonance Energy Transfer (FRET). The FRET donor, in this case Cer-AC5, because the receptor was labelled with YFP, was excited at 430 ± 12 nm and the fluorescence of Cerulean (Cer) and YFP was recorded simultaneously at 488 ± 20 nm and 534 ± 10 nm, respectively. The individual fluorescences of both fluorophores, F_{CFP} and F_{YFP}, respectively, were corrected for background fluorescence and spectral crosstalk as detailed in the methods section. Finally, $\frac{F_{YFP}}{F_{CFP}}$ was calculated and is presented in most following figures. This ratio is also referred to as "FRET-ratio". The cells were continuously superfused with buffer or agonist-containing buffer, during the experiments. As shown in Figure 13 no FRET-signal was observed between α_{2A}-AR-YFP and Cer-AC5.

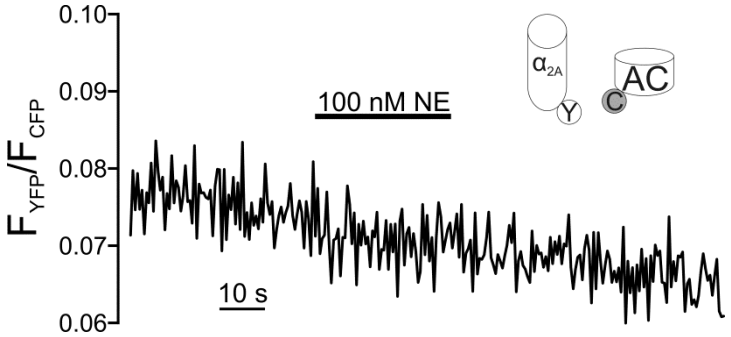

Figure 13: No FRET between α_{2A}-AR and AC5

HEK293T cells were transiently transfected with Cer-AC5, α_{2A}-AR-YFP and unlabelled Gi1-protein subunits. Cerulean (Cer) was excited at 430 ± 12 nm and the fluorescence of Cer and YFP simultaneously recorded at 488 ± 20 nm (F_{CFP}) and 534 ± 10 nm (F_{YFP}), respectively. The FRET-ratio derived from the corrected individual fluorescences (please refer to the methods section for further) is presented in this figure. Cells were continuously superfused with buffer or norepinephrine (NE)-containing buffer (indicated by the line). No FRET was observed between Cer-AC5 and the YFP-labelled α_{2A}-AR. This recording is representative for 6 experiments.

3.4.3 Interaction between AC5 and G-proteins

Generally, the observed agonist-dependent changes between YFP-AC5 and the labelled Gs- and Gi-protein subunits where rather small in amplitude (Figure 14). The agonist induced FRET-change between CFP-labelled Gα-subunits and YFP-AC5 resulted in slightly larger amplitudes, than FRET-changes between Cer-$G\beta_1\gamma_2$ and YFP-AC5: $\Delta F_{YFP}/F_{CFP}$ of 0.021 ± 0.005 (n=7) and 0.012 ± 0.002 (n=7), respectively (values for Gs-protein).

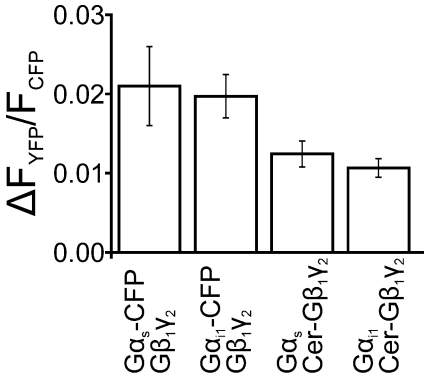

Figure 14: FRET-change between YFP-AC5 and G-protein subunits upon stimulation with agonist

The bar graph shows the averaged increase in FRET upon agonist stimulation (mean ± S.E.M., n≥6). HEK293T cells were transiently transfected with YFP-AC5, labelled and unlabelled G-protein subunits as indicated and β_2-AR (for Gs-proteins) or α_{2A}-AR (for Gi1-proteins). Cells were stimulated with either 1 µM isoprenaline (Gs-protein) or 10 µM norepinephrine (Gi-proteins) and the change in FRET between baseline and agonist-induced FRET-signal was measured.

The small amplitudes might be explained by a distance between the fluorophores larger than the Förster radius. Combined with the low expression level of the labelled partners this resulted in a low signal/noise-ratio. Nevertheless, the assays were reliable and allowed reproducible induction of agonist-dependent changes in FRET between YFP-AC5 and G-protein subunits, which are described in more detail in the following chapters.

3.4.3.1 Interaction between AC5 and $G\alpha_s$-subunits

To make sure the small amplitude were not due to unfavourable expression of the FRET-partners, the expression ratio between $G\alpha_s$-CFP and YFP-AC5 was analysed analogous to control experiments for the FRET between $G\alpha_{i1}$ and AC5 (compare section 3.5.1.1). The expression ratio between CFP and YFP was 0.57 ± 0.07 (mean ± S.E.M., n=12) ranging from 0.2 to 1, i.e. 5-fold overexpression of YFP-AC5 over $G\alpha_s$-CFP to equal expression, respectively. An excess of FRET-acceptor is ideal, because in this condition every donor has an acceptor to interact with.

Upon stimulation of the cotransfected β_2-adrenergic receptor (β_2-AR) the FRET between $G\alpha_s$-CFP and YFP-AC5 increased. After a transient peak that reached about 150 % of the final plateau value, the reaction plateaued after 5-6 seconds (Figure 15). This transient peak occurred at concentrations as low as 10 nM isoprenaline (Figure 15C). It could also be induced by another receptor (A_{2A}-adenosin receptor). Switching the fluorophores on $G\alpha_s$ and AC5 did not affect the transient peak either (Figure 15E). It was not observed at agonist concentrations below 10 nM Iso. However, these conditions resulted in a slow development of the FRET-signal and might have thereby blunted the development of this transient peak.

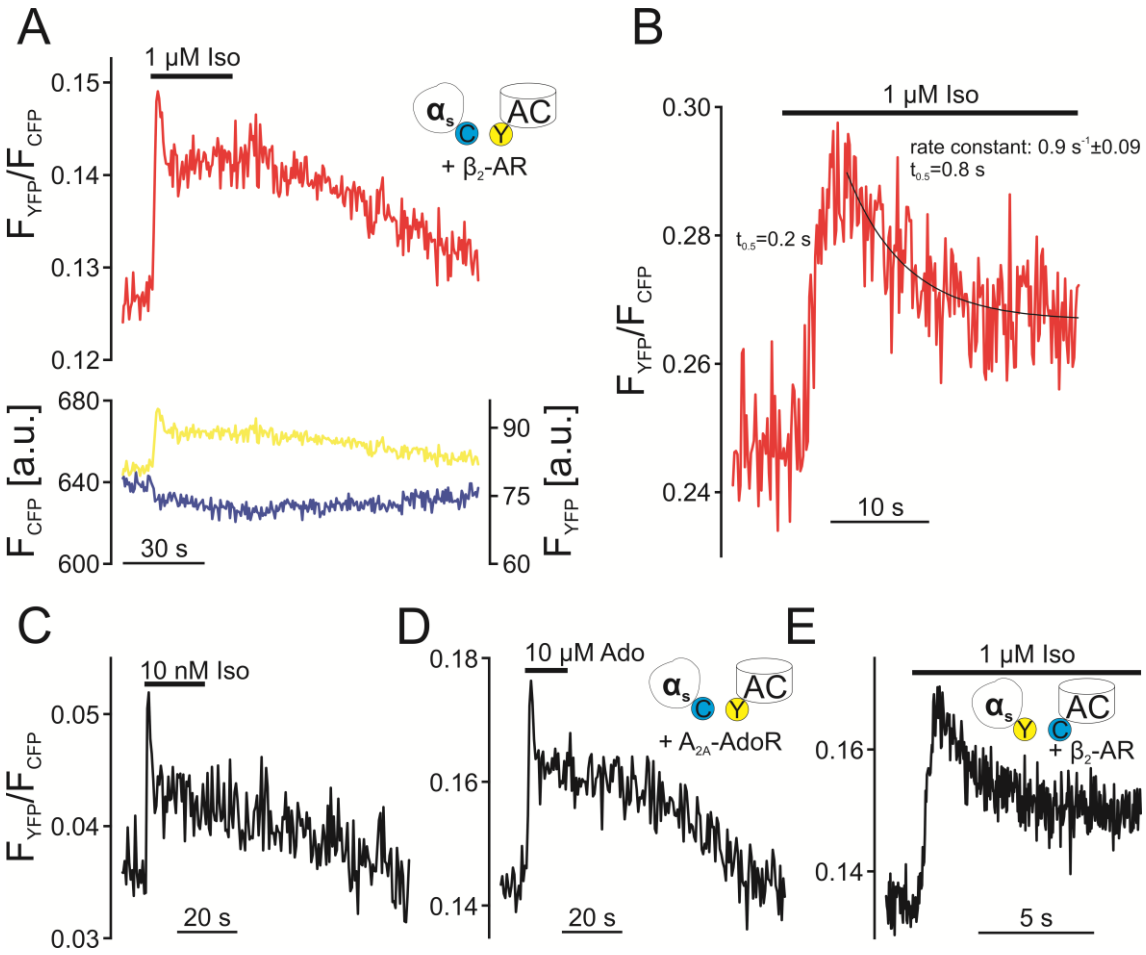

Figure 15: Agonist-dependent FRET between AC5 and Gα$_s$ is characterised by a transient peak

Depicted are representative single cell FRET recordings for HEK293T cells transiently transfected with the labelled constructs as indicated by the icons (Y: YFP, e.g. YFP-AC5; C: CFP, e.g. Gα$_s$-CFP) together with the indicated unlabelled receptor and Gβ$_1$γ$_2$-subunits. Cells were continuously superfused with buffer or agonist-containing buffer. Superfusion with agonist-containing buffer is indicated by the line in this and the following figures. The fluorescence of CFP was excited at 430 ± 12 nm and the fluorescence of CFP and YFP (F_{CFP} and F_{YFP}) was simultaneously recorded at 488 ± 20 nm and 534 ± 10 nm, respectively. The sampling rate was 2 Hz, if not indicated otherwise. The individual fluorescences (***A***, lower panel) were corrected for background fluorescence and spectral crosstalk (please refer to the methods section for further details). The FRET-ratio (F_{YFP}/F_{CFP}) was calculated and is depicted in the upper panel of ***A***. ***A)*** Upon stimulation with isoprenaline (Iso, as indicated) F_{YFP} increased, while F_{CFP} was decreased (lower panel). This indicated an increase in FRET between Gα$_s$-CFP and YFP-AC5, which is better visualised by the increase in the ratio trace (upper panel). Please note the characteristic transient peak before the plateau in the agonist-mediated FRET-increase. ***B)*** This sample recording (acquired at 33 Hz) shows the onset-kinetics of the reaction for the same conditions as used in ***A***. Recordings like this were used to calculate the kinetics summarised in Figure 17C. The transient peak also occurs at agonist concentrations as low as 10 nM Iso (***C***, equal transfection as in ***A***), when a different receptor (A_{2A}-adenosine receptor) is cotransfected and stimulated (***D***) or after exchange of the fluorophores of AC5 and Gα$_s$ (***E***, this is a 33 Hz recording).

The onset of the FRET-change upon agonist stimulation was fast, the $t_{0.5}$ to the maximum of the peak being in the sub-second range (0.26 s, see Figures 15 and 17) and similar to the activation-kinetics of the Gs-protein as published previously (Hein et al., *J. Biol. Chem.* 2006). The half-life for the transition from peak to plateau was about 0.9 s (λ=0.77 ± 0.09 s^{-1}, n=7).

To verify the specificity of the observed FRET-signal between $G\alpha_s$ and AC5 a negative control was looked for. Although Gq-proteins might be cross-talking to the cAMP pathway (Sassone-Corsi, *Cold Spring Harb. Perspect. Biol.* 2012), ACs are not considered to be a target for Gq-protein signalling themselves and therefore no FRET-signal is expected to develop.

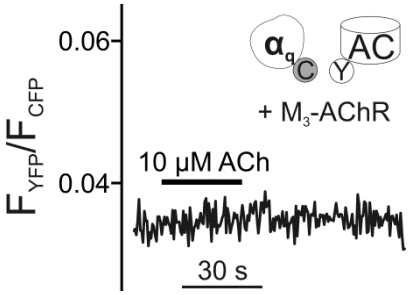

Figure 16: No FRET between $G\alpha_q$-CFP and YFP-AC5

HEK293T cells were transiently transfected with $G\alpha_q$-CFP, YFP-AC5, unlabelled M_3-acetylcholine receptor and $G\beta_1\gamma_2$. The experiments where performed as described in Figure 15. Application of acetylcholine (ACh, as indicated) does not result in FRET between AC5 and $G\alpha_q$. This sample trace is representative for 4 experiments.

The absence of FRET between $G\alpha_q$ and AC5 confirmed the reliability of the $G\alpha_s$/AC5-FRET-signal.

3.4.3.2 Interaction between AC5 and Gβγ-subunits

Gβγ-subunits bind to the N-terminus of AC5 and are necessary for $G\alpha_s$-mediated activation of the enzyme. Using $G\beta_1$-Cer as the FRET-donor for YFP-AC5 an agonist-dependent FRET-increase was observed. The kinetics of this FRET-increase were indistinguishable from those of the $G\alpha_s$/AC5-FRET (Figure 17).

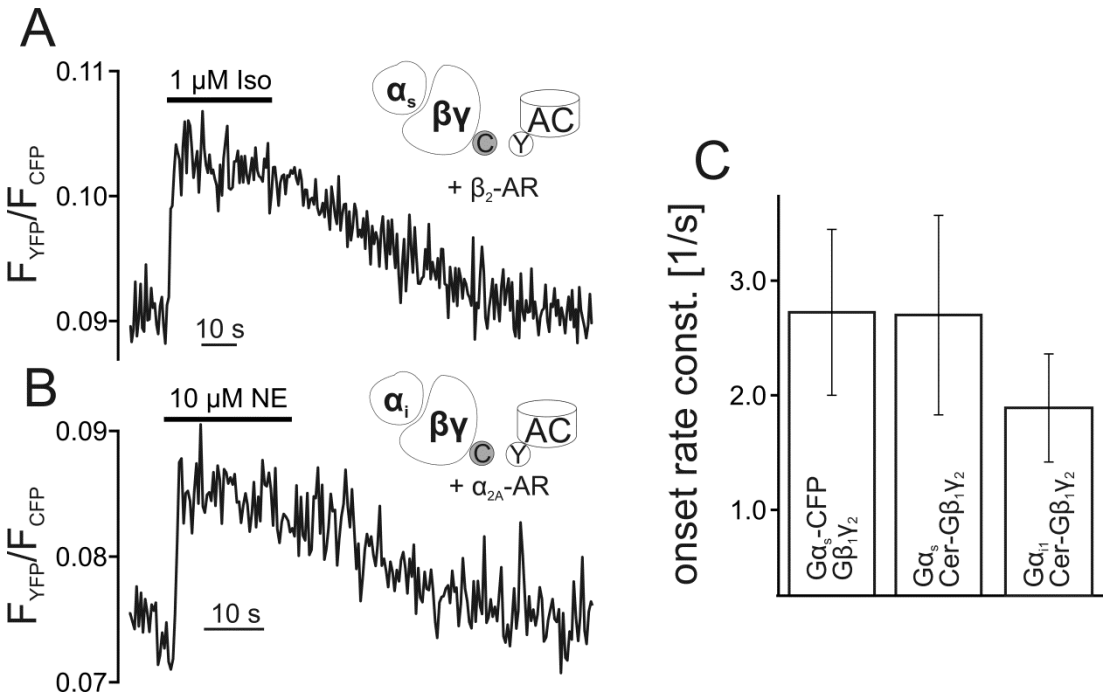

Figure 17: Agonist-dependent FRET between AC5 and Gβγ-subunits

HEK293T cells were transiently transfected with YFP-AC5, Cer-$G\beta_1$, $G\gamma_2$ and $G\alpha_s$ or $G\alpha_{i1}$, respectively. β_2-AR or α_{2A}-AR were cotransfected to stimulate Gs- or Gi-proteins, respectively. Experiments were performed in analogy to those depicted in Figure 15. ***A)*** Upon stimulation of the β_2-AR with isoprenaline (Iso, as indicated) FRET develops between AC5 and Gβγ-subunits derived from Gs-proteins. ***B)*** Gi-protein-derived Gβγ-subunits also showed FRET with AC5 upon stimulation of the α_{2A}-AR with norepinephrine (NE). ***C)*** The bar graph depicts the average onset rate constant of the FRET-increase between YFP-AC5 and the indicated labelled partners upon agonist stimulation (mean ± S.E.M., n≥6). All conditions showed similar kinetics, the $t_{0.5}$ values ranging from 0.367 s ($G\alpha_{i1}$, Cer-$G\beta_1\gamma_2$) to 0.255 s ($G\alpha_s$-CFP, $G\beta_1\gamma_2$, measured to maximum of the peak).

The similar onset of the FRET-change between AC5 and the different Gs-protein subunits is in line with reports of their simultaneous binding to the AC's N-terminus (Sadana et al., *Mol. Pharmacol.* 2009). Interestingly, the characteristic peak in the onset of FRET between $G\alpha_s$ and AC5 was not observed in FRET-experiments between AC5 and $G\beta_1\gamma_2$-subunits. This points at additional conformational changes that might occur between AC5 and $G\alpha_s$ upon activation.

Signalling complexes including Gi-coupled receptors and AC5 have been reported (Rebois et al., *Cell. Signal.* 2012) and it can easily be imagined that Gi1-proteins are participating in those complexes. As depicted in Figure 17 Gi-derived $G\beta_1\gamma_2$-subunits also change FRET with AC5 in an agonist-dependent manner. The according FRET-signal closely resembles that of Gs-derived Gβγ-subunits. This indicates that Gi-derived Gβγ-subunits interact with AC5 in a similar manner as those derived from Gs-proteins.

Having observed not only FRET-changes between Gs-derived Gβγ and AC5, but also AC5 and Gi-derived Gβγ, the FRET between AC5 and $G\alpha_{i1}$ was investigated next.

3.4.3.3 Interaction between AC5 and $G\alpha_{i1}$-subunits

Upon agonist stimulation of the cotransfected α_{2A}-AR an increase in FRET between YFP-AC5 and $G\alpha_{i1}$-CFP was observed. This increase closely resembled the FRET-increase observed with $G\beta_1\gamma_2$ and AC5, it did not show the transient peak observed in the $G\alpha_s$/AC5 FRET (Figure 18). In the following, the FRET-assay to resolve the interaction between $G\alpha_{i1}$-CFP and YFP-AC5 is termed Gαi/AC5-FRET assay. The different shape of the FRET-signal might be due to the different binding sites of the Gα-subunits in AC5. But consistently at higher (saturating) concentrations, the FRET-traces showed a transient increase in the FRET-ratio upon agonist washout. To make sure, that this transient was not a unique property of the cotransfected α_{2A}-AR, the receptor was exchanged for the type 2 muscarinic acetylcholine receptor (M_2-AChR). Obviously the observed transient is not dependent on the receptor, as it occurred in these experiments as well (compare representative samples in Figure 18).

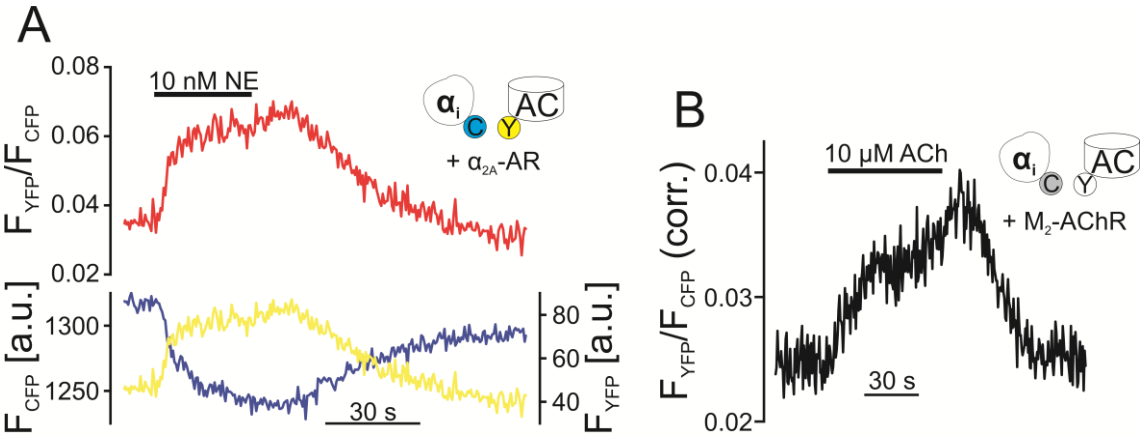

Figure 18: Agonist-dependent FRET between $G\alpha_{i1}$ and AC5

HEK cells were transfected with YFP-AC5, $G\alpha_{i1}$-CFP, α_{2A}-AR and $G\beta_1\gamma_2$. ***A)*** The representative single-cell FRET-recording shows the FRET-change induced by agonist stimulation of the receptor by norepinephrine (NE, as indicated). Upon agonist washout a transient increase in the FRET-ratio was observed, which was also represented by the opposing course of the individual fluorescence traces. ***B)*** The transient occurred also in cells transfected with the M_2-AChR, instead of the α_{2A}-AR. This recording was corrected for bleaching.

Agonist-mediated changes in FRET were small in the Gαi/AC5-FRET assay and of similar amplitude as those of the $G\alpha_s$/AC5-FRET. The specificity of this signal was controlled by checking for unspecific FRET between Gi1-proteins and non-interacting membrane proteins like CD86 T-cell receptor. No agonist-dependent FRET-change

could be elicited between $G\alpha_{i1}$-CFP and CD86-YFP, thereby verifying the changes observed in the Gαi/AC5-FRET (Figure 19).

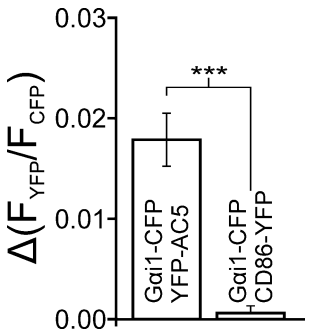

Figure 19: Agonist-induced FRET-change between $G\alpha_{i1}$ and AC5

The Gαi/AC5-FRET pair showed a robust signal, which was not observed in the control condition. Depicted is the average agonist-dependent FRET-increase (mean ± S.E.M., n≥8). Statistics were obtained by a t-Test (*** p≤0.001).

In the initial Gαi/AC5-experiments high agonist concentrations were applied, frequently 1 µM NE and higher. These concentrations were applied in order to induce saturating conditions with the highest possible amplitude. As revealed by later experiments, this was not the optimal approach.

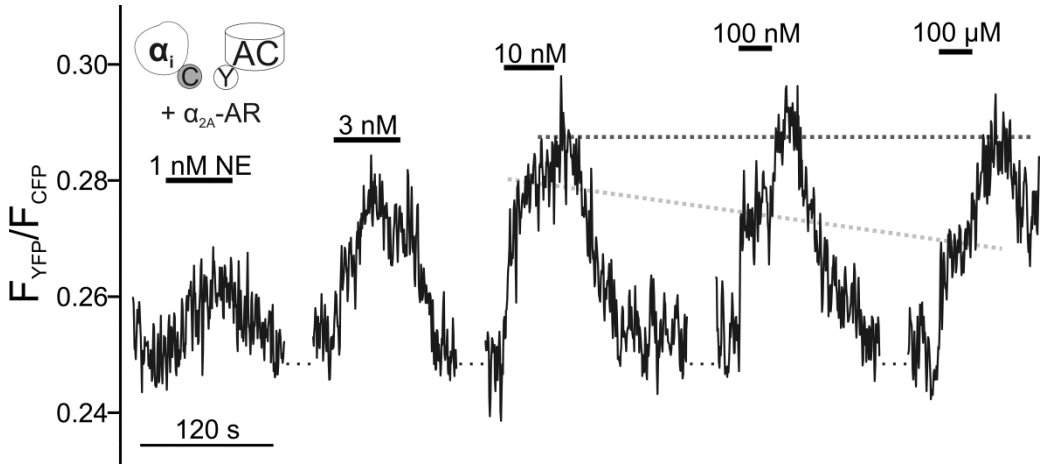

Figure 20: High agonist concentrations reduce the amplitude of the FRET-change between $G\alpha_{i1}$-CFP and YFP-AC5

HEK cells were transiently transfected with the plasmids for the Gαi/AC5-FRET assay and sequentially stimulated with increasing concentrations of NE (as indicated). Concentrations of 10 nM NE and more reliably showed the transient increase in FRET upon agonist washout. While the transient increase reached about the same level after each stimulation (dark grey line), the actual agonist-induced FRET-change was reduced with each increasing concentration above 10 nM NE (light grey line). This recording was corrected for bleaching and smoothened using Savitzky-Golay algorism. The X-axis was interrupted as indicated by the dotted lines.

As shown in the representative recording in Figure 20 the transient could be observed consistently after the application of 10 nM NE or more. Furthermore, increasing agonist concentrations reduced the amplitude of the actual agonist-induced FRET-change, while the overall amplitude (i.e. agonist-induced FRET-signal plus transient) was not affected. This observation might hint at self-inhibitory effects of the signalling pathway, possibly mediated through the α_{2A}-AR as described previously (Hommers et al., *J. Biol. Chem.* 2010).

The application of high agonist concentrations also resulted in another phenotype, especially in the presence of higher receptor expression as used in these initial experiments. However, the following has not been verified at lower amounts of transfected receptor. Upon stimulation with 10 µM NE and subsequent agonist withdrawal the transient occurs as expected, but the recovery is incomplete. A second stimulation no longer leads to the expected agonist-dependent FRET-increase (Figure 21). Nevertheless, the transient is elicited again upon agonist washout. Even a very brief application of ~1 s is sufficient to stimulate the transient. If agonist is applied again within the transient of a previous stimulation, the FRET-ratio drops back to the amplitude of the initial agonist-induced stimulation and recovered to the transient's maximum level after withdrawal.

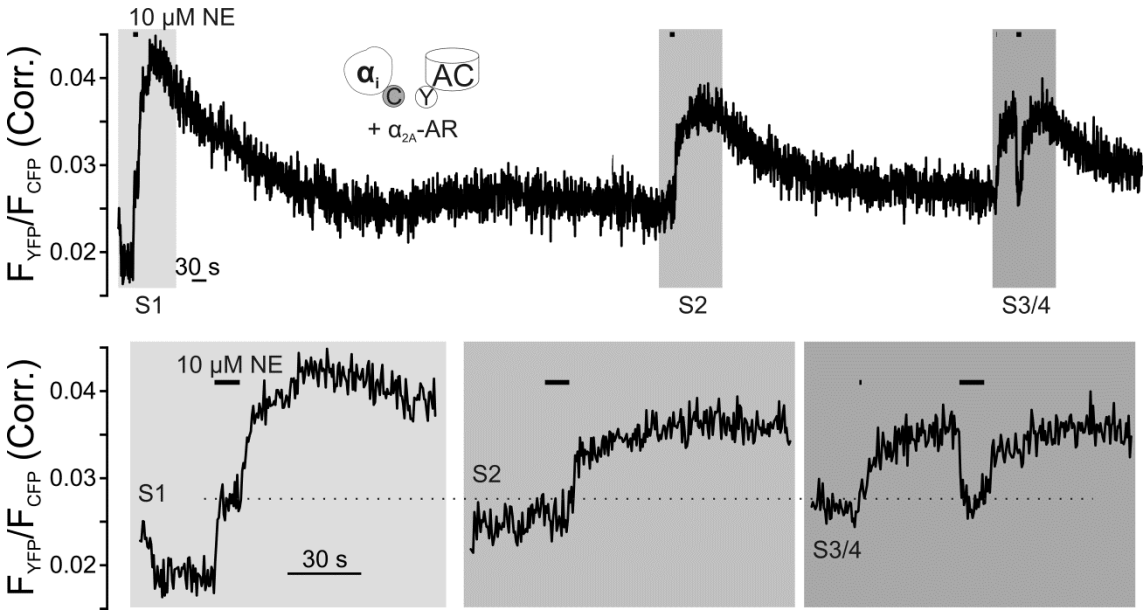

Figure 21: Incomplete recovery of the FRET-signal between Gα$_{i1}$-CFP and YFP-AC5 after high concentrations of agonist

HEK cells were transfected with the Gαi/AC5-FRET assay and subjected to single cell FRET-recording. During the recording the cell was repeatedly stimulated with 10 µM NE as indicated by the black lines. The upper panel shows the complete recording, while the lower panel shows magnifications of the individual agonist applications. The first stimulation (*S1*) resulted in an agonist-dependent FRET-increase between Gα$_{i1}$-CFP and YFP-AC5 (dotted line). It further elicited the transient increase upon agonist washout. The FRET-ratio did not recover to baseline again, but to the level of the agonist-induced amplitude of the first stimulation. The second stimulation (*S2*) showed no agonist-dependent amplitude, but the transient FRET-increase occurred. This transient was also elicited by an about 1 s long stimulation (*S3/4*). Agonist application within the transient's maximum resulted in a decrease of the FRET-ratio back to the level of the first agonist-induced amplitude. The recording was corrected for bleaching.

These observations raised the question, whether the offset-kinetics of the Gαi/AC5-FRET were different, especially slower, than that of G-protein deactivation. This was especially interesting in the light of differences in the sensitivity towards agonist that were observed. As this is part of the major findings of this study, it was assigned an individual section below (section 3.5).

As Go-proteins belong to the same major family of G-proteins, the agonist-dependent FRET with AC5 was tested as well. Even though they have been reported to regulate AC2 (Nasman et al., *J. Neurochem.* 2002) they had also been reported to not interact with AC5 (Xie et al., *Sci. Signal.* 2012). This allowed for the verification of the FRET-signal between Gα$_{i1}$ and AC5 using a negative control from the same G-protein family.

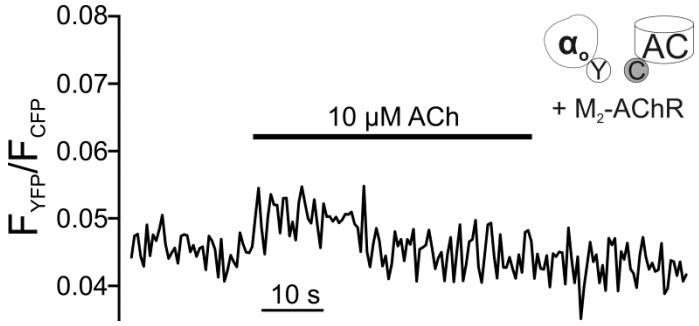

Figure 22: No FRET between Gα$_o$ and AC5

HEK cells were transfected with Gα$_o$-YFP, Cer-AC5, M_2-acetylcholine receptor and Gβ$_1$γ$_2$. Activation of the receptor by acetylcholine (ACh) does not result in FRET between the two proteins. This trace is representative for 3 experiments.

As shown in Figure 22 no agonist-dependent change in FRET between Gα$_o$-YFP and Cer-AC5 could be elicited. This verified the previous reports and corroborated the Gαi/AC5-observations.

Some preliminary experiments between Gα$_{i1}$ and AC5 hinted at a high sensitivity of the interaction between the two partners. It seemed that this interaction was even more sensitive, than expected by the activation of the Gi-protein. Therefore, the Gαi/AC5-FRET and the Gi1-protein activity, also assessed by FRET, were compared directly under similar experimental conditions.

3.5 Sensitivity of agonist-mediated Gi1-protein activation and Gα$_{i1}$/AC5-interaction

Our lab has previously developed and published an assay to investigate the activation of the Gi1-protein by means of FRET (Bünemann et al., *Proc. Natl. Acad. Sci. U. S. A.* 2003). This assay resolves agonist-dependent changes in the conformation of the Gi1-protein. Upon receptor stimulation FRET increases between Gα$_{i1}$-YFP and Gβγ-Cer. This argues in favour of subunit rearrangement, rather than subunit dissociation, as the latter would be expected to induce a loss in FRET. Figure 23 shows a representative recording of this assay.

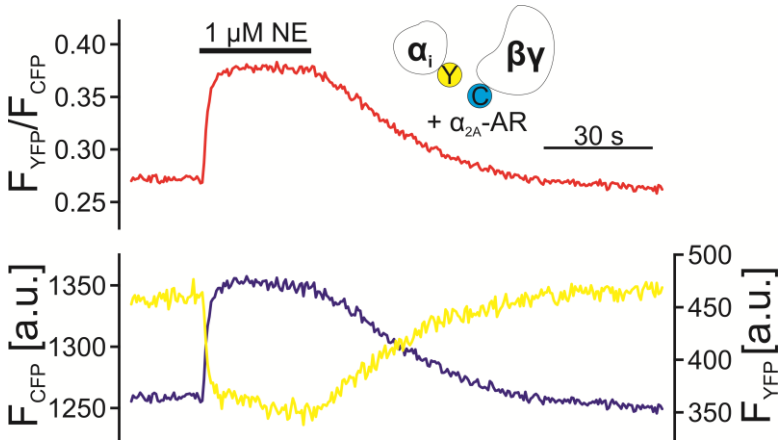

Figure 23: Agonist-dependent FRET-change in the Gi1-protein

This representative single cell recording shows the agonist-dependent FRET-changes between $G\alpha_{i1}$-YFP and Cer-$G\beta_1$. $G\gamma_2$ and α_{2A}-AR were cotransfected. Stimulation of the α_{2A}-AR with norepinephrine (NE) resulted in an increase in FRET between the G-protein subunits as represented by the increase in the FRET-ratio (upper panel) and the opposing movement of the individual fluorescence traces (lower panel). The signal was reversible upon agonist washout.

The assay was adapted to the experimental conditions of the Gαi/AC5-FRET assay to directly compare them. The assay to resolve conformational changes in the G-protein will be referred to as Gαi/Gβγ-FRET, hereafter.

3.5.1 Direct comparison of the sensitivity of Gi1-protein activation and $G\alpha_{i1}$/AC5-interaction towards agonist-mediated receptor stimulation

To investigate the sensitivity of Gαi/AC5-FRET and Gi1-protein activation concentration-response curves were recorded for both conditions. HEK293T cells, transiently transfected with either the Gαi/AC5- or Gαi/Gβγ-FRET assay, were superfused with increasing concentrations of agonist. To obtain a control value for each cell the agonist was washed off after the highest concentration and the saturating concentration was applied again. To avoid incomplete recovery in the Gαi/AC5-FRET after application of high agonist concentrations (see Figure 21 and section 3.6.1 for details) the agonist washout was performed after application of 10 nM NE (Figure 24A). Preliminary experiments revealed this to be a usually saturating concentration. Therefore, not all of the higher concentrations had to be tested. Please refer to the methods section for a detailed description of how the amplitudes were measured and normalised.

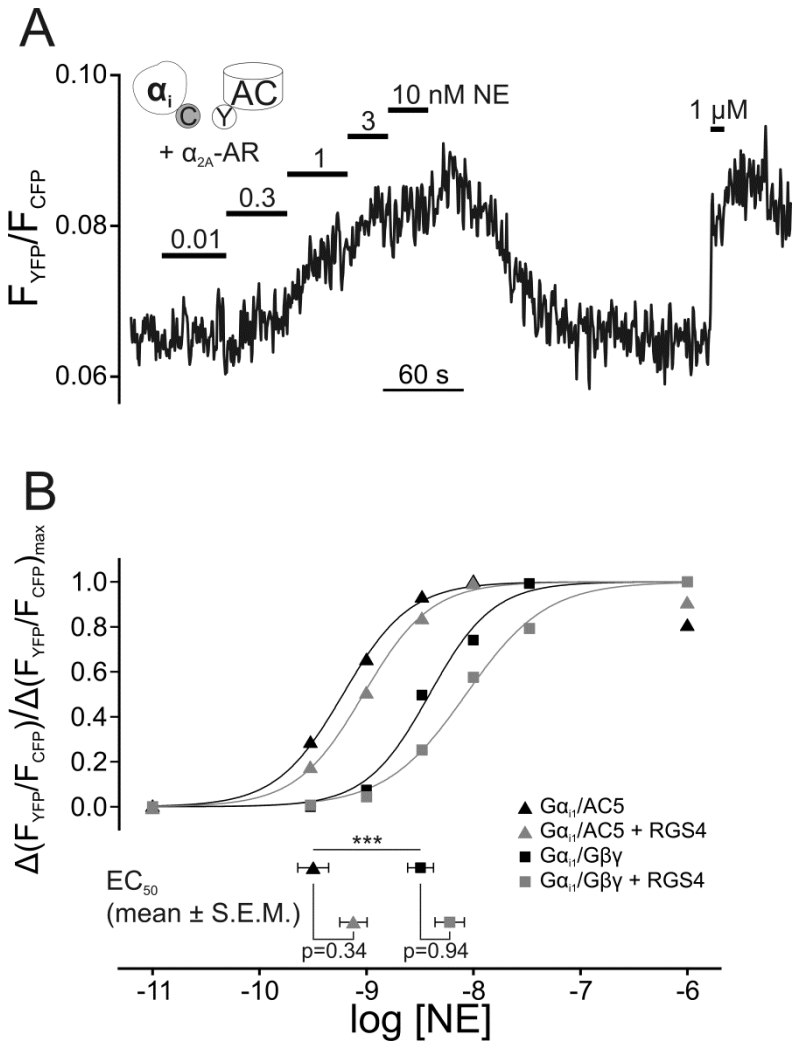

Figure 24: Different sensitivity of Gi1-protein activation and Gαi/AC5-FRET

A) This representative single-cell FRET-recording of HEK cells transfected with the Gαi/AC5-FRET assay depicts the dependence of the FRET-signal on the agonist-concentration. Agonist was washed out after the application of 10 nM NE to record the transient increase in the FRET-ratio. 1 µM NE was applied for comparison after the FRET-change had recovered to baseline. This recording was corrected for bleaching and smoothened using Savitzky-Golay algorism. The transient's maximum after 10 nM NE was set as the amplitude for 10 nM NE in order to avoid contribution of the unknown inhibitory component. The other amplitudes were normalised to this value to obtain concentration-response curves. ***B)*** Representative concentration-response curves from single-cell recordings for NE-evoked changes in Gαi/AC5- and Gαi/Gβγ-FRET (upper panel). RGS4 was cotransfected as indicated. The lower panel shows the average EC_{50}-values (mean ± S.E.M., n≥11). Statistics were obtained with ANOVA and Bonferroni post-hoc test (*** $p<0.001$).

As shown in Figure 24B Gi1-protein activation has an EC_{50} of 3.2 nM norepinephrine (NE). Contrastingly, the EC_{50} for the FRET-changes between $G\alpha_{i1}$ and AC5 is indeed shifted leftwards by one order of magnitude to 0.3 nM NE. If RGS4 was coexpressed with either assay, the EC_{50}-values tended to be increased. This effect was not

statistically significant, though. The effect of RGS4 was tested and is presented in this figure, because of a possible involvement of the interaction dynamics in the sensitivity shift, which are presented later in section 3.6.

Certain experimental conditions can alter the apparent sensitivity of the assays. Confounding conditions are receptor-overexpression in the AC5-containing assay or excess of the FRET-donor, i.e. $G\alpha_{i1}$-CFP. In order to rule out these influences, the receptor expression was analysed as well as the relative expression of the FRET-partners.

3.5.1.1 Verification of equal expression levels of the α_{2A}-AR

Higher expression levels of the receptor can result in seemingly higher agonist sensitivity of an assay as reported previously (Bunemann et al., *J. Biol. Chem.* 2001). Western-Blots against the HA-tag on the receptor N-terminus were performed to investigate the expression levels. Both assays, Gαi/Gβγ-FRET and Gαi/AC5-FRET, showed about equal expression of the receptor with a tendency towards a little less expression in the Gαi/AC5-assay (Figure 25). Quantification of the Western-Blot resulted in an average expression ratio of 75.6 ± 9.9 % for the $G\alpha_{i1}$/AC5-condition in comparison to the Gαi/Gβγ-assay (mean with S.E.M., n=3). Therefore, different receptor levels could most likely not account for the difference in sensitivity.

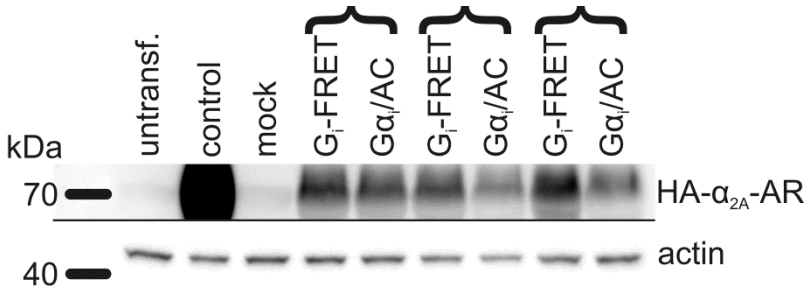

Figure 25: Western-Blot analysis of the expression of HA-tagged α_{2A}-AR

Three independent transfections (black brackets) were analysed for α_{2A}-AR expression. Cells were transfected with components of the Gαi/Gβγ-FRET (G_i-FRET) or Gαi/AC5-FRET assay ($G\alpha_i$/AC). Untransfected cells (untransf.) and cells only transfected with empty pcDNA3 (mock) were used as negative controls. Cells only transfected with α_{2A}-AR (control) were used as a positive control. Whole-cell lysates were obtained as detailed in the methods section. The HA-tag on the receptor was detected by a monoclonal antibody (HA.11 Clone 16B12, mouse, Covance). After stripping of the membrane actin was detected using a monoclonal antibody (Anti-actin clone C4, mouse, Merck Millipore).

The RGS4-construct used in these assays was also tagged with HA. Accordingly, its expression was also analysed by means of Western-Blotting, but the protein was not

detected. Either the expression of HA-tagged RGS4 was too low for proper detection by the used antibodies, or the protocol to obtain the cell-lysates was inadequate for the analysis of cytosolic proteins.

3.5.1.2 Determination of the relative expression level of the FRET- partners

Apart from differences in receptor levels, the relative expression of the FRET-partners could also be a reason for the high sensitivity observed in the Gαi/AC5-assay in comparison to the Gαi/Gβγ-FRET. Strong overexpression of the FRET-donor ($G\alpha_{i1}$-CFP) over YFP-AC5 could theoretically lead to the saturation of the FRET-acceptor already at a small portion of activated G-proteins and therefore result in seemingly higher sensitivity of the assay. As mentioned in section 3.2, substantial amounts of overexpressed AC5 tended to accumulate inside the cell. YFP-AC5, localised in such compartments, did not interact with membrane-bound G-protein subunits. Conclusively, the analysis of whole-cell lysates or membrane preparations from whole cells would result in expression levels not reflecting the actual situation at the cell membrane. To determine the relative expression levels of $G\alpha_{i1}$-CFP and YFP-AC5 the fluorescence intensity of CFP and YFP was analysed at the cell membrane and compared to a reference construct. The reference construct YFP-β_2-AR-CFP (Dorsch et al., *Nat. Methods* 2009) expresses YFP and CFP with a stoichiometry of 1:1. Please refer to the methods section for a detailed description of the measurement and data analysis. As shown in Figure 26, both FRET-partners are about equally expressed at the membrane.

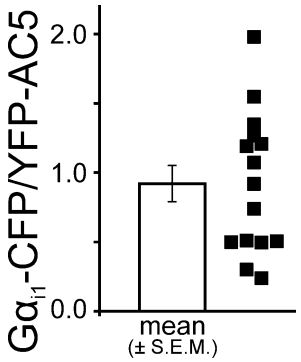

Figure 26: Relative expression of Gαi/AC5-FRET-partners at the cell membrane

The fluorescence of the reference construct YFP-β_2-AR-CFP (Dorsch et al., *Nat. Methods* 2009) was analysed by individual excitation of both fluorophores and the fluorescence ratio for this 1:1-stoichiometry of CFP and YFP was calculated. Furthermore, the fluorescence intensity of $G\alpha_{i1}$-CFP or YFP-AC5 was measured individually in cells transfected with the Gαi/AC5-FRET assay and related to the fluorescence ratio of the control construct. Please refer to the methods and results sections for details on measurement and calculations. Depicted is the average ratio (left column) of CFP/YFP (mean ± S.E.M., n=15), which represents the expression of $G\alpha_{i1}$ in relation to AC5. The data points depicted in the right part represent the individual values obtained in these experiments

On average, $G\alpha_{i1}$-CFP and YFP-AC5 were expressed equally, the ratio being 0.92 ± 0.13 (mean ± S.E.M., n=15). The individual expression ratio ranged from 0.3 to 2 (i.e. 3-fold overexpression of AC5 over $G\alpha_{i1}$ or 2-fold excess of $G\alpha_{i1}$ over AC5, respectively).

Using these methods and the correction factor obtained from the reference construct, the datasets of the kinetics and concentration-response curve experiments were analysed retrospectively. In the kinetics experiments the expression ratio of $G\alpha_{i1}$-CFP over YFP-AC5 was 0.96 ± 0.14 (mean ± S.E.M., n=12; ranging from 0.3 to 1.8). The concentration-response experiments show an expression-ratio of 1.17 ± 0.32 (mean ± S.E.M., n=15; ranging from 0.3 to 5.4). The experiment showing 5-fold excess of CFP over YFP was an outlier, though, as the next lower expression ratio was 1.3 (i.e. only minor overexpression of $G\alpha_{i1}$-CFP over YFP-AC5). However, the dataset in question yielded no outlying EC_{50}.

In conclusion, the higher sensitivity observed in the Gαi/AC5-FRET assay in comparison to the Gαi/Gβγ-FRET cannot be attributed to differences in receptor expression or unfavourable expression levels of the FRET-partners.

3.5.2 Verification of the sensitivity of $G\alpha_{i1}$/AC5-interaction and Gi1-protein activity with endogenous G-proteins using downstream functional readouts

The experiments described so far to investigate the sensitivity of the $G\alpha_{i1}$/AC5-interaction and the Gi1-protein had relied on heterologous expressed fluorescently labelled proteins. This protein overexpression might cause artificial interaction between the investigated partners. Endogenous G-proteins were used to verify the observed differences between the agonist-dependent sensitivity of G-protein activation and $G\alpha_{i1}$/AC5-interaction. Because the interaction of unlabelled proteins cannot be easily determined, functional downstream readouts were used. The GIRK channel, an effector of Gβγ-subunits, is classically used to monitor Gi-protein activity. G-protein-mediated regulation of AC5 results in alterations of cAMP levels. Therefore the Gi-protein-dependent activity of the GIRK channel was compared to the inhibition of cAMP production.

3.5.2.1 GIRK channel activity as a functional readout for Gi1-protein activity

The initial publication of the Gαi/Gβγ-FRET assay showed that the concentration-response of the FRET assay very closely resembled that of the GIRK channel activity (Bünemann et al., *Proc. Natl. Acad. Sci. U. S. A.* 2003). In order to verify the concentration-response of the Gαi/Gβγ-assay under the given experimental conditions collaboration with Dr. Andreas Rinne was established, who performed electrophysiological recordings of the GIRK channel (Figure 27).

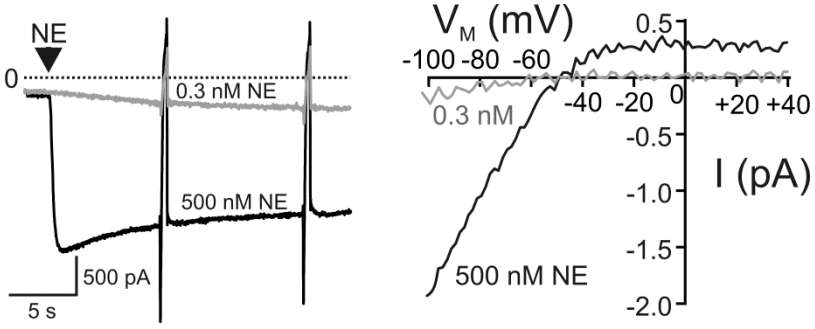

Figure 27: Receptor-induced GIRK channel activity

Representative whole-cell patch recording of agonist-induced GIRK currents. The experiments were performed at a holding potential of -90 mV and GIRK activity was measured as inward currents. The calculated reversing potential E_K was -48 mV. The cell was stimulated with the indicated concentration of NE. Between two stimulations the agonist was washed off by superfusing the cell with agonist-free buffer to allow the baseline recovery of the current (not shown). The spikes in the trace are voltage ramps from -120 mV to +60 mV (duration: 500 ms) used to generate the voltage-current plot for the channel (right panel). Refer to methods section and Rinne et al. (*Proc. Natl. Acad. Sci. U. S. A.* 2013) for further details on these experiments.

For these measurements different concentrations of NE were applied, always including 500 nM NE for normalisation purposes. The resulting EC_{50} for the GIRK activity concentration-response (Figure 30 later in this section) was very similar to that obtained from the Gαi/Gβγ-FRET experiments.

3.5.2.2 AC regulation assessed by dual control of cAMP generation through Gs- and Gi-pathways

Having confirmed the sensitivity of the Gαi/Gβγ-FRET with a functional readout, the Gi-protein-dependent inhibition of cAMP production was to be analysed. However, reduction of cellular cAMP levels by activation of inhibitory pathways cannot be easily determined. Therefore, a protocol was established to investigate the dual control of cAMP generation by stimulatory and inhibitory G-proteins at the same time. HEK293T cells were transiently transfected with Epac1-camps, the FRET-based sensor for cAMP, together with AC5 and α_{2A}-AR. The cells were continuously superfused with 3 nM Iso for 9 min, thereby stimulating cAMP production via endogenous β_2-ARs and Gs-proteins (Figure 28). During the Iso-application 0.3 nM NE was added to stimulate endogenous Gi/o-proteins. The concentration for NE was chosen according to the EC_{50} of the Gαi/AC5-FRET-change as detailed above. Application of NE, during the continuous treatment with Iso, resulted in a robust increase of the ratio, reflecting cAMP degradation. Control experiments without coexpression of either receptor or AC5 revealed the dependence of this effect on both partners.

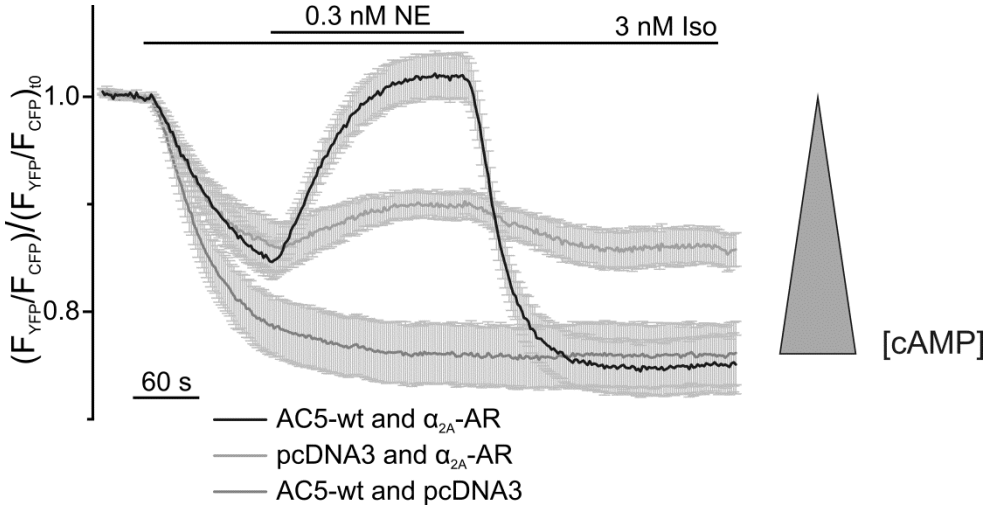

Figure 28: Dual regulation of cAMP measured with FRET

HEK cells were transfected with Epac1-camps together with AC5-wt and α_{2A}-AR as indicated to measure cAMP levels. The graph shows average traces obtained from 8-10 single-cell recordings (mean ± S.E.M.). Stimulation of endogenous β_2-ARs by Iso resulted in a loss of FRET indicating the generation of cAMP. NE-mediated activation of the cotransfected α_{2A}-AR inhibited AC-dependent cAMP generation and increased the FRET again. This occured only in cells that were cotransfected with α_{2A}-AR. Cells without cotransfected AC5-wt reacted less to both Iso and NE. These recordings were performed with a sampling rate of 0.5 Hz.

One aspect of the cAMP recordings was especially notable. 0.3 nM NE led to an increase in the FRET-ratio that plateaued above the initial baseline before the application of Iso. This reflects a decrease of basal cAMP levels of the cells and hinted at a very sensitive Gi-dependent regulation of AC5.

3.5.2.2.1 Dual control of sREACh-labelled AC5 in comparison to wild-type AC5

As mentioned previously, the CNG-channel-based bioluminescent cAMP-assays failed to characterise Gi-mediated AC5-inhibition (compare with section 3.3). In order to avoid problems with the combined use of Epac1-camps and YFP-AC5 the non-fluorescent construct sREACh-AC5 was cloned. This construct was measured under analogous experimental conditions like that depicted in Figure 28 to investigate the Gi-signalling competence of the labelled AC5 (Figure 29).

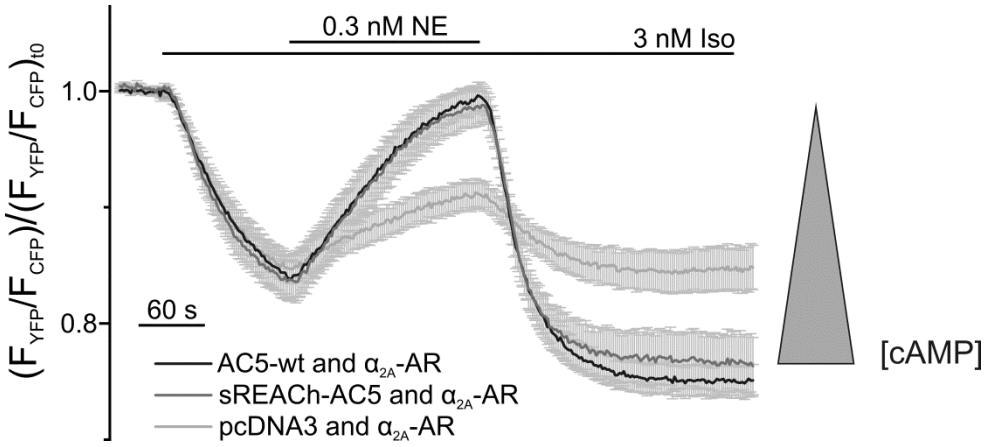

Figure 29: Comparison of sREACh-AC5 and AC5-wt with respect to regulation of cAMP
HEK cells were transfected with Epac1-camps and the indicated constructs to monitor cellular [cAMP]. These experiments were performed analogous to those depicted in Figure 28. Presented are average curves (mean ± S.E.M.) of 10 recordings for each condition. Note, that the traces of non-fluorescently labelled sREACh-AC5 (dark grey) and AC5-wt (black) are very similar in kinetics and amplitude.

sREACh-AC5 reached 95.6 ± 6.1 % (mean ± S.E.M., n=10) of the α_{2A}-AR-induced inhibition of cAMP generation of wild-type AC5. The curves were virtually identical, confirming that sREACh-AC5 showed also wt-like kinetics of dual control through Gs- and Gi-proteins. Together with data from the bioluminescence-assays described in section 3.3 YFP-AC5 was considered to be fully Gs- and Gi-signalling-competent as well.

3.5.2.3 Comparison of the concentration-response of cAMP regulation and GIRK channel activity

Similar to the experiments detailed above (section 3.5.2.2) concentration-response curves were recorded. Cells were superfused with three increasing concentrations of NE during each experiment, always including 3 nM NE for normalisation. These experiments revealed that 0.3 nM NE did not elicit the maximum inhibition of cAMP generation, but rather about 85 %. The final concentration-response curve had an EC_{50} of about 0.08 nM NE, which was even further right-shifted to the already very sensitive FRET between $G\alpha_{i1}$ and AC5. The curve was also quite steep, with a Hill slope of 5.9, which was possibly caused by further amplification mechanisms involved in the regulation of cAMP and the non-linear detection of [cAMP] by Epac1-camps.

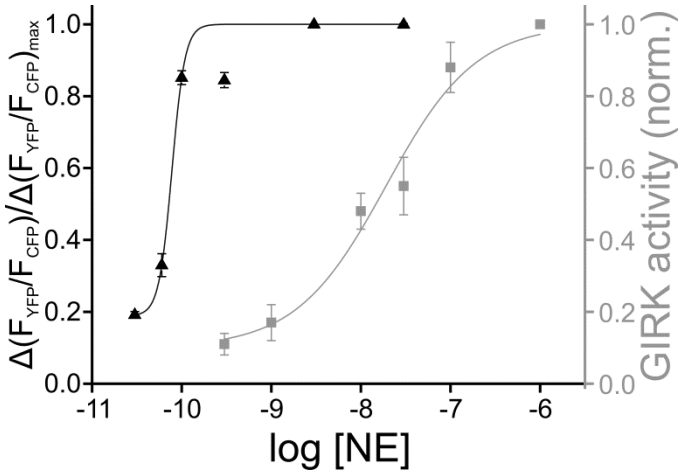

Figure 30: Concentration-response of cAMP regulation and GIRK activity towards receptor stimulation

Concentration-response curves for GIRK channel activity (squares) and NE-mediated inhibition of Iso-induced cAMP generation (triangles) were obtained from similar experiments as depicted in Figures 27 and 28, respectively. The GIRK channel activity at a given concentration was normalised to the maximum activity at 500 nM NE (mean ± S.E.M., n≥5). For this set of cAMP experiments three increasing concentrations of NE, always including 3 nM NE, were sequentially applied under continuous application of 3 nM Iso. The respective FRET-changes were normalised to the maximum FRET-change observed between the application of 3 nM NE and the final plateau of 3 nM Iso after NE withdrawal (mean ± S.E.M., n≥7). The data were fitted to concentration-response curves resulting in an EC_{50} of 0.08 nM NE (slope of 5.9) for the inhibition of Iso-induced cAMP elevation and 19 nM NE (slope of 0.9) for the GIRK channel activity, respectively.

The comparison of the two functional readouts revealed an even larger left-shift between the Gi-protein activity-mediated effect (GIRK) and the $G\alpha_{i1}$/AC5-interaction-mediated regulation of cAMP (EC_{50} of 19 and 0.08 nM NE, respectively). Both curves showed outlying values (0.3 nM NE for cAMP and 30 nM NE for GIRK). These values had not been measured together with their respective next lower values. Therefore it cannot be concluded, which of the values is more reliable (the lower or higher of each pair, respectively).

3.6 Kinetics of the interaction between YFP-AC5 and $G\alpha_{i1}$-CFP upon washout of the agonist

Having ruled out other causes that might shift the sensitivity of the assays (refer to sections 3.5.1.1 and 3.5.1.2) the kinetics of the interaction seemed to be a relevant mediator of the high sensitivity observed for the Gαi/AC5-FRET in comparison to Gi1-protein activation. Considering the G-protein cycle the following hypothesis was postulated.

Due to the G-protein cycle (compare Figure 3) there is always a fine-tuned balance between active and inactive G-protein subunits. An inhibition of G-protein deactivation through AC5 would therefore result in a shift towards a larger amount of AC-bound active G-protein subunits. This increased amount of active G-proteins should result in a higher sensitivity of the assay, which in turn should be visible in a left-shift of concentration-response curves. As already reported, this increased sensitivity was observed (compare Figure 24). Therefore, the kinetics of G-protein activation and Gαi/AC5-FRET were compared under similar experimental conditions.

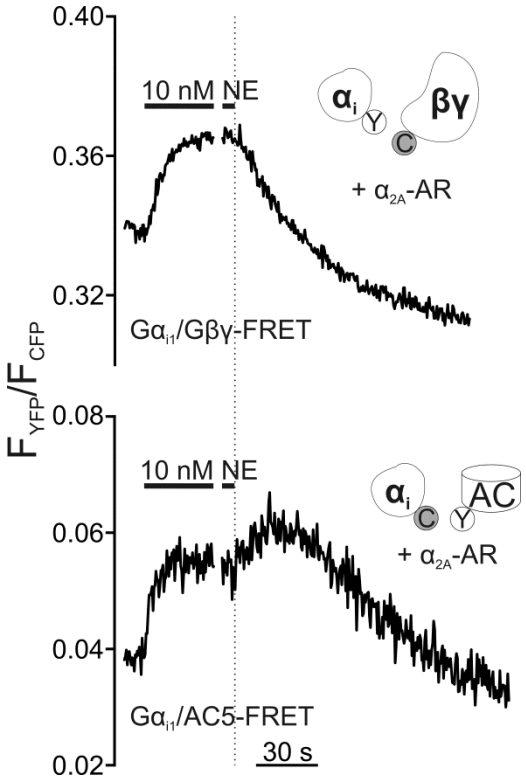

Figure 31: Interaction between $G\alpha_{i1}$-CFP and YFP-AC5 is prolonged in comparison to Gi1-protein deactivation

HEK cells were transfected with either Gαi/Gβγ- or Gαi/AC5-FRET assays and single-cell FRET-recordings were performed to analyse agonist-dependent changes in FRET. The representative traces (not corrected for bleaching) were aligned to the start of the agonist application. Furthermore, the X-axis were interrupted in the plateau of NE application to better show the different kinetics of Gi1-protein reassociation and $G\alpha_{i1}$/AC5-dissociation.

Although the amplitudes of the individual assays differed by about a factor of 2, the respective onset-kinetics were very similar. This was especially obvious, when both assays were scaled to the same amplitude (compare black squares and grey triangles in Figure 32).

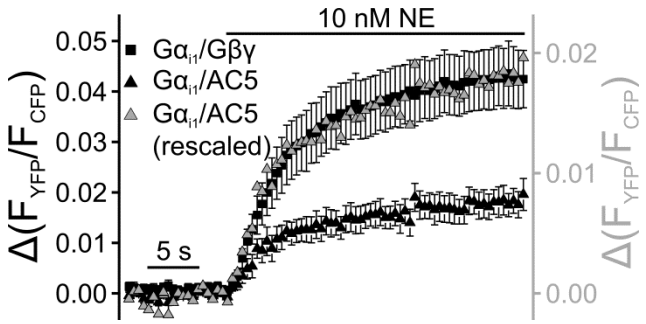

Figure 32: Similar kinetics of Gi1-protein activation and $G\alpha_{i1}$/AC5-association

The average FRET-change upon stimulation with NE is depicted as mean ± S.E.M. for 12 cells of each condition. The amplitude of the Gαi/Gβγ-FRET (black squares) is about twice as large as that of the Gαi/AC5-FRET assay (black triangles). The grey triangles represent the Gαi/AC5-data scaled to the amplitude of the Gαi/Gβγ-assay for better comparison of the kinetics.

In contrast to the similar onset-kinetics of both conditions, the offset after agonist-withdrawal was significantly delayed. The recovery of the FRET-signal between $G\alpha_{i1}$ and AC5 was prolonged in comparison to the deactivation of the Gi1-protein (Figure 33, black triangles vs. black squares, respectively). This prolonged interaction between AC5 and $G\alpha_{i1}$ might slow down the G-protein cycle, as at least the reassociation of the Gi1-protein subunits will be delayed. RGS4 was overexpressed to accelerate G-protein deactivation and thereby the recovery of the FRET-signal of the Gαi/AC5-condition. As shown in Figure 33A, RGS4 significantly accelerated Gi1-protein deactivation. RGS4 reduced the $t_{0.5}$ for Gi1-protein deactivation by about 50 % from 29.3 s to 15.8 s. However, RGS4 did not significantly influence the dissociation of $G\alpha_{i1}$-CFP and YFP-AC5 (Figure 33B and C).

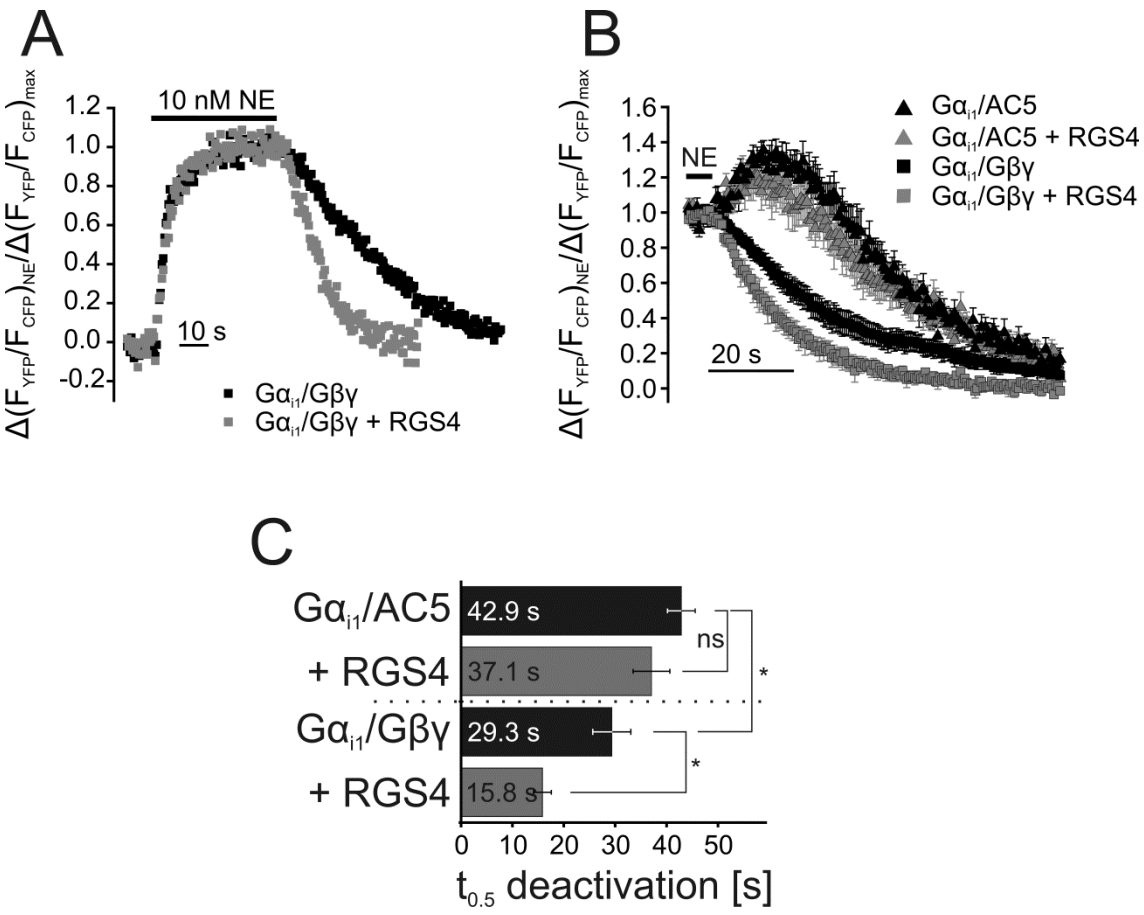

Figure 33: Kinetics of Gi1-protein deactivation and interaction of $G\alpha_{i1}$ and AC5

A) The representative sample traces depict the agonist-dependent change in FRET between $G\alpha_{i1}$ and $G\beta_1\gamma_2$. RGS4 accelerated the subunit rearrangement upon agonist-washout. The traces were normalised to the amplitude of the agonist-induced FRET-change. ***B)*** The average traces (mean ± S.E.M., n≥12) show the normalised agonist washout phase after withdrawal of 10 nM NE. RGS4 accelerated Gi1-protein deactivation and subunit reassociation in comparison to the RGS4-free condition. The generally slower dissociation kinetics of the Gαi/AC5-FRET assay was not affected by RGS4. ***C)*** The bar graph presents the average $t_{0.5}$ of the conditions presented in ***B*** (mean ± S.E.M., n≥12). Gi1-protein deactivation took about half as long as $G\alpha_{i1}$/AC5-dissociation. The difference was even larger, if RGS4 was cotransfected. Statistics were obtained using ANOVA and Bonferroni's post-hoc test (*: $p<0.05$; ns: not significant).

Because of the prolonged interaction between $G\alpha_{i1}$ and AC5 it was concluded that AC5 shifted the balance of the G-protein cycle, thereby causing the higher sensitivity observed in comparison to Gi1-protein activity. However, these experiments did not allow to determine, whether AC5 shows prolonged interaction with $G\alpha_{i1}$-GTP or $G\alpha_{i1}$-GDP.

3.6.1 Long components in the $G\alpha_{i1}$/AC5-interaction detected by FRET

Experiments, as depicted in Figure 21, revealed a tendency for incomplete recovery of the FRET-signal between $G\alpha_{i1}$-CFP and YFP-AC5. This hinted at the presence of

additional long components in the FRET-signal. To investigate this in more detail cells were stimulated twice with 1 µM NE with different washout times in between. A long component would delay the recovery of the Gαi/AC5-FRET-signal back to baseline. Conclusively, a second stimulation would not be elicited from the initial baseline, but from an elevated value according to the washout of the preceding stimulation. This would reduce the actual agonist-induced amplitude of the second stimulation. However, the longer the washout between the two stimulations, the further the ratio should have recovered to baseline and the second amplitude should ultimately be similar to the first one. Figure 34A (next page) presents a representative stimulation of such an experimental setting. 5 min of washing between the stimulations only recover the second amplitude by about 56.5 ± 10.1 % (mean ± S.E.M., n=14).

Between two stimulations the agonist was washed out for 2, 5 or 10 minutes. The amplitude of both stimulations was compared, as well as the transient increase over the agonist-dependent FRET-change. Even 10 minutes of agonist washout between the stimulations only recovered the second amplitude by about 76 ± 7.7 % (n=11). Contrastingly, 2 minutes of agonist washout recover the amplitude of the Gαi/Gβγ-FRET by 90.6 ± 4.5 % (n=3). The transient of the Gαi/AC5-FRET-signal was not affected by the different washout times. These results provide evidence for the presence of further, very slow components in the interaction between $G\alpha_{i1}$ and AC5 that might contribute to the high sensitivity. Future studies are necessary to reveal possible underlying mechanisms.

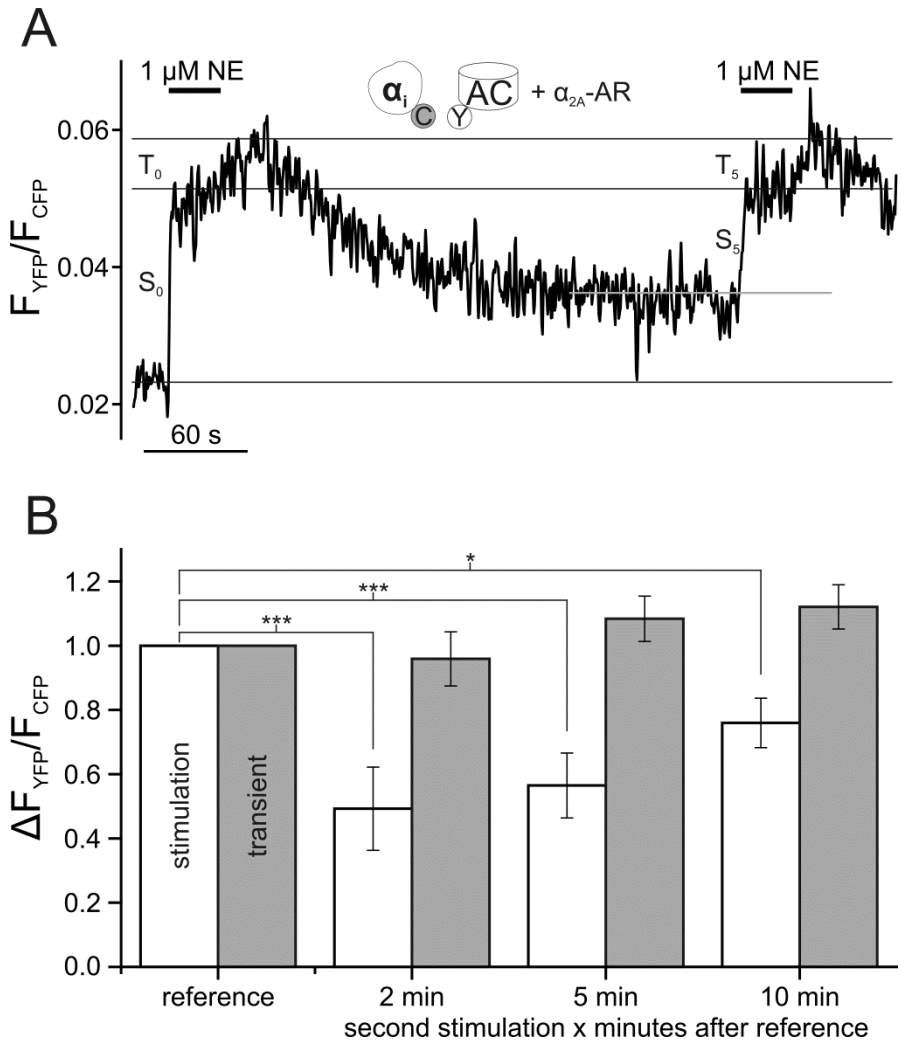

Figure 34: Amplitude of a second stimulation of Gαi/AC5-FRET after different times of agonist washout

Cells transfected with the Gαi/AC5-FRET assay were stimulated for 30 s with NE. The agonist was washed out for 2, 5 or 10 minutes, before being applied a second time. Panel ***A*** shows a representative recording of such an experiment with 5 minutes of washout between the stimulations. The recording was corrected for bleaching using the maximum of the transients and the agonist-evoked amplitude as references. Furthermore, the curve was smoothened using Savitzky-Golay algorism. S_0 is the amplitude of the reference, first stimulation, calculated as the difference in FRET before and during agonist application. The amplitude of the second stimulation after 5 minutes of agonist washout (S_5) was measured as the difference between the agonist-evoked amplitude and the FRET-ratio prior to this stimulation (grey line). The amplitude of the transients (T_0 and T_5) was measured as the difference in FRET between the agonist-induced amplitude and the transients' maxima. Amplitude and transient change of the second agonist application (S_5 and T_5, in this example) were normalised to those evoked by the reference application. ***B)*** The bar graph compares agonist-stimulated amplitude and the transient increase of the second stimulation with the according reference values. The actual agonist-induced amplitude increased with longer washout times. Statistics were obtained using ANOVA and Dunnett's multiple comparison test (*, $p \leq 0.01$; ***, $p \leq 0.001$). All transient values after washout are not significantly different from the first transient, which is not indicated in the figure.

4 Discussion

Regulation of the second messenger cAMP is the common outcome of stimulatory and inhibitory G-protein signalling. The development of optical methods, as reviewed by Lohse et al. (*Pharmacol. Rev.* 2012), together with structural information (Sunahara et al., *Annu. Rev. Pharmacol. Toxicol.* 1996; Tesmer and Sprang, *Curr. Opin. Struct. Biol.* 1998) and data from reconstituted systems for purified proteins, reviewed by Albert Gilman (*Annu. Rev. Pharmacol. Toxicol.* 2012), painted a detailed picture of the regulatory mechanisms in the signalling pathway from GPCR to cAMP. However, research on ACs has been hampered for several reasons. Currently, no full-length structure of the mammalian enzyme is available, not least because of the enzyme's size and hydrophobicity (Gilman, *Annu. Rev. Pharmacol. Toxicol.* 2012). Therefore, interaction sites and conformational changes in the transition from inactive to active state can only be guessed to a certain extent from the biochemical data available. Immunological methods like Western-Blotting and immunofluorescence are impaired by the lack of suitable antibodies that specifically detect individual isoforms and discriminate for example between AC5 and AC6. Furthermore, fluorescently labelled ACs have been reported to not always localise to the plasma membrane (Sadana et al., *Mol. Pharmacol.* 2009), a problem possibly interfering with interaction studies with other membrane-bound proteins like receptors or G-proteins. Altogether research on ACs is difficult. Some studies already utilised FRET and BRET (Bioluminescence Resonance Energy Transfer) to investigate direct interaction between ACs, receptors and G-proteins (Sadana et al., *Mol. Pharmacol.* 2009; Rebois et al., *Cell. Signal.* 2012), but those experiments were performed under steady-state conditions. Investigation of AC-dynamics had to rely on cAMP measurements and the dynamics of the interaction between ACs and their respective signalling partners remained elusive.

This study closed a gap in the available microscopic assays of the signalling pathway from GPCR to cAMP and thereby provides a new tool to perform biochemical research on ACs in intact cells. Fluorescently labelled AC isoforms were cloned and investigated together with fluorescent G-protein subunits using FRET-microscopy. Using the newly developed assay the agonist-dependent dynamic interaction between AC5 and several G-protein subunits ($G\alpha_s$, $G\alpha_{i1}$ and $G\beta_1\gamma_2$) was resolved. Furthermore, a highly sensitive $G\alpha_{i1}$-mediated inhibition of AC5 compared to other Gi-protein effectors was observed

and evidence gathered that the interaction dynamics between AC5 and $G\alpha_{i1}$ are a major contributor to the high sensitivity of cAMP regulation.

4.1 Interaction of YFP-AC5 with G-protein subunits

YFP-AC5, the brightest of the newly cloned constructs, was similar to a fluorescently labelled AC5 previously published by Carmen W. Dessauer's group (Sadana et al., *Mol. Pharmacol.* 2009), which had served as a template. However, it is essential to control proper functionality of proteins that were tagged with GFP derivatives.

It was noticed that overexpressed fluorescently labelled AC5 tended to localise to intracellular compartments, a fact also reported by others (Sadana et al., *Mol. Pharmacol.* 2009). Experiments designed to determine the subcellular localisation of endogenous ACs failed, because of the lack of suitable antibodies (Figure 9). Problems concerning the specificity of antibodies against ACs have also been reported previously (Gottle et al., *J. Pharmacol. Exp. Ther.* 2009). Therefore, it can currently not be concluded, whether the intracellular distribution reflects the natural expression pattern or is an artefact of the overexpression and/or fluorescent label.

The functionality of the newly generated construct was investigated by means of cAMP generation assays. YFP-labelled AC5 showed wild-type-like (wt-like) regulation through Gs- and Gi-proteins alike. Bioluminescence-based cAMP-assays (Wunder et al., *Mol. Pharmacol.* 2008) revealed a two-component concentration-response to forskolin stimulation in cells that expressed either YFP-AC5 or AC5-wt (Figure 10). However, forskolin can permeate cell membranes and activate intracellular ACs, including overexpressed ACs that were not trafficked to the membrane and might therefore not be under the control of G-proteins. A second set of experiments, where cAMP generation was enhanced by stimulating the Gs-pathway, showed that YFP-AC5 was basically indistinguishable from AC5-wt (Figure 11). Detection of Gi-mediated inhibition of cAMP levels is hard to determine with most assays, because those assays usually use cAMP increase-based readouts. Therefore, Gi-dependent regulation of YFP-AC5 could not be investigated using the bioluminescent assays. The FRET-based cAMP sensor Epac1-camps (Nikolaev et al., *J. Biol. Chem.* 2004) can detect dynamic changes in cellular cAMP levels and thereby resolve Gi-dependent inhibition of Gs-induced cAMP generation. However, YFP-AC5 regulation could not be investigated directly by Epac1-camps experiments, because the fluorophore of the AC would have

severely impaired the sensor's signal/noise-ratio. sREACh (Murakoshi et al., *Brain Cell Biol.* 2008) is a variant of YFP that was cloned to be non-fluorescent, but has otherwise equal protein properties (i.e. size and build) like the other GFP derivatives. It was therefore cloned to AC5 to generate a non-fluorescent construct that closely resembled YFP-AC5. sREACh-AC5 was used to assess dual control by Gs- and Gi-proteins using Epac1-camps and showed the same course of cAMP-generation and -inhibition as wild-type AC5 (Figure 29). Taken together YFP-AC5 was concluded to be fully functional and under proper dual control through stimulatory and inhibitory G-proteins.

The kinetics of the interaction between proteins could be affected by the fusion of fluorescent labels, although the labelled proteins retain their functionality. This was, for example, reported for the interaction between $G\alpha_{i3}$ and GIRK channels, where tagging with fluorescent proteins slowed the interaction under certain conditions (Berlin et al., *J. Biol. Chem.* 2011). However, in the present study fluorescently labelled AC5 showed wt-like kinetics of Gs- and Gi-mediated regulation of cAMP (Figure 29), arguing against this hypothesis. Further functional or regulatory impairments cannot be ruled out. To properly investigate this, unlabelled, preferentially endogenously expressed proteins should be used. However, there are currently no suitable methods available to investigate such interactions in living cells.

Biochemical studies proposed complexes of AC2 and AC5 with G-protein subunits (Rebois et al., *J. Cell Sci.* 2006; Sadana et al., *Mol. Pharmacol.* 2009). By means of donor fluorescence recovery after acceptor photobleaching no specific interaction between G-protein subunits and AC5 was detected in the absence of agonist-stimulation (Figure 12). These results argue against the existence of preformed complexes. However, they do not rule them out entirely, either. Under non-stimulated conditions the orientation of the fluorophores might be unfavourable and/or the distance between them might be too large for FRET to occur. The fast onset-kinetics between G-protein subunits and AC5 (Figures 17 and 32), which are in the same range as the G-protein activation-kinetics (Bünemann et al., *Proc. Natl. Acad. Sci. U. S. A.* 2003; Hein et al., *J. Biol. Chem.* 2006), argue in favour of signalling complexes. In the course of this study the presence of preformed complexes was not investigated further. Nevertheless, future studies could address this, e.g. by using dual colour fluorescence recovery after photobleaching assays (FRAP) as described by Dorsch et al. (*Nat. Methods* 2009).

The interaction between a GPCR (α_{2A}-AR) and AC5 was investigated, but no FRET was observed (Figure 13). A signalling complex between AC2, Gs-proteins and β_2-adrenergic receptors has been reported in a study using BRET (Rebois et al., *Cell. Signal.* 2012) and co-immunoprecipitation revealed interaction between the β_2-AR and AC5/6 (Lavine et al., *J. Biol. Chem.* 2002). The BRET-experiments had a larger Förster radius than the FRET-pair used in this study and might therefore resolve interactions over distances that might be too large for FRET. As the basal interaction between the receptor and the AC by means of donor fluorescence recovery after acceptor photobleaching was not determined in this study, it remains an open question, whether the observations for the β_2-AR and type II and V ACs would also hold true for the α_{2A}-AR and AC5.

Upon agonist application a FRET-signal developed between all investigated CFP-labelled G-protein subunits and YFP-AC5. The FRET-amplitudes observed in the experiments (Figure 14 and 32) were small in comparison to other FRET assays (Bünemann et al., *Proc. Natl. Acad. Sci. U. S. A.* 2003; Hein et al., *J. Biol. Chem.* 2006; Wolters and Bünemann, *Naunyn-Schmiedeberg's Arch. Pharmacol.* 2013). This limitation might be caused by a distance between the fluorophores larger than the Förster radius or an unfavourable orientation. In context of the interaction between G-proteins the amplitude of the FRET-change is of less importance, though. Furthermore, the observed low signal/noise-ratio was probably due to the low expression of the labelled partners. However small, the signals were reproducible and their specificity was proven by the opposing course of the individual fluorescence traces, the reversibility of the signal upon agonist withdrawal and the kinetics of the FRET-changes. Furthermore, no such FRET-changes were observed upon replacement of YFP-AC5 with control proteins such as CD86-YFP (Dorsch et al., *Nat. Methods* 2009), a T-cell receptor that does not interact with G-proteins (Figures 19). In addition, FRET-changes remained consistent upon exchange of the receptor and also when the fluorophores were exchanged (Figures 15 and 18).

The specificity of the observed FRET-signals between AC5 and the different G-protein subunits was further controlled by negative control experiments with non-AC5-interacting G-proteins. Gq-proteins are not presumed to interact with ACs at all, their effectors being phospholipases. Go-proteins have also been reported to not interact with AC5 (Xie et al., *Sci. Signal.* 2012). These proteins might be even better suited as a

negative control, because they belong to the same family as the AC5-interacting Gi-proteins. FRET occurred in neither combination (Figures 16 and 22), which verified the observations for the other G-protein subunits.

Although the amplitudes of the newly developed assays were small, they were still reliable. The signal/noise-ratio was sufficient to reveal distinct signal-"phenotypes" for the interaction between AC5 and different G-protein subunits. It further resolved divergences in sensitivity and interaction-kinetics in the Gi-protein/AC-pathway, which will be discussed later in this section.

Agonist-mediated interaction between $G\alpha_s$ or Gs-derived $G\beta_1\gamma_2$ and AC5 resulted in the development of FRET with similar onset-kinetics and only slightly different plateau values (Figures 14-17). The $t_{0.5}$ to maximum stimulation of these interactions is in the same range as observed previously for the activation of Gs-proteins (Hein et al., *J. Biol. Chem.* 2006), although a different receptor (β_2-AR instead of β_1-AR) was used. Previous reports of FRET-assays revealed a kinetic gap between the activation of the G-protein and the generation of cAMP, the $t_{0.5}$ being in the sub-second range and 30 s, respectively) (Nikolaev et al., *J. Biol. Chem.* 2004; Hein et al., *J. Biol. Chem.* 2006). During these studies it became evident that the interaction between the G-protein and AC5 is not the rate-limiting step in the signalling-cascade from GPCR to cAMP. Given the fast onset kinetics of Epac1-camps observed *in vitro* of less than 2 s (Nikolaev et al., *J. Biol. Chem.* 2004) and the fast diffusion of cAMP in cells, the enzymatic rate of AC5 presumably in combination with cAMP-degredation through PDEs is most likely the cause for the observed delay.

The observation of FRET between AC5 and $G\alpha_s$ and Gs-derived $G\beta\gamma$ is in line with previous reports about the joint regulation of AC5 by all Gs-protein subunits (Sadana et al., *Mol. Pharmacol.* 2009). Interestingly, however, the FRET-signals between AC5 and the different subunits were easily distinguishable. While the interaction between Gs-derived $G\beta\gamma$ and AC5 showed exponential onset-kinetics as observed in G-protein-FRET assays, $G\alpha_s$ produced a transient peak before the final plateau. This peak was not affected by exchange of the receptor or "swapping" of the fluorescent proteins (Figures 15). At lower concentrations it seemed to be missing, but onset-kinetics were so slow, that the development of the peak might have been blunted. As the transient peak was not observed with $G\beta\gamma$-subunits, it is unlikely to be due to events upstream of the

Gs-protein/AC5-interaction, such as Gs-protein activity. Due to the lack of full-length structures of AC5, it can currently only be speculated about the precise nature of this observation. The group of Carmen W. Dessauer reported that the AC's N-terminus is involved in the interaction with Gβγ-subunits, provides a binding site for $G\alpha_s$-GDP and also interacts with the catalytic core (C1-domain) (*Mol. Pharmacol.* 2009). The authors speculate that this interaction enhances or facilitates binding of $G\alpha_s$-GTP to the AC's catalytic domain C2. $G\alpha_s$ has been shown to interact with C1 and C2 domains (Sunahara et al., *J. Biol. Chem.* 1997; Tesmer et al., *Science* 1997), presumably to bring the two domains into the closed/active conformation. Taken together it can be imagined, that the observed transient peak in FRET reflects a combination of conformational changes that occur in the $G\alpha_s$/AC5-complex. This could e.g. be the transition of the activated $G\alpha_s$-subunit from the binding site on the N-terminus (where the AC is labelled) to that on the catalytic core. A C-terminally labelled AC might result in a different FRET-signal between these two partners and provide further insight. However, this speculative hypothesis needs experimental verification.

FRET was not only observed between AC5 and Gs-derived $G\beta_1\gamma_2$-subunits, but also with $G\beta_1\gamma_2$ from Gi-proteins. The resulting signals were virtually identical with regard to amplitudes and kinetics. So far there have been no reports about different interaction sites for the two Gβγ-populations. The current results hint at binding to the same site. Furthermore, no reports on competition between Gs- and Gi-derived Gβγ for the same binding site were found. This question was not addressed in this study, though. It might be possible to investigate this by FRET between labelled Gβγ-subunits and AC5 in the presence of $G\alpha_s$ and $G\alpha_{i1}$. If there are two competing pools of Gβγ, the activation of one pathway (e.g. Gs) should reduce the signal evoked by the other (e.g. Gi). It has been reported that Gs- and Gi-proteins may compete for the pool of Gβγ (Hippe et al., *Naunyn-Schmiedeberg's Arch. Pharmacol.* 2013). In the heterologous overexpression system usually used for FRET-studies like the current one, the expression of Gβγ will most likely not be limiting, though. However, the stoichiometry between Gβγ and AC5 should be controlled in such experiments. Gβγ is usually better expressed at the cell membrane than AC5. Therefore, it might be preferable to use Cerulean or CFP-tagged AC5. This would not only prevent early saturation of the FRET-signal that could occur if the donor-labelled Gβγ is expressed in excess of the acceptor-carrying AC5, but also a reduction of the signal/noise-ratio.

After the observations described above, agonist-dependent FRET-changes between $G\alpha_{i1}$ and AC5 were investigated. Interestingly, this interaction showed a new signal phenotype. While the onset-kinetics fairly much resembled that of the Gαi/Gβγ-assay (Figure 32), compare also (Bünemann et al., *Proc. Natl. Acad. Sci. U. S. A.* 2003), and being only insignificantly slower than the interaction between AC5 and Gs-proteins (Figure 15 and 17), the offset was completely different. In contrast to the exponential recovery observed in the Gαi/Gβγ-assay, this interaction showed an additional transient increase in the FRET-ratio upon agonist-washout, before recovering to baseline (Figures 31 and 33). Even more interestingly, very long kinetic components seemed to be involved in this interaction (Figures 34), which reduced the amplitude of a second stimulation (see also section 4.3 for a detailed discussion).

Several explanations can be imagined for the observed transient increase in the FRET-ratio between $G\alpha_{i1}$ and AC5. It might be due to self-inhibitory properties of the α_{2A}-AR as have been previously reported (Hommers et al., *J. Biol. Chem.* 2010). In line with this hypothesis is the observation that the actual FRET-amplitude was reduced at higher agonist-concentrations, while the overall-amplitude (maximum amplitude of the transient) was not affected (see Figure 21 for an example). The self-inhibition of the signalling pathway should result in a bell-shaped concentration-response for cAMP regulation. Such an effect was not observed, though, at least not in the concentration range that could be tested in these studies. Because NE is also an agonist on the β_2-AR, which is endogenously expressed in HEK293T cells, more than 10 nM NE reliably stimulated this receptor and resulted in cAMP generation. This cross-signalling did not allow to measure cAMP concentration-responses at more 10 nM NE. 10 nM NE was about the lowest concentration that reliably elicited the transient increase upon agonist washout, and the expected bell-shape might only occur above this concentration. Contrastingly, the FRET between Gi-derived Gβγ and AC5 was virtually identical to that observed between AC5 and Gs-derived Gβγ and showed no signs of self-inhibitory components. This argues against such a mechanism. On the other hand, the observed transient might reflect yet another conformational change, that occurs after the agonist is withdrawn and the signalling complex between $G\alpha_{i1}$ and AC5 resumes its initial conformation again. This hypothesis is strengthened by the observation, that agonist-application within the transient leads to a decline in the FRET-ratio back to the initial amplitude of the previous stimulation (Figure 21). The existence of larger signalling

complexes (Rebois et al., *Cell. Signal.* 2012), that include Gs- and Gi-proteins, their respective receptors and AC5, might explain both observations. However, based on the results from acceptor photobleaching experiments, no indication for such complexes was observed in this study.

4.2 Sensitivity of G-protein-mediated regulation of AC5

Preliminary experiments had hinted at a very sensitive interaction between $G\alpha_{i1}$ and AC5, a result verified in the later course of this work. The actual interaction between the partners was found to be 10-times more sensitive towards agonist-mediated stimulation, than expected from the activity of the Gi1-protein (Figure 24). Li et al. had reported the different sensitivity of cAMP- and G-protein-dependent pathways in frog cardiac myocytes (*J. Gen. Physiol.* 1994). They observed two distinct effects of M_2-AChR stimulation, which in their sensitivity were also shifted by more than one order of magnitude: The cAMP-dependent inhibition of Ca^{2+} currents occurred at lower agonist concentrations than necessary to activate GIRK channels in a Gi-protein activity-dependent manner. Furthermore, the dopamine D_3 receptor, a receptor that only weakly activates Gi-proteins, had been reported to efficiently inhibit AC5 (Robinson and Caron, *Mol. Pharmacol.* 1997). These studies hinted at a very sensitive inhibition of ACs, especially AC5, through Gi-proteins. Both studies used cAMP production or even further downstream effects as readouts and they might have been influenced by downstream regulatory mechanisms or the stoichiometry of the expressed partners. Therefore, the underlying mechanism for the increased sensitivity remained elusive. The results reported herein indicate that the direct interaction between $G\alpha_{i1}$ and AC5 already causes this sensitivity-shift.

Physiologically the possibility to increase the sensitivity of the regulation of one effector over the other could be highly relevant. It would allow for huge differences in the regulation of several effectors by the same pool of receptors and G-protein subtypes in identical cells and thereby provide a potent fine-tuning mechanism for cellular responses. Evidence for such divergence was found, when the regulation of targets downstream of G-protein activity and G-protein/AC5-interaction was investigated. The higher sensitivity observed in the $G\alpha_{i1}$/AC5-interaction also translated into functional readout. The Gi-mediated inhibition of AC5-dependent cAMP production was even more significantly left-shifted in comparison to GIRK activity, than the $G\alpha_{i1}$/AC5-interaction was compared to the Gi1-protein activation. The obtained EC_{50}-values

differed by more than two orders of magnitude. It must be noted, that the concentration-response of the GIRK channel, as measured in collaboration by Dr. Andreas Rinne under similar experimental conditions, was slightly right-shifted in comparison to the Gi1-protein activity (EC_{50} of 19 nM and 3 nM NE, respectively). Bünemann et al. showed, that GIRK channel activity closely resembles Gi1-protein activity, as assessed by FRET (*Proc. Natl. Acad. Sci. U. S. A.* 2003). The concentration-response curves presented in Figure 30 seem to include outlying values. These values lie in the steepest part of the curve and thereby negatively affect curve fitting and EC_{50} calculation. Due to the experimental settings, these values could not be measured with their entire respective neighbours at the same time. Nevertheless, the curves are shifted further apart than the $G\alpha_{i1}$/AC5-interaction and Gi1-protein activation, which is possibly caused by further regulatory mechanisms in the functional assays. The steepness of the cAMP-inhibition concentration-response-curve (slope of 5.9) hints at such effects. At this point it should be noted, that the cAMP measurements, as detailed above, were conducted without cotransfected G-proteins. The dual control of AC5 relies on Gs- and Gi/o-proteins endogenously expressed in HEK cells. Go-proteins obviously do not interact with AC5 (Xie et al., *Sci. Signal.* 2012) and are therefore unlikely to attribute to the observed effect. HEK293T cells do not express large quantities of $G\alpha_{i1}$-subunits either. Therefore, Gi2/3-proteins are presumable major contributors to the observed strong inhibition of AC5-dependent Gs-stimulated cAMP elevation. Although this remains speculative, it seems likely that the observations reported herein for the interaction between $G\alpha_{i1}$ and AC5 would also hold true for $G\alpha_{i2}$ and $G\alpha_{i3}$.

It was noted during the investigation of the dual control of AC5-mediated cAMP production through Gs- and Gi-proteins, that the Iso-stimulated cAMP generation was more than completely inhibited by activation of inhibitory pathways with 0.3 nM NE. This became obvious in the fact that the FRET-ratio would increase to levels above the initial baseline value, which indicated a reduction of cAMP below the basal level of the cell, prior to stimulation (Figures 28 and 29). This might be caused by the not-saturating stimulation of ACs through 3 nM Iso. It has been reported that Gi-proteins cannot completely inhibit AC5, if this is fully activated by large amounts of $G\alpha_s$ in combination with forskolin (Chen-Goodspeed et al., *J. Biol. Chem.* 2005). However, the Epac1-camps-based cAMP measurements relied on endogenous G-protein levels, in which

Gi-proteins might be more abundant than Gs-proteins, thereby dominating AC5-regulation.

The high sensitivity observed in the $G\alpha_{i1}$/AC5-interaction could have several reasons. First, the receptor expression in the AC5-including assay might be higher than in the Gαi/Gβγ-assay. This would shift the apparent sensitivity to the left. As assessed by Western-Blot-analysis, the expression of the receptor was about equal in both assays (Figure 25). If at all, it was slightly less in the Gαi/AC5-cells (Figure 25). Altogether different receptor expression levels were ruled out to cause the observed shift. Another possible explanation might be found in a different stoichiometry of the FRET-partners. Should the FRET donor, i.e. $G\alpha_{i1}$-CFP, be expressed in excess of the acceptor, i.e. YFP-AC5, the resulting interaction would be saturated at low amounts of activated G-proteins. One usually aims for a higher expression of the FRET-acceptor than -donor. In the assay presented herein, this was not easily achievable, because of the already discussed low membrane expression of YFP-AC5. Making use of a control plasmid containing CFP and YFP (Dorsch et al., *Nat. Methods* 2009), the stoichiometry of the partners at the cell membrane was analysed (Figure 26). On average, both partners are expressed about equally in the $G\alpha_{i1}$/AC5-interaction assays. In conclusion, differences in membrane expression levels were also ruled out to cause the shifted sensitivity. Therefore, the kinetics of the interaction remained the most likely explanation.

4.3 Prolonged kinetics of the $G\alpha_{i1}$/AC5-interaction

As detailed in the introduction (see section 1.2.4) G-proteins cycle through their activation and deactivation process. The already discussed high sensitivity led to the hypothesis that AC5 possibly interferes with the dynamics of the G-protein cycle (Figure 35). As the G-protein cycle provides a fine-tuned balance between active and inactive G-proteins, the prolongation of the active state of the G-proteins could possibly shift this equilibrium. If AC5 would now prevent the deactivation of the Gi-protein, then the amount of active G-proteins bound to AC5 would be increased, resulting in a left-shifted sensitivity of the assay.

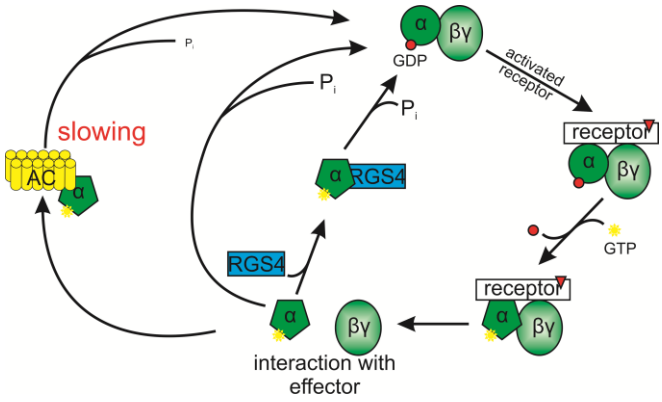

Figure 35: Possible interaction of AC5 with the G-protein cycle

AC5 slows the Gi-protein cycle and thereby causes a shift in the balance between active and inactive Gi-proteins.

To investigate this further, interaction kinetics between $G\alpha_{i1}$ and AC5 were compared to that of the Gi1-protein as assessed by Gαi/Gβγ-FRET. Even though the amplitude of both assays differs by about a factor of 2, the onset-kinetics were very similar (Figure 32). Contrastingly, the offset-kinetics were significantly different. The deactivation of the Gi1-protein occured with a half-time of about 30 s while the interaction between $G\alpha_{i1}$ and AC5 lasted longer ($t_{0.5}$ is about 43 s).

The regulator of G-protein signalling type 4 (RGS4) is known to enhance the GTPase activity of $G\alpha_{i1}$ *in vitro* and thereby accelerate G-protein-deactivation *in vivo* (Doupnik et al., *Proc. Natl. Acad. Sci. U. S. A.* 1997). Accordingly, RGS4 significantly accelerated G-protein deactivation. Contrastingly, RGS4 failed to reduce the interaction of $G\alpha_{i1}$ with AC5 and the dissociation time was not significantly affected (Figure 33). At this point, it is hard to say, whether the prolonged interaction between $G\alpha_{i1}$ and AC5 is the result of either a slower GTPase activity of the $G\alpha_{i1}$-subunit or the prolonged interaction between AC5 and $G\alpha_{i1}$-GDP. During these studies, RGS4 was not coexpressed with the functional cAMP experiments discussed in section 4.2. However, RGS4 showed no significant effect on the concentration-response of the $G\alpha_{i1}$/AC5-interaction or Gi-protein activation (Figure 24) and the interaction-kinetics (Figure 33). It is therefore likely that cAMP-measurements will not be affected, either. Biochemical studies revealed on the other hand that AC5 is regulated by $G\alpha_{i1}$-GTP and $G\alpha_{i1}$-GDP to similar extent (Dessauer et al., *J. Biol. Chem.* 1998). Presumably, the dissociation of $G\alpha_{i1}$ from AC5 and the reassociation of the former with Gβγ to the inactive heterotrimer is the main cause to relieve the inhibitory effect on AC5. Therefore, on a functional level, the question of whether AC5 shows prolonged interaction with $G\alpha_{i1}$-GTP

or -GDP might be less relevant. The lack of effect of RGS4 on interaction kinetics between $G\alpha_{i1}$ and AC5 could have different reasons. RGS4 binding to the $G\alpha_{i1}$-subunit could be sterically hindered and accordingly the $G\alpha_{i1}$-subunit is retained in its active state for a longer period. It can also be imagined, that RGS4 deactivates the $G\alpha_{i1}$-subunit in a normal time-course, but $G\alpha_{i1}$-GDP stays bound to the AC, which delays reassembly of the inactive Gi1-protein. Furthermore, AC5 could reduce the endogenous GTPase activity of $G\alpha_{i1}$ and thereby prolong the interaction. Which of the mentioned reasons is likely, or whether further mechanisms are contributing to the long interaction between AC5 and $G\alpha_{i1}$ can currently not be answered. However, the observed prolonged interaction likely causes a shift in the equilibrium of the G-protein cycle and thereby provides an explanation for the observed higher sensitivity.

It could be argued that RGS4, which accelerates the G-protein deactivation, should accordingly right-shift the concentration-response of the G-protein activity or $G\alpha_{i1}$/AC5-interaction. Even though RGS4-coexpression indeed tended to reduce the sensitivity of either assay (Figure 24), the effect did not reach statistical significance. This is in line with previous reports (Doupnik et al., *Proc. Natl. Acad. Sci. U. S. A.* 1997), but there is no consensus about the underlying mechanism.

A discrepancy remains between the shift in the sensitivity of the interaction and that in kinetics. Whereas the interaction of $G\alpha_{i1}$ and AC5 is 10-times more sensitive than the activation of Gi1-proteins, their offset-kinetics are only separated by a factor of about 1.5. Therefore the prolonged interaction between the partners might not be the only cause for the increased sensitivity. The low expression of the fluorophores makes the assay prone to bleaching, which can "imitate" recovery of the FRET-ratio. In combination with the small amplitude, the assay might not be sensitive enough to resolve minor differences between real and "bleaching-accelerated" recovery. Especially because of the bleaching, the experimental setup might not have been long enough to properly resolve the kinetics. However, the hypothesis of a prolonged interaction is strengthened by a phenomenon observed at higher concentration of agonist. Especially if larger amounts of receptor were expressed, application of agonist resulted in a very slow recovery of the $G\alpha_{i1}$/AC5-interaction. Even after 10 minutes of agonist washout, a second stimulation would only reach about 80 % of the amplitude of the initial stimulation (Figure 34). It remains elusive, though, why this long component

was less important, if not totally missing at 10 nM NE, the concentration used for the actual kinetics experiments (Figure 33).

To the author's knowledge, this study provides the first direct evidence, that the interaction between an effector and the G-protein can actually prolong the G-protein cycle of the effector-associated pool of G-proteins. This in turn results in an increased sensitivity of the G-protein-mediated regulation of the effector. Whether AC5 could or would alter the kinetics of the Gαi/Gβγ-FRET assay, remains an open question. As already discussed, AC5 does not always localise to the plasma membrane, if expressed in higher amounts. In order to investigate an influence of AC5 on the Gαi/Gβγ-FRET assay, AC5 would have to be expressed in excess to the fluorescent G-protein at the cell membrane. Currently there are no experimental conditions that would ensure this and accordingly this open question cannot be addressed.

4.4 Conclusion

This work reports the generation of a FRET-based assay to investigate the dynamics of the interaction between G-protein-subunits and AC5, thereby complementing the tool-box of microscopic methods for the GPCR/G-protein/effector signalling pathway. Furthermore, a protocol was established to resolve Gi-protein-mediated regulation of cellular cAMP. The new FRET-assays resolved the interaction between AC5 and different G-protein subunits. A basal interaction between inactive G-proteins and AC5 was not observed, but agonist-mediated changes in FRET were resolved. Notably, the interaction between AC5 and different G-protein subunits also resulted in different FRET-signal phenotypes. These reflect most likely different conformational changes upon agonist-mediated interaction, possibly involving several steps. The agonist-dependent interaction between G-proteins and AC5 occurred fast, the onset half-times being in the range of 300 ms. This is much closer to the already reported half-times of G-protein activation (also being in the sub-second range), than to the half-time of cAMP-production ($t_{0.5}$ of about 30 s). The rate-limiting step in the signalling cascade from GPCR to cAMP is therefore presumably the enzymatic activity of AC5 with only little influence by the subsequent detection of cAMP by the FRET-based Epac1-camps. In addition to the kinetic analysis, an increased sensitivity towards agonist-mediated stimulation of the interaction between $G\alpha_{i1}$ and AC5 was observed in comparison to the activity of the Gi1-protein. This shifted sensitivity became even more evident, when the according functional consequences, cAMP production and GIRK channel activity, respectively, were investigated. The high sensitivity of the molecular interaction of $G\alpha_{i1}$ and AC5 could explain the differences observed between cAMP-dependent and Gi-protein activity-mediated effects reported herein and previously (Li et al., *J. Gen. Physiol.* 1994). Different kinetics of the $G\alpha_{i1}$/AC5-dissociation and the Gi1-protein deactivation provide a putative mechanism for the extreme sensitivity of AC5 towards Gi-dependent regulation. RGS4 did not affect the kinetics of AC5-bound G-proteins, which hints at an AC5-dependent slowing of the G-protein cycle, because the reassembly of the inactive G-protein is inhibited. Taken together this leads to the hypothesis that the dynamics of G-protein/effector-interactions might serve to fine-tune GPCR-mediated signal transduction in an effector-dependent manner.

5 Summary

The signalling pathway from G-protein-coupled receptors to the second messenger cAMP is present in virtually all cells and of major physiological and pathophysiological importance. The membrane-spanning receptors can easily be targeted by pharmaceutical compounds and therapies to treat diseases like hypertension, asthma or pain affect cellular cAMP-levels. Biochemical studies have revealed a lot of important information about the interaction of the proteins participating in this signalling cascade, namely the receptors, the G-proteins and adenylyl cyclases. The development of new microscopic methods allowed to dynamically investigate protein/protein-interactions. While these techniques have already been widely used to investigate *in vivo* signalling dynamics of the receptors, G-proteins and second messengers, research on adenylyl cyclases (ACs) mainly relied on *in vitro* methods or steady-state interaction studies.

An assay, based on Förster Resonance Energy Transfer (FRET), was developed within this study, to investigate the dynamic interaction between G-proteins and ACs in living cells, thereby providing a platform for biochemical analysis *in vivo*. Furthermore, a protocol was established to resolve Gi-protein-mediated regulation of cAMP in single living cells by means of FRET. For the assays, a fluorescently labelled AC5 was cloned. Bioluminescence-based cAMP measurements proved the constructs wild-type-like functionality with respect to stimulation through forskolin and Gs-proteins. The new protocol for FRET-based cAMP measurements verified Gs- and Gi-protein signalling competence of the labelled AC5.

The new assay was used to analyse agonist-dependent interaction between AC5 and $G\alpha_s$-, $G\alpha_{i1}$- and $G\beta_1\gamma_2$-subunits, respectively. Although no basal interaction between the G-protein subunits and AC5 was observed, all subunits showed an increase in FRET upon agonist-stimulation of the according receptors. Interestingly, the different combinations of AC5 and G-protein subunits showed distinct FRET-signals. The agonist-dependent $G\beta_1\gamma_2$/AC5-FRET increase and decrease followed an exponential course, closely resembling other FRET-signals observed for G-proteins. FRET between $G\alpha_s$ and AC5 was characterised by a transient peak in the onset of the signal. Contrastingly, $G\alpha_{i1}$ and AC5 showed an additional transient increase in their FRET-signal upon agonist withdrawal. The signal-phenotypes observed between Gα-subunits and AC5 possibly indicate additional conformational changes within the G-protein/AC5

complex. The onset-kinetics of the interaction between AC5 and G-protein-subunits were fast and in the same range as previously observed G-protein activation-kinetics.

The interaction between $G\alpha_{i1}$ and AC5 was found to be especially sensitive and proved to be left-shifted in comparison to the activation of the Gi1-protein itself. Downstream events of Gi-dependent regulation of AC5 and Gi-protein activity further verified this difference on a functional level. Gi-dependent inhibition of AC5-regulated cAMP levels was determined with the newly established protocol for the FRET-based cAMP sensor Epac1-camps. In comparison to GIRK currents, which reflect Gi1-protein activity, the receptor-induced Gi-protein-mediated inhibition of stimulated AC5 activity was shifted by two orders of magnitude. This was in line with previous reports on higher sensitivity of cAMP-involving over Gi-protein activity-dependent pathways. After appropriate controls ruled out confounding mechanisms that could shift the apparent sensitivity of the assay, the interaction kinetics between AC5 and $G\alpha_{i1}$ remained as a major contributing cause. Indeed the interaction of $G\alpha_{i1}$-subunits with AC5 was prolonged in comparison to the deactivation of the Gi1-protein and could not be accelerated by RGS4. This indicates a slow dissociation of AC5 and $G\alpha_{i1}$, which prevents the deactivation and reassembly of the Gi1-protein, thereby affecting the dynamics of the G-protein cycle. Presumably, the balance in the G-protein cycle between inactive and active G-proteins is shifted towards a higher amount of AC5-bound active G-proteins, providing the putative molecular mechanism for the high sensitivity observed in the interaction studies.

5 Zusammenfassung

Praktisch alle Zellen des menschlichen Körpers verfügen über den Signalweg vom G-Protein-gekoppelten Rezeptor zum sog. „second messenger“ (zweiter Botenstoff) cAMP. Diese Signalkaskade ist von großer physiologischer und pathophysiologischer Bedeutung. Die in die Zellmembran eingelassenen Rezeptoren sind leicht zugänglich für pharmakologische Wirkstoffe. Daher beeinflussen verschiedene Krankheitstherapien, z.B. die Behandlungen von Bluthochdruck, Asthma und Schmerzen, direkt oder indirekt die zellulären cAMP-Spiegel. Biochemische Studien konnten bereits wichtige Informationen liefern über die Interaktion der an diesem Signalweg beteiligten Proteine. Dazu gehören die Rezeptoren selbst, die G-Proteine und die Adenylylzyklasen. Durch die Entwicklung neuartiger mikroskopischer Methoden konnten diese Interaktionen auch dynamisch untersucht werden. Derartige Techniken wurden bereits vielfach verwendet, um die Dynamik der Rezeptoraktivierung, des G-Proteins und des second messengers cAMP *in vivo* zu untersuchen. Die Erforschung der Adenylylzyklasen (AC) stützte sich bisher aber hauptsächlich auf *in vitro* Methoden oder Untersuchungen des Gleichgewichtszustandes der Interaktion der AC mit anderen Proteinen.

Während dieser Arbeit wurde, basierend auf dem Förster Resonanzenergietransfer (FRET), eine neue Untersuchungsmethode entwickelt. Mit ihr ist es möglich, die dynamische Interaktion zwischen G-Proteinen und ACs zu erforschen und biochemische Studien in lebenden Zellen durchzuführen. Darüber hinaus wurde ein Protokoll für FRET-Messungen in lebenden Zellen etabliert, mit dessen Hilfe die Regulation von cAMP durch inhibitorische Gi-Proteine verfolgt werden kann. Um diese Versuche zu ermöglichen, wurde eine fluoreszenzmarkierte Typ V AC (AC5) kloniert. Dieses Konstrukt zeigte eine Wildtyp-ähnliche Funktionalität in Biolumineszenz-basierten cAMP-Untersuchungen, in denen Forskolin und stimulatorische G-Protein-Signalwege eingesetzt wurden. Mittels des neu entwickelten Protokolls für FRET-basierte cAMP-Untersuchungen konnte darüber hinaus nachgewiesen werden, dass die markierte AC5 auch durch Gi-Proteine reguliert wird. Auch hier unterschied sie sich nicht von unmarkierter AC5.

Der neue Assay wurde verwendet, um die agonistabhängige Interaktion zwischen der AC5 und den verschiedenen G-Proteinuntereinheiten ($G\alpha_s$, $G\alpha_i$ und $G\beta_1\gamma_2$) zu untersuchen. Nach der Stimulation zugehöriger Rezeptoren wurde für alle Paarungen die Entwicklung eines FRET-Signals beobachtet, obwohl nicht festgestellt werden konnte, dass die Proteine unter nicht-stimulierten Bedingungen miteinander interagieren. Bemerkenswerterweise waren diese Signale für alle Paarungen unterschiedlich ausgeprägt. Der agonistabhängige Anstieg

im FRET zwischen $G\beta_1\gamma_2$-Untereinheiten und AC5 folgte einem monoexponentiellem Verlauf, ähnlich dem, der aus anderen G-Protein-Versuchen bekannt war. Der FRET-Anstieg zwischen der $G\alpha_s$-Untereinheit und AC5 war durch ein Maximum vor dem Signalplateau charakterisiert. Im Gegensatz zu diesen Kurvenverläufen zeigte das FRET-Signal zwischen der $G\alpha_{i1}$-Untereinheit und AC5 einen zusätzlichen vorübergehenden Anstieg, sobald der Agonist ausgewaschen wurde. Die verschiedenen Signalformen, die zwischen AC5 und den Gα-Untereinheiten beobachtet wurden, werden vermutlich durch zusätzliche Konformationsänderungen im G-Protein/AC-Komplex hervorgerufen. Für alle untersuchten G-Protein-Untereinheiten konnte festgestellt werden, dass sich die FRET-Signale mit der AC5 schnell entwickelten und im gleichen zeitlichen Rahmen abliefen, wie die schon bekannte Aktivierung der G-Proteine an sich.

Die Interaktion zwischen $G\alpha_{i1}$-Untereinheit und AC5 stellte sich als besonders sensitiv heraus. Weitere Untersuchungen konnten belegen, dass die Empfindlichkeit dieser Wechselwirkung tatsächlich linksverschoben war gegenüber der Aktivierung des Gi1-Proteins an sich. Diese Verschiebung konnte durch die Untersuchung nachfolgender Signalschritte auch auf funktioneller Ebene bestätigt werden. Hierzu wurde die Gi-Protein-abhängige Inhibierung der AC5 mittels des neu etablierten Protokolls zur FRET-basierten cAMP-Messung durch den Epac1-camps-Sensor gemessen. Im Vergleich zur Aktivität des GIRK-Kanals, der klassischerweise zur Bestimmung der Aktivität des Gi-Proteins verwendet wird, zeigte sich, dass die Rezeptor-abhängige, Gi-Protein-vermittelte Regulation der AC5 um zwei Zehnerpotenzen sensitiver war. Dieses Ergebnis bestätigt frühere Berichte, die ebenfalls eine deutlich höhere Sensitivität von cAMP-Signalwegen, im Vergleich zu Gi-Protein-Aktivitäts-basierten Signalen, gefunden hatten. Durch geeignete Kontrollen konnte ausgeschlossen werden, dass die Verschiebung der Sensitivität durch experimentelle Bedingungen hervorgerufen wurde. Somit blieb die Interaktionskinetik als wichtiger Einfluss übrig. Tatsächlich wurde entdeckt, dass die Interaktion der $G\alpha_{i1}$-Untereinheit und AC5 länger andauerte, als durch die Deaktivierung des Gi1-Proteins zu vermuten war. RGS4 konnte diese lange Interaktion auch nicht signifikant verkürzen. Dieses Ergebnis deutet auf eine langsame Dissoziation von $G\alpha_{i1}$ und AC5 hin, welche die Deaktivierung des Gi1-Proteins und nachfolgend die Formierung der inaktiven Konformation verzögert. Dadurch wird die Dynamik des G-Protein-Zyklus beeinflusst und vermutlich das Gleichgewicht zwischen inaktiven und aktiven G-Proteinen derart verschoben, dass mehr aktive, AC5-gebundene G-Proteine vorhanden sind. Dieser molekulare Mechanismus könnte die mutmaßliche Erklärung für die beobachtete hohe Sensitivität in den Interaktionsstudien liefern.

6 Literature

Baldwin, J. M. (1994). "Structure and function of receptors coupled to G proteins." *Curr. Opin. Cell Biol.* **6**(2): 180-190.

Becker, W. (2012). "Fluorescence lifetime imaging--techniques and applications." *J. Microsc.* **247**(2): 119-136.

Berlin, S., V. A. Tsemakhovich, R. Castel, T. Ivanina, C. W. Dessauer, T. Keren-Raifman and N. Dascal (2011). "Two distinct aspects of coupling between Galpha(i) protein and G protein-activated K+ channel (GIRK) revealed by fluorescently labeled Galpha(i3) protein subunits." *J. Biol. Chem.* **286**(38): 33223-33235.

Blumenthal, S. A. (2012). "Earl Sutherland (1915-1974) [corrected] and the discovery of cyclic AMP." *Perspect. Biol. Med.* **55**(2): 236-249.

Bokoch, G. M., T. Katada, J. K. Northup, E. L. Hewlett and A. G. Gilman (1983). "Identification of the predominant substrate for ADP-ribosylation by islet activating protein." *J. Biol. Chem.* **258**(4): 2072-2075.

Bousquet, P., J. Feldman and J. Schwartz (1984). "Central cardiovascular effects of alpha adrenergic drugs: differences between catecholamines and imidazolines." *J. Pharmacol. Exp. Ther.* **230**(1): 232-236.

Bünemann, M., M. Frank and M. J. Lohse (2003). "Gi protein activation in intact cells involves subunit rearrangement rather than dissociation." *Proc. Natl. Acad. Sci. U. S. A.* **100**(26): 16077-16082.

Bunemann, M., M. M. Bucheler, M. Philipp, M. J. Lohse and L. Hein (2001). "Activation and deactivation kinetics of alpha 2A- and alpha 2C-adrenergic receptor-activated G protein-activated inwardly rectifying K+ channel currents." *J. Biol. Chem.* **276**(50): 47512-47517.

Chen-Goodspeed, M., A. N. Lukan and C. W. Dessauer (2005). "Modeling of Galpha(s) and Galpha(i) regulation of human type V and VI adenylyl cyclase." *J. Biol. Chem.* **280**(3): 1808-1816.

Childress, A. C. and F. R. Sallee (2012). "Revisiting clonidine: an innovative add-on option for attention-deficit/hyperactivity disorder." *Drugs Today (Barc)* **48**(3): 207-217.

Chruscinski, A. J., D. K. Rohrer, E. Schauble, K. H. Desai, D. Bernstein and B. K. Kobilka (1999). "Targeted disruption of the beta2 adrenergic receptor gene." *J. Biol. Chem.* **274**(24): 16694-16700.

Chung, C. T., S. L. Niemela and R. H. Miller (1989). "One-step preparation of competent Escherichia coli: transformation and storage of bacterial cells in the same solution." *Proc. Natl. Acad. Sci. U. S. A.* **86**(7): 2172-2175.

Cooper, D. M. (2005). "Compartmentalization of adenylate cyclase and cAMP signalling." *Biochem. Soc. Trans.* **33**(Pt 6): 1319-1322.

Currie, K. P. (2010). "G protein modulation of CaV2 voltage-gated calcium channels." *Channels (Austin)* **4**(6): 497-509.

Dessauer, C. W. (2002). "Kinetic analysis of the action of P-site analogs." *Methods Enzymol.* **345**: 112-126.

Dessauer, C. W., M. Chen-Goodspeed and J. Chen (2002). "Mechanism of Galpha i-mediated inhibition of type V adenylyl cyclase." *J. Biol. Chem.* **277**(32): 28823-28829.

Dessauer, C. W., J. J. Tesmer, S. R. Sprang and A. G. Gilman (1998). "Identification of a Gialpha binding site on type V adenylyl cyclase." *J. Biol. Chem.* **273**(40): 25831-25839.

Deupi, X. and J. Standfuss (2011). "Structural insights into agonist-induced activation of G-protein-coupled receptors." *Curr. Opin. Struct. Biol.* **21**(4): 541-551.

Dorsch, S., K. N. Klotz, S. Engelhardt, M. J. Lohse and M. Bunemann (2009). "Analysis of receptor oligomerization by FRAP microscopy." *Nat. Methods* **6**(3): 225-230.

Doupnik, C. A., N. Davidson, H. A. Lester and P. Kofuji (1997). "RGS proteins reconstitute the rapid gating kinetics of gbetagamma-activated inwardly rectifying K+ channels." *Proc. Natl. Acad. Sci. U. S. A.* **94**(19): 10461-10466.

Edwards, H. V., F. Christian and G. S. Baillie (2012). "cAMP: novel concepts in compartmentalised signalling." *Semin. Cell Dev. Biol.* **23**(2): 181-190.

Edwards, H. V., J. D. Scott and G. S. Baillie (2012). "PKA phosphorylation of the small heat-shock protein Hsp20 enhances its cardioprotective effects." *Biochem. Soc. Trans.* **40**(1): 210-214.

Engelman, E. and C. Marsala (2013). "Efficacy of adding clonidine to intrathecal morphine in acute postoperative pain: meta-analysis." *Br. J. Anaesth.* **110**(1): 21-27.

Essayan, D. M. (2001). "Cyclic nucleotide phosphodiesterases." *J. Allergy Clin. Immunol.* **108**(5): 671-680.

Fan, P., Z. Jiang, I. Diamond and L. Yao (2009). "Up-regulation of AGS3 during morphine withdrawal promotes cAMP superactivation via adenylyl cyclase 5 and 7 in rat nucleus accumbens/striatal neurons." *Mol. Pharmacol.* **76**(3): 526-533.

Fedorowicz, Z., M. Nasser, V. A. Jagannath, J. H. Beaman, K. Ejaz and E. J. van Zuuren (2012). "Beta2-adrenoceptor agonists for dysmenorrhoea." *Cochrane Database Syst. Rev.* **5**: CD008585.

Förster, T. (1948). "Zwischenmolekulare Energiewanderung und Fluoreszenz." *Annalen der Physik* **437**(1-2): 55-75.

Frank, M., L. Thumer, M. J. Lohse and M. Bunemann (2005). "G Protein activation without subunit dissociation depends on a G{alpha}(i)-specific region." *J. Biol. Chem.* **280**(26): 24584-24590.

Fredriksson, R., M. C. Lagerstrom, L. G. Lundin and H. B. Schioth (2003). "The G-protein-coupled receptors in the human genome form five main families. Phylogenetic analysis, paralogon groups, and fingerprints." *Mol. Pharmacol.* **63**(6): 1256-1272.

Gancedo, J. M. (2013). "Biological roles of cAMP: variations on a theme in the different kingdoms of life." *Biol. Rev. Camb. Philos. Soc.*

Gao, X., R. Sadana, C. W. Dessauer and T. B. Patel (2007). "Conditional stimulation of type V and VI adenylyl cyclases by G protein betagamma subunits." *J. Biol. Chem.* **282**(1): 294-302.

Gilman, A. G. (2012). "Silver spoons and other personal reflections." *Annu. Rev. Pharmacol. Toxicol.* **52**: 1-19.

Gloerich, M. and J. L. Bos (2010). "Epac: defining a new mechanism for cAMP action." *Annu. Rev. Pharmacol. Toxicol.* **50**: 355-375.

Gottle, M., J. Geduhn, B. Konig, A. Gille, K. Hocherl and R. Seifert (2009). "Characterization of mouse heart adenylyl cyclase." *J. Pharmacol. Exp. Ther.* **329**(3): 1156-1165.

Halls, M. L. and D. M. Cooper (2011). "Regulation by Ca2+-signaling pathways of adenylyl cyclases." *Cold Spring Harb. Perspect. Biol.* **3**(1): a004143.

Hebert, T. E., S. Moffett, J. P. Morello, T. P. Loisel, D. G. Bichet, C. Barret and M. Bouvier (1996). "A peptide derived from a beta2-adrenergic receptor

transmembrane domain inhibits both receptor dimerization and activation." *J. Biol. Chem.* **271**(27): 16384-16392.

Hein, L., J. D. Altman and B. K. Kobilka (1999). "Two functionally distinct alpha2-adrenergic receptors regulate sympathetic neurotransmission." *Nature* **402**(6758): 181-184.

Hein, P., M. Frank, C. Hoffmann, M. J. Lohse and M. Bunemann (2005). "Dynamics of receptor/G protein coupling in living cells." *EMBO J.* **24**(23): 4106-4114.

Hein, P., F. Rochais, C. Hoffmann, S. Dorsch, V. O. Nikolaev, S. Engelhardt, C. H. Berlot, M. J. Lohse and M. Bunemann (2006). "Gs activation is time-limiting in initiating receptor-mediated signaling." *J. Biol. Chem.* **281**(44): 33345-33351.

Hippe, H. J., M. Ludde, K. Schnoes, A. Novakovic, S. Lutz, H. A. Katus, F. Niroomand, B. Nurnberg, N. Frey and T. Wieland (2013). "Competition for Gbetagamma dimers mediates a specific cross-talk between stimulatory and inhibitory G protein alpha subunits of the adenylyl cyclase in cardiomyocytes." *Naunyn-Schmiedeberg's Arch. Pharmacol.*

Holthoff, H. P., S. Zeibig, V. Jahns-Boivin, J. Bauer, M. J. Lohse, S. Kaab, S. Clauss, R. Jahns, A. Schlipp, G. Munch and M. Ungerer (2012). "Detection of anti-beta1-AR autoantibodies in heart failure by a cell-based competition ELISA." *Circ. Res.* **111**(6): 675-684.

Holz, G. G., G. Kang, M. Harbeck, M. W. Roe and O. G. Chepurny (2006). "Cell physiology of cAMP sensor Epac." *J. Physiol.* **577**(Pt 1): 5-15.

Hommers, L. G., C. Klenk, C. Dees and M. Bunemann (2010). "G proteins in reverse mode: receptor-mediated GTP release inhibits G protein and effector function." *J. Biol. Chem.* **285**(11): 8227-8233.

Hughes, T. E., H. Zhang, D. E. Logothetis and C. H. Berlot (2001). "Visualization of a functional Galpha q-green fluorescent protein fusion in living cells. Association with the plasma membrane is disrupted by mutational activation and by elimination of palmitoylation sites, but not be activation mediated by receptors or AlF4." *J. Biol. Chem.* **276**(6): 4227-4235.

Ishikawa-Ankerhold, H. C., R. Ankerhold and G. P. Drummen (2012). "Advanced fluorescence microscopy techniques--FRAP, FLIP, FLAP, FRET and FLIM." *Molecules* **17**(4): 4047-4132.

Jensen, J. B., J. S. Lyssand, C. Hague and B. Hille (2009). "Fluorescence changes reveal kinetic steps of muscarinic receptor-mediated modulation of phosphoinositides and Kv7.2/7.3 K+ channels." *J. Gen. Physiol.* **133**(4): 347-359.

Kheirbek, M. A., J. A. Beeler, W. Chi, Y. Ishikawa and X. Zhuang (2010). "A molecular dissociation between cued and contextual appetitive learning." *Learn. Mem.* **17**(3): 148-154.

Kheirbek, M. A., J. P. Britt, J. A. Beeler, Y. Ishikawa, D. S. McGehee and X. Zhuang (2009). "Adenylyl cyclase type 5 contributes to corticostriatal plasticity and striatum-dependent learning." *J. Neurosci.* **29**(39): 12115-12124.

Kim, K. S., H. Kim, I. S. Baek, K. W. Lee and P. L. Han (2011). "Mice lacking adenylyl cyclase type 5 (AC5) show increased ethanol consumption and reduced ethanol sensitivity." *Psychopharmacology (Berl.)* **215**(2): 391-398.

Kim, K. S., K. W. Lee, K. W. Lee, J. Y. Im, J. Y. Yoo, S. W. Kim, J. K. Lee, E. J. Nestler and P. L. Han (2006). "Adenylyl cyclase type 5 (AC5) is an essential mediator of morphine action." *Proc. Natl. Acad. Sci. U. S. A.* **103**(10): 3908-3913.

Kimple, A. J., D. E. Bosch, P. M. Giguere and D. P. Siderovski (2011). "Regulators of G-protein signaling and their Galpha substrates: promises and challenges in their use as drug discovery targets." *Pharmacol. Rev.* **63**(3): 728-749.

Krasel, C., M. Bunemann, K. Lorenz and M. J. Lohse (2005). "Beta-arrestin binding to the beta2-adrenergic receptor requires both receptor phosphorylation and receptor activation." *J. Biol. Chem.* **280**(10): 9528-9535.

Kritzer, M. D., J. Li, K. Dodge-Kafka and M. S. Kapiloff (2012). "AKAPs: the architectural underpinnings of local cAMP signaling." *J. Mol. Cell. Cardiol.* **52**(2): 351-358.

Lavine, N., N. Ethier, J. N. Oak, L. Pei, F. Liu, P. Trieu, R. V. Rebois, M. Bouvier, T. E. Hebert and H. H. Van Tol (2002). "G protein-coupled receptors form stable complexes with inwardly rectifying potassium channels and adenylyl cyclase." *J. Biol. Chem.* **277**(48): 46010-46019.

Li, Y., R. Hanf, A. S. Otero, R. Fischmeister and G. Szabo (1994). "Differential effects of pertussis toxin on the muscarinic regulation of Ca2+ and K+ currents in frog cardiac myocytes." *J. Gen. Physiol.* **104**(5): 941-959.

Linder, J. U. (2006). "Class III adenylyl cyclases: molecular mechanisms of catalysis and regulation." *Cell. Mol. Life Sci.* **63**(15): 1736-1751.

Lohse, M. J., V. O. Nikolaev, P. Hein, C. Hoffmann, J. P. Vilardaga and M. Bunemann (2008). "Optical techniques to analyze real-time activation and signaling of G-protein-coupled receptors." *Trends Pharmacol. Sci.* **29**(3): 159-165.

Lohse, M. J., S. Nuber and C. Hoffmann (2012). "Fluorescence/bioluminescence resonance energy transfer techniques to study G-protein-coupled receptor activation and signaling." *Pharmacol. Rev.* **64**(2): 299-336.

Ludwig, A., X. Zong, M. Jeglitsch, F. Hofmann and M. Biel (1998). "A family of hyperpolarization-activated mammalian cation channels." *Nature* **393**(6685): 587-591.

McCudden, C. R., M. D. Hains, R. J. Kimple, D. P. Siderovski and F. S. Willard (2005). "G-protein signaling: back to the future." *Cell. Mol. Life Sci.* **62**(5): 551-577.

Metrich, M., M. Berthouze, E. Morel, B. Crozatier, A. M. Gomez and F. Lezoualc'h (2010). "Role of the cAMP-binding protein Epac in cardiovascular physiology and pathophysiology." *Pflugers Arch.* **459**(4): 535-546.

Milligan, G. (2013). "The Prevalence, Maintenance and Relevance of GPCR Oligomerization." *Mol. Pharmacol.*

Mou, T. C., N. Masada, D. M. Cooper and S. R. Sprang (2009). "Structural basis for inhibition of mammalian adenylyl cyclase by calcium." *Biochemistry (Mosc.)* **48**(15): 3387-3397.

Murakoshi, H., S. J. Lee and R. Yasuda (2008). "Highly sensitive and quantitative FRET-FLIM imaging in single dendritic spines using improved non-radiative YFP." *Brain Cell Biol.* **36**(1-4): 31-42.

Nasman, J., J. P. Kukkonen, T. Holmqvist and K. E. Akerman (2002). "Different roles for Gi and Go proteins in modulation of adenylyl cyclase type-2 activity." *J. Neurochem.* **83**(6): 1252-1261.

Nikolaev, V. O., M. Bunemann, L. Hein, A. Hannawacker and M. J. Lohse (2004). "Novel single chain cAMP sensors for receptor-induced signal propagation." *J. Biol. Chem.* **279**(36): 37215-37218.

Nikolaev, V. O., M. Bunemann, E. Schmitteckert, M. J. Lohse and S. Engelhardt (2006). "Cyclic AMP imaging in adult cardiac myocytes reveals far-reaching beta1-adrenergic but locally confined beta2-adrenergic receptor-mediated signaling." *Circ. Res.* **99**(10): 1084-1091.

Northup, J. K., P. C. Sternweis, M. D. Smigel, L. S. Schleifer, E. M. Ross and A. G. Gilman (1980). "Purification of the regulatory component of adenylate cyclase." *Proc. Natl. Acad. Sci. U. S. A.* **77**(11): 6516-6520.

Palczewski, K., T. Kumasaka, T. Hori, C. A. Behnke, H. Motoshima, B. A. Fox, I. Le Trong, D. C. Teller, T. Okada, R. E. Stenkamp, M. Yamamoto and M. Miyano (2000). "Crystal structure of rhodopsin: A G protein-coupled receptor." *Science* **289**(5480): 739-745.

Papa, S., D. D. Rasmo, Z. Technikova-Dobrova, D. Panelli, A. Signorile, S. Scacco, V. Petruzzella, F. Papa, G. Palmisano, A. Gnoni, L. Micelli and A. M. Sardanelli (2012). "Respiratory chain complex I, a main regulatory target of the cAMP/PKA pathway is defective in different human diseases." *FEBS Lett.* **586**(5): 568-577.

Patschan, D., S. Patschan, J. T. Wessels, J. U. Becker, S. David, E. Henze, M. S. Goligorsky and G. A. Muller (2010). "Epac-1 activator 8-O-cAMP augments renoprotective effects of syngeneic [corrected] murine EPCs in acute ischemic kidney injury." *Am. J. Physiol. Renal Physiol.* **298**(1): F78-85.

Pavan, B., C. Biondi and A. Dalpiaz (2009). "Adenylyl cyclases as innovative therapeutic goals." *Drug Discov. Today* **14**(19-20): 982-991.

Peschke, E. (2008). "Melatonin, endocrine pancreas and diabetes." *J. Pineal Res.* **44**(1): 26-40.

Pierre, S., T. Eschenhagen, G. Geisslinger and K. Scholich (2009). "Capturing adenylyl cyclases as potential drug targets." *Nat. Rev. Drug Discov.* **8**(4): 321-335.

Pinto, C., M. Hubner, A. Gille, M. Richter, T. C. Mou, S. R. Sprang and R. Seifert (2009). "Differential interactions of the catalytic subunits of adenylyl cyclase with forskolin analogs." *Biochem. Pharmacol.* **78**(1): 62-69.

Rasmussen, S. G., H. J. Choi, D. M. Rosenbaum, T. S. Kobilka, F. S. Thian, P. C. Edwards, M. Burghammer, V. R. Ratnala, R. Sanishvili, R. F. Fischetti, G. F. Schertler, W. I. Weis and B. K. Kobilka (2007). "Crystal structure of the human beta2 adrenergic G-protein-coupled receptor." *Nature* **450**(7168): 383-387.

Rasmussen, S. G., B. T. DeVree, Y. Zou, A. C. Kruse, K. Y. Chung, T. S. Kobilka, F. S. Thian, P. S. Chae, E. Pardon, D. Calinski, J. M. Mathiesen, S. T. Shah, J. A. Lyons, M. Caffrey, S. H. Gellman, J. Steyaert, G. Skiniotis, W. I. Weis, R. K. Sunahara and B. K. Kobilka (2011). "Crystal structure of the beta2 adrenergic receptor-Gs protein complex." *Nature* **477**(7366): 549-555.

Rebois, R. V., K. Maki, J. A. Meeks, P. H. Fishman, T. E. Hebert and J. K. Northup (2012). "D2-like dopamine and beta-adrenergic receptors form a signaling complex that integrates Gs- and Gi-mediated regulation of adenylyl cyclase." *Cell. Signal.* **24**(11): 2051-2060.

Rebois, R. V., M. Robitaille, C. Gales, D. J. Dupre, A. Baragli, P. Trieu, N. Ethier, M. Bouvier and T. E. Hebert (2006). "Heterotrimeric G proteins form stable complexes with adenylyl cyclase and Kir3.1 channels in living cells." *J. Cell Sci.* **119**(Pt 13): 2807-2818.

Rinne, A., A. Birk and M. Bunemann (2013). "Voltage regulates adrenergic receptor function." *Proc. Natl. Acad. Sci. U. S. A.* **110**(4): 1536-1541.

Robinson, S. W. and M. G. Caron (1997). "Selective inhibition of adenylyl cyclase type V by the dopamine D3 receptor." *Mol. Pharmacol.* **52**(3): 508-514.

Roseberry, A. G., M. Bunemann, J. Elavunkal and M. M. Hosey (2001). "Agonist-dependent delivery of M(2) muscarinic acetylcholine receptors to the cell surface after pertussis toxin treatment." *Mol. Pharmacol.* **59**(5): 1256-1268.

Ross, E. M. (2011). "Galpha(q) and phospholipase C-beta: turn on, turn off, and do it fast." *Sci. Signal.* **4**(159): pe5.

Sadana, R., N. Dascal and C. W. Dessauer (2009). "N terminus of type 5 adenylyl cyclase scaffolds Gs heterotrimer." *Mol. Pharmacol.* **76**(6): 1256-1264.

Salahpour, A., S. Angers, J. F. Mercier, M. Lagace, S. Marullo and M. Bouvier (2004). "Homodimerization of the beta2-adrenergic receptor as a prerequisite for cell surface targeting." *J. Biol. Chem.* **279**(32): 33390-33397.

Salim, S., S. Sinnarajah, J. H. Kehrl and C. W. Dessauer (2003). "Identification of RGS2 and type V adenylyl cyclase interaction sites." *J. Biol. Chem.* **278**(18): 15842-15849.

Santoro, B., D. T. Liu, H. Yao, D. Bartsch, E. R. Kandel, S. A. Siegelbaum and G. R. Tibbs (1998). "Identification of a gene encoding a hyperpolarization-activated pacemaker channel of brain." *Cell* **93**(5): 717-729.

Sassone-Corsi, P. (2012). "The cyclic AMP pathway." *Cold Spring Harb. Perspect. Biol.* **4**(12).

Sharman, J. L., H. E. Benson, A. J. Pawson, V. Lukito, C. P. Mpamhanga, V. Bombail, A. P. Davenport, J. A. Peters, M. Spedding, A. J. Harmar and I. Nc (2013). "IUPHAR-DB: updated database content and new features." *Nucleic Acids Res.* **41**(Database issue): D1083-1088.

Shcherbo, D., E. M. Merzlyak, T. V. Chepurnykh, A. F. Fradkov, G. V. Ermakova, E. A. Solovieva, K. A. Lukyanov, E. A. Bogdanova, A. G. Zaraisky, S. Lukyanov and D. M. Chudakov (2007). "Bright far-red fluorescent protein for whole-body imaging." *Nat Methods* **4**(9): 741-746.

Shimomura, O., F. H. Johnson and Y. Saiga (1962). "Extraction, purification and properties of aequorin, a bioluminescent protein from the luminous hydromedusan, Aequorea." *J. Cell. Comp. Physiol.* **59**: 223-239.

Sinnarajah, S., C. W. Dessauer, D. Srikumar, J. Chen, J. Yuen, S. Yilma, J. C. Dennis, E. E. Morrison, V. Vodyanoy and J. H. Kehrl (2001). "RGS2 regulates signal transduction in olfactory neurons by attenuating activation of adenylyl cyclase III." *Nature* **409**(6823): 1051-1055.

Smrcka, A. V. (2008). "G protein betagamma subunits: central mediators of G protein-coupled receptor signaling." *Cell. Mol. Life Sci.* **65**(14): 2191-2214.

Sunahara, R. K., C. W. Dessauer and A. G. Gilman (1996). "Complexity and diversity of mammalian adenylyl cyclases." *Annu. Rev. Pharmacol. Toxicol.* **36**: 461-480.

Sunahara, R. K., C. W. Dessauer, R. E. Whisnant, C. Kleuss and A. G. Gilman (1997). "Interaction of Gsalpha with the cytosolic domains of mammalian adenylyl cyclase." *J. Biol. Chem.* **272**(35): 22265-22271.

Sutherland, E. W. and T. W. Rall (1957). "THE PROPERTIES OF AN ADENINE RIBONUCLEOTIDE PRODUCED WITH CELLULAR PARTICLES, ATP, Mg++, AND EPINEPHRINE OR GLUCAGON." *J. Am. Chem. Soc.* **79**(13): 3608-3608.

Sutherland, E. W. and G. A. Robison (1966). "The role of cyclic-3',5'-AMP in responses to catecholamines and other hormones." *Pharmacol. Rev.* **18**(1): 145-161.

Tang, W. J. and Q. Guo (2009). "The adenylyl cyclase activity of anthrax edema factor." *Mol. Aspects Med.* **30**(6): 423-430.

Tesmer, J. J. and S. R. Sprang (1998). "The structure, catalytic mechanism and regulation of adenylyl cyclase." *Curr. Opin. Struct. Biol.* **8**(6): 713-719.

Tesmer, J. J., R. K. Sunahara, A. G. Gilman and S. R. Sprang (1997). "Crystal structure of the catalytic domains of adenylyl cyclase in a complex with Gsalpha.GTPgammaS." *Science* **278**(5345): 1907-1916.

Tesmer, J. J., R. K. Sunahara, R. A. Johnson, G. Gosselin, A. G. Gilman and S. R. Sprang (1999). "Two-metal-Ion catalysis in adenylyl cyclase." *Science* **285**(5428): 756-760.

Timofeyev, V., R. E. Myers, H. J. Kim, R. Woltz, P. Sirish, J. Heiserman, N. Li, A. Singapuri, T. Tang, V. Yarov-Yarovoy, E. N. Yamoah, K. Hammond and N. Chiamvimonvat (2013). "Adenylyl Cyclase Subtype-Specific Compartmentalization: Differential Regulation of L-type Ca2+ Current in Ventricular Myocytes." *Circ. Res.*

Tsien, R. Y. (1998). "The green fluorescent protein." *Annu. Rev. Biochem.* **67**: 509-544.

Uhlen, M., P. Oksvold, L. Fagerberg, E. Lundberg, K. Jonasson, M. Forsberg, M. Zwahlen, C. Kampf, K. Wester, S. Hober, H. Wernerus, L. Bjorling and F. Ponten (2010). "Towards a knowledge-based Human Protein Atlas." *Nat. Biotechnol.* **28**(12): 1248-1250.

Vatner, S. F., M. Park, L. Yan, G. J. Lee, L. Lai, K. Iwatsubo, Y. Ishikawa, J. E. Pessin and D. E. Vatner (2013). "Adenylyl Cyclase Type 5 in Cardiac Disease, Metabolism and Aging." *Am. J. Physiol. Heart Circ.Physiol.*

Vatner, S. F., D. E. Vatner and L. Yan (2012). "Models of longevity (calorie restriction and AC5 KO): result of three bad hypotheses." *Aging (Albany NY)* **4**(10): 662-663.

Vatner, S. F., L. Yan, Y. Ishikawa, D. E. Vatner and J. Sadoshima (2009). "Adenylyl cyclase type 5 disruption prolongs longevity and protects the heart against stress." *Circ. J.* **73**(2): 195-200.

Watson, N., M. E. Linder, K. M. Druey, J. H. Kehrl and K. J. Blumer (1996). "RGS family members: GTPase-activating proteins for heterotrimeric G-protein alpha-subunits." *Nature* **383**(6596): 172-175.

Wiege, K., S. R. Ali, B. Gewecke, A. Novakovic, F. M. Konrad, K. Pexa, S. Beer-Hammer, J. Reutershan, R. P. Piekorz, R. E. Schmidt, B. Nurnberg and J. E. Gessner (2013). "Galphai2 is the essential Galphai protein in immune complex-induced lung disease." *J. Immunol.* **190**(1): 324-333.

Willoughby, D. and D. M. Cooper (2006). "Ca2+ stimulation of adenylyl cyclase generates dynamic oscillations in cyclic AMP." *J. Cell Sci.* **119**(Pt 5): 828-836.

Willoughby, D., N. Masada, S. Wachten, M. Pagano, M. L. Halls, K. L. Everett, A. Ciruela and D. M. Cooper (2010). "AKAP79/150 interacts with AC8 and regulates Ca2+-dependent cAMP synthesis in pancreatic and neuronal systems." *J. Biol. Chem.* **285**(26): 20328-20342.

Wise, A., M. A. Watson-Koken, S. Rees, M. Lee and G. Milligan (1997). "Interactions of the alpha2A-adrenoceptor with multiple Gi-family G-proteins: studies with

pertussis toxin-resistant G-protein mutants." *Biochem. J.* **321 (Pt 3)**(3): 721-728.

Wittpoth, C., K. Scholich, Y. Yigzaw, T. M. Stringfield and T. B. Patel (1999). "Regions on adenylyl cyclase that are necessary for inhibition of activity by beta gamma and Gialpha subunits of heterotrimeric G proteins." *Proc. Natl. Acad. Sci. U. S. A.* **96**(17): 9551-9556.

Wolters, V. and M. Bünemann (2013). "Dynamics of interaction between Gq subunits and GRK2." *Naunyn-Schmiedeberg's Arch. Pharmacol.* **386**(Suppl 1): S93.

Wu, C., C. Orozco, J. Boyer, M. Leglise, J. Goodale, S. Batalov, C. L. Hodge, J. Haase, J. Janes, J. W. Huss, 3rd and A. I. Su (2009). "BioGPS: an extensible and customizable portal for querying and organizing gene annotation resources." *Genome Biol.* **10**(11): R130.

Wunder, F., A. Rebmann, A. Geerts and B. Kalthof (2008). "Pharmacological and kinetic characterization of adrenomedullin 1 and calcitonin gene-related peptide 1 receptor reporter cell lines." *Mol. Pharmacol.* **73**(4): 1235-1243.

Xie, K., I. Masuho, C. Brand, C. W. Dessauer and K. A. Martemyanov (2012). "The complex of G protein regulator RGS9-2 and Gbeta(5) controls sensitization and signaling kinetics of type 5 adenylyl cyclase in the striatum." *Sci. Signal.* **5**(239): ra63.

Yan, L., D. E. Vatner, J. P. O'Connor, A. Ivessa, H. Ge, W. Chen, S. Hirotani, Y. Ishikawa, J. Sadoshima and S. F. Vatner (2007). "Type 5 adenylyl cyclase disruption increases longevity and protects against stress." *Cell* **130**(2): 247-258.

Zhang, G., Y. Liu, A. E. Ruoho and J. H. Hurley (1997). "Structure of the adenylyl cyclase catalytic core." *Nature* **386**(6622): 247-253.

Zhang, X. and U. S. Eggert (2013). "Non-traditional roles of G protein-coupled receptors in basic cell biology." *Mol. Biosyst.* **9**(4): 586-595.

Publications

Manuscript under revision:

M. Milde, A. Rinne, F. Wunder, S. Engelhardt and M. Bünemann "Dynamics of $G\alpha_{i1}$ interaction with type 5 adenylyl cyclase reveal molecular basis for high sensitivity of Gi-mediated inhibition of cAMP production"

This manuscript was submitted to *Biochemical Journal* under the paper number BJ2013/0554. By the time of this thesis, it had been returned to the authors for minor revision.

Oral presentation:

M. Milde, M. Bünemann: Gi protein activity is sensitised by type 5 adenylyl cyclase (AC5) *Proceedings of the British Pharmacological Society* at http://www.pa2online.org/abstracts/vol10issue1abst010p.pdf

Posters:

M. Milde, M. Bünemann: Prolonged binding of Gαi to type V adenylyl cyclase potentiates receptor-mediated regulation of cAMP *Naunyn Schmiedebergs Arch Pharmacol* **386**, S55 (2013)

M. Milde, M. Bünemann: Adenylyl cyclase type V sensitises its regulation by inhibitory G-proteins *Naunyn Schmiedebergs Arch Pharmacol* **385**, S59 (2012)

M. Milde, M. Bünemann: Dynamics of G-protein interaction with adenylyl cyclase V *Naunyn Schmiedebergs Arch Pharmacol* **383**, 47 (2011)

Curriculum Vitae

This page containes personal information. It is therefore excluded from online publication.

Diese Seite enthält persönliche Daten. Sie ist daher nicht Bestandteil der Online-Veröffentlichung.

Erklärung

Ich versichere, dass ich meine Dissertation

„Interaction dynamics between heterotrimeric G-proteins and type V adenylyl cyclase determine sensitivity of effector regulation“

selbständig ohne unerlaubte Hilfe angefertigt und mich dabei keiner anderen, als der von mir ausdrücklich bezeichneten Quellen bedient habe.

Die Dissertation wurde in der jetzigen oder einer ähnlichen Form noch bei keiner anderen Hochschule eingereicht und hat noch keinen sonstigen Prüfungszwecken gedient.

Marburg, 10. Juni 2013

.....

(Markus Milde)

Acknowledgements

This cannot go without words of thanks to those who directly or indirectly made this work possible.

First of all, I would like to thank Prof. Dr. Moritz Bünemann very much for providing the interesting subject, giving me the opportunity to work in his lab and do my thesis under his supervision. I appreciated the working atmosphere and his open ear in many questions.

Thanks to Dr. Andreas Rinne for the collaboration on the GIRK experiments. Dr. Frank Wunder is kindly acknowledged as well, for his help in characterising the new construct with the screening-platform of Bayer.

Thank you to Eva-Lisa Bodmann for her help in cloning the "PCR-resistant" AC5.

I am very grateful for Sandra Engel's invaluable help with and fortitude in performing those sometimes frustrating cAMP experiments.

Thanks to Dr. Cornelius Krasel for answering any question I had and allowing me to gather experience in lecturing.

Emma Esser proofread all this and I am very grateful for her comments. Together with Nikol Gröning she also kept most administrative things from our hands and minds, a work that cannot be acknowledged too much.

Many, many thanks to Valerie Wolters not least for partially sharing and taking over responsibility for the Nikon microscope.

Furthermore, I like to thank Dr. Eva Öxler for her helpful discussions and her friendship.

Thanks to all members of the Bünemann-Lab in Marburg, for your help – especially in proofreading –, the nice and friendly atmosphere and trying to cheer me, when things sometimes got rough. Anna-Lena Müller has to be mentioned here for issuing the "leisure time ban". Thanks as well to the other colleagues in the Institute of Pharmacology and Clinical Pharmacy in Marburg.

I would further like to thank the members of the Institute of Pharmacology and Toxicology in Würzburg, namely the old Bünemann-Lab members Dr. Ruth Werthmann, Dr. Kathrin von Hayn, Dr. Leif Hommers, Kerstin Hadamek and Monika Frank for training me and helping with every question and problem a "newbie" comes up with.

Last, but not least, I heartily thank my whole family for all the support, encouragement and understanding in all those years.

"Adenylyl Cyclase is a hateful enzyme."
(Gilman, *Annu. Rev. Pharmacol. Toxicol.* 2012)

It's not that bad, but I would have preferred to know that earlier…